UNIVERSITY OF THESSALY

SCHOOL OF ENGINEERING

DEPARTMENT OF MECHANICAL ENGINEERING

DYNAMICS OF VEHICLE-BRIDGE INTERACTION SYSTEM

by

Dimitrios Simos

Supervisor: **Dr. Costas Papadimitriou**

Submitted in partial fulfillment of the requirements for the degree of Diploma in Mechanical Engineering at the University of Thessaly

Volos, 2022

UNIVERSITY OF THESSALY

SCHOOL OF ENGINEERING

DEPARTMENT OF MECHANICAL ENGINEERING

DYNAMICS OF VEHICLE-BRIDGE INTERACTION SYSTEM

by

Dimitrios Simos

Supervisor: **Dr. Costas Papadimitriou**

Submitted in partial fulfillment of the requirements for the degree of Diploma in Mechanical Engineering at the University of Thessaly

Volos, 2022

Approved by the Committee on Final Examination:

Advisor	**Dr. Costas Papadimitriou**, Professor of Structural Dynamics, Department of Mechanical Engineering, University of Thessaly
Member	**Dr. Konstantinos Ampountolas**, Associate Professor of Automatic Control and Optimization Theory, Department of Mechanical Engineering, University of Thessaly
Member	**Dr. Spyros A. Karamanos**, Professor of Structural Mechanics, Department of Mechanical Engineering, University of Thessaly

Date Approved: [September 19, 2022]

Acknowledgements

I express my sincere gratitude to my supervisor Dr. Costas Papadimitriou who patiently assisted me with every problem I encountered working on this thesis and for the opportunity to study such an interesting topic.

I would also like to thank the members of the committee Dr. Konstantinos Ampountolas and Dr. Spyros A. Karamanos for the careful reading of my work and their valuable suggestions.

I am also thankful to Tulay Ercan for giving me precious advice especially in the Chapter 5 of the thesis and answering my many questions.

Finally, I am grateful to my friends and family, for their support all these years.

DYNAMICS OF VEHICLE-BRIDGE INTERACTION SYSTEM

DIMITRIOS SIMOS

Department of Mechanical Engineering, University of Thessaly,2022

Abstract

Over the last years, there is a significant need for new transportation systems. In this context many cities have expanded their transportation system by adding highway and railway bridges. The dynamic interaction between the vehicle and the bridge, is a topic of high interest, as it directly affects the safety and comfort of the passengers during travelling. The design parameters of both vehicles and bridges, are a major factor effecting the dynamic response of the system.

The present thesis studies the dynamic response of the vehicle-bridge interaction system and presents the influence of the subsystems parameters in the final response. The localized Lagrange multipliers method and the extended modified bridge system (EMBS) method, with the aid of Newmark-β time-integration method, are two solving methods used for the evaluation of the system's response.

The investigation of the parameters effect in the systems response was carried out using two models of the vehicle-bridge system. The vehicles models were introduced in MATLAB, while the finite element model of the bridge was designed and analyzed in COMSOL Multiphysics software. Finally, the simulation of the dynamic interaction of the two subsystems (vehicle-bridge) was carried out in MATLAB, using self-written code developed specifically for the purpose of this thesis.

ΔΥΝΑΜΙΚΗ ΤΗΣ ΑΛΛΗΛΕΠΙΔΡΑΣΗΣ ΤΟΥ ΣΥΣΤΗΜΑΤΟΣ ΟΧΗΜΑΤΟΣ-ΓΕΦΥΡΑΣ

ΔΗΜΗΤΡΙΟΣ ΣΙΜΟΣ

Τμήμα Μηχανολόγων Μηχανικών, Πανεπιστήμιο Θεσσαλίας,2022

Περίληψη

Τα τελευταία χρόνια παρουσιάζεται αισθητή ανάγκη για νέα συστήματα μεταφοράς. Στο πλαίσιο αυτό πολλές πόλεις ανά τον κόσμο επεκτείνουν το σύστημα μεταφορών τους χτίζοντας αυτοκινητοδρομικές και σιδηροδρομικές γέφυρες. Η μελέτη της δυναμικής αλληλεπίδρασης μεταξύ της γέφυρας και των οχημάτων που την διασχίζουν αποτελεί θέμα μεγάλου ενδιαφέροντος, αφού επηρεάζει άμεσα την ασφάλεια και την άνεση των επιβατών. Οι παράμετροι σχεδιασμού τόσο των οχημάτων όσο και των γεφυρών , αποτελούν κυρίαρχο παράγοντα ως προς την δυναμική απόκριση του συστήματος.

Η παρούσα διπλωματική, μελετά την δυναμική αλληλοεπίδραση του συστήματος οχήματος-γέφυρας και παρουσιάζει την επιρροή διάφορων παραμέτρων των υποσυστημάτων στην τελική απόκριση. Η μέθοδος των τοπικών πολλαπλασιαστών του Lagrange και η μέθοδος του εκτεταμένου συστήματος της γέφυρας (EMBS), με την βοήθεια της χρονικής ολοκλήρωσης μέσω της μεθόδου του Newmark-β, είναι οι δύο μέθοδοι που χρησιμοποιούνται για τον υπολογισμό της απόκρισης του συστήματος.

Η ανάλυση για την επίδραση των παραμέτρων στην δυναμική απόκριση του συστήματος πραγματοποιήθηκε για δύο μοντέλα οχήματος-γέφυρας. Τα μοντέλα του οχήματος αναπτύχθηκαν στην MATLAB, ενώ το μοντέλο πεπερασμένων στοιχείων της γέφυρας σχεδιάστηκε και αναλύθηκε στο λογισμικό της COMSOL Multiphysics. Τελικώς, η προσομοίωση της δυναμικής αλληλοεπίδρασης των δύο υποσυστημάτων (οχήματος-γέφυρας) πραγματοποιήθηκε στην MATLAB, χρησιμοποιώντας κώδικα που αναπτύχθηκε ειδικά για τους σκοπούς της διπλωματικής εργασίας.

Contents

LIST OF FIGURES

LIST OF TABLES

Chapter 1

1 Introduction

1.1 Background

In the last decades, there has been a significant need for new transportation systems due to traffic problems in major cities of the word. This need has led to a rapid development of highway communication around the word. The increasing number of bridges, the emergence of new bridge's structure, the need of improved, safer and faster means of transportation (vehicles, trains etc.), require advanced and accurate simulation methods in order to study the dynamics of a vehicle-bridge interaction system. When a vehicle runs across a bridge, the weight of the vehicle, the irregularities of the bridge and even the acceleration or braking of the vehicle can lead to excessive vibrations. Those vibrations will be transferred to the bridge through the vehicle's wheels and so on.

Following the pioneer works of Stokes (1849) and Willis (1849) in the mid-19 century, the vibration of bridges caused by the passage vehicles has been investigated by a great number of researchers. By modeling a moving vehicle as a moving load, moving mass, or moving sprung mass considering the suspension effects, the dynamic response of bridges induced by moving vehicles has been studied from time to time (Timoshenko 1950, Fryba 1972).

Nowadays finite element (FE) analysis offers the opportunity to study and solve the interaction system of bridge and running vehicle with virtually no limit, in a detailed description. Numerical studies in VBI aim primarily at the detailed numerical simulation of involved vehicle-bridge system and at the accurate and efficient time-integration of the VBI problem.

The examination of the dynamics of the interaction of the coupled system (VBI) and the accurate prediction of the system's responses remains a topic of high interest as in the design phase it is necessary to ensure that all the parameters of the system are within a safe range and provide both safety and comfort for the passengers and structural health for the bridge.

1.2 Aim and structure of the study

The major goal of this study is to create and study a simplified model of vehicle-bridge interaction system. The vehicle-bridge system is modeled in MATLAB interacting with COMSOL Multiphysics, using self-written code. For comparison reasons, the response of the system is studied with two solving methods (Lagrange and EMBS) where in both cases the time-integration follows the Newmark-β method. The model will last be used to study the influence of the model's parameters in the system's response.

Chapter 2

2 Theoretical modelling

2.1 Introduction

There is a great variety regarding to the complexity and design of a vehicle. However, when in motion, every vehicle vibrates because of its mass, stiffness and damping properties. Similarly, the variety of bridges considering their size, architecture, materials is even greater. Still, regardless of the bridge's features the passing vehicle excites the bridge to vibrations. Throughout this study the vehicle elements are considered as rigid bodies with mass, and they are interconnected with linear springs and dampers. It is also assumed that there is no internal elastic deformation in the system and the wheels and body of the vehicle are vibrating with small displacements. Finally, the bridge subsystem is modelled with Euler-Bernoulli beam elements.

2.2 Kinetic model of vehicle subsystem

Let $[\boldsymbol{m_v}]$, $[\boldsymbol{c_v}]$ and $[\boldsymbol{k_v}]$ respectively denote the mass, damping and stiffness matrices of a typical vehicle, and $\{\boldsymbol{u_v}\}$ the displacement vector of the vehicle. According to the Newtons 2nd law of motion the vehicles equation of motion can be written as:

$$[\boldsymbol{m_v}]\{\ddot{\boldsymbol{u}}_{\boldsymbol{v}}\}+[\boldsymbol{c_v}]\{\dot{\boldsymbol{u}}_{\boldsymbol{v}}\}+[\boldsymbol{k_v}]\{\boldsymbol{u_v}\}-[\boldsymbol{W^v}]\{\boldsymbol{\lambda_N}\} = \{\boldsymbol{F_v}\} \quad (2.1)$$

where,
$\boldsymbol{\lambda_N(t)}$ is the time varying vector of the contact forces between the vehicle and the bridge/road
$\boldsymbol{W^v}$ is the contact direction matrix associating the contact forces with the DOFs of the vehicle
$\boldsymbol{F_v}$ is the vector of the external forces
Note that the index **N** of the contact forces represents the total number of wheels, of the equivalent vehicle model on each case.

The dimensions of the above matrices depend on the degrees of freedom of the vehicle model. Assuming $\boldsymbol{ndofs}$ for the vehicle's DOFs, the dimensions of the above matrices are:
$[\boldsymbol{m_v}] = [\boldsymbol{c_v}] = [\boldsymbol{k_v}] = [\boldsymbol{ndofs} \times \boldsymbol{ndofs}]$

$\{\ddot{\boldsymbol{u}}_{\boldsymbol{v}}\} = \{\dot{\boldsymbol{u}}_{\boldsymbol{v}}\} = \{\boldsymbol{u_v}\} = \{\boldsymbol{F_v}\} = \{\boldsymbol{ndofs} \times \boldsymbol{1}\}$

Lastly, assuming $\boldsymbol{N\_wheels}$ (number of the wheels of the vehicle), the dimensions of $[\boldsymbol{W^v}]$ and $\{\boldsymbol{\lambda_N}\}$ become:
$[\boldsymbol{W^v}] = [\boldsymbol{ndofs} \times \boldsymbol{N\_wheels}]$ and specifically,

$$[\boldsymbol{W^v}] = \begin{bmatrix} \boldsymbol{zeros(N\_wheels, ndofs - N\_wheels)} \\ \boldsymbol{eye(N\_wheels)} \end{bmatrix}$$

where, **zeros** is a $[\boldsymbol{N\_wheels} \times (\boldsymbol{ndofs} - \boldsymbol{N\_wheels})]$ matrix full of zeros , **eye** is an identity matrix with ones on the main diagonal (for the vertical direction case)
and
$\{\boldsymbol{\lambda_N}\} = \{\boldsymbol{N\_wheels} \times \boldsymbol{1}\}$, as there is a contact force for each wheel on the vertical direction

2.3 Dynamic model of the bridge subsystem

Like the vehicle subsystem, the EOM of the bridge subsystem is:

$$[\boldsymbol{m_b}]\{\ddot{\boldsymbol{u}}_\boldsymbol{b}\} + [\boldsymbol{c_b}]\{\dot{\boldsymbol{u}}_\boldsymbol{b}\} + [\boldsymbol{k_b}]\{\boldsymbol{u_b}\} + \left[\boldsymbol{W^b}\right]\{\boldsymbol{\lambda_N}\} = \{\boldsymbol{F_b}\} \quad (2.2)$$

Note that $\boldsymbol{m_b}, \boldsymbol{c_b}\ and\ \boldsymbol{k_b}$ are, respectively, the mass, damping and stiffness matrices of the bridge and depend on the structural and geometrical characteristics of the bridge (see 2.3.1)

$\boldsymbol{F_b}$ is the external force vector

$\boldsymbol{W^b}$ is the contact direction matrix connecting the contact forces with the DOFs of the bridge The contact direction matrix of the bridge denotes the location of the vehicle's wheels and is used to transfer the forces from the wheels to the equivalent nodes of the bridge element at each time step of the simulation. To formulate the $\boldsymbol{W^b}$ matrix, Hermitian interpolation functions for beam elements are being used (Appendix 3).

At this point it is quite important to point out that $\boldsymbol{W^b}(\boldsymbol{x_N})$ is a time varying matrix and depends on the wheel's location at each time. Assuming that the vehicle's speed is constant and the vehicle is in linear motion, the wheels position can be found as:

$$\boldsymbol{x_N} = \boldsymbol{vt_i} - \boldsymbol{d_N} \quad (2.3)$$

where,
$\boldsymbol{x_N}$: N-wheel's position
$\boldsymbol{v}$: vehicle's velocity
$\boldsymbol{t_i}$: time of interest
$\boldsymbol{d_N}$: distance between the first and N-st wheel of the vehicle

To specify if the wheel acts on the bridge element during the time of interest, function $\boldsymbol{h}(\boldsymbol{x})$ is introduced:

$$\boldsymbol{h}(\boldsymbol{x_i}) = \boldsymbol{H}\left(\frac{\boldsymbol{x_i}}{\boldsymbol{v}}\right) - \boldsymbol{H}\left(\frac{\boldsymbol{x_i} - \boldsymbol{L}}{\boldsymbol{v}}\right) \quad (2.4)$$

The $\boldsymbol{h}(\boldsymbol{x_i})$ function consists of $\boldsymbol{H}(\boldsymbol{x})$,which is the Heaviside step function, that activates and deactivates the action of a wheel on the bridge when a vehicle comes through.

Subsequently,

$$\boldsymbol{h(x_i)} = \begin{cases} \mathbf{1}, & \boldsymbol{wheel\ on\ bridge} \\ \mathbf{0}, & \boldsymbol{wheel\ off\ bridge} \end{cases}$$

In order to evaluate the contact direction matrix $\boldsymbol{W^b(x_i)}$ at each time, $\boldsymbol{h(x_i)}$ function is integrated into $\boldsymbol{W^b(x_i)}$ by multiplying $\boldsymbol{W^b}$ with $\boldsymbol{h(x_i)} = \mathbf{1}$ in case that the wheel acts on the bridge or with $\boldsymbol{h(x_i)} = \mathbf{0}$ in case not.
For better understanding of the contact direction matrix see section 4.4 (Application on a 2D bridge)

Assuming $\boldsymbol{ndofs\_bridge}$ for the bridge's DOFs, the dimensions of the structure's matrices are:

$[\boldsymbol{m_b}] = [\boldsymbol{c_b}] = [\boldsymbol{k_b}] = [\boldsymbol{ndofs\_bridge} \times \boldsymbol{ndofs\_bridge}]$

$\left[\boldsymbol{W^b}\right] = [\boldsymbol{ndofs\_bridge} \times \boldsymbol{N\_wheels}]$

$\{\ddot{\boldsymbol{u}}_\boldsymbol{b}\} = \{\dot{\boldsymbol{u}}_\boldsymbol{b}\} = \{\boldsymbol{u_b}\} = \{\boldsymbol{F_b}\} = \{\boldsymbol{ndofs\_bridge} \times \mathbf{1}\}$

$\{\boldsymbol{\lambda_N}\} = \{\boldsymbol{N\_wheels} \times \mathbf{1}\}$

Where, $\boldsymbol{ndofs\_bridge} = (\boldsymbol{ndofs\ per\ node}) \times (\boldsymbol{mesh\ elements} + \mathbf{1})$ (see section 4.4)

As mentioned earlier the mass, stiffness and damping matrices of the system are different, depending on the structure system of interest. In the next section the structural matrices for the case of Euler-Bernoulli beams are introduced.

2.3.1 Euler-Bernoulli beam

As mentioned in the beginning of this study, the bridge subsystem is modeled with Euler-Bernoulli beams. As we can see in the literature [1] a general 3D beam element consists of six Dofs per node (Figure 2-1). The longitudinal axis of the beam is denoted by x, and the two transverse principal axes of the cross section of the beam by y and z. The six degrees of freedom correspond to three translations and three rotations on each node, giving 12-DOFs for a beam element.

$$\{u\} = \langle u_{xA}\ u_{yA}\ u_{zA}\ u_{xB}\ u_{yB}\ u_{zB} \rangle^T$$
$$\{\theta\} = \langle \theta_{xA}\ \theta_{yA}\ \theta_{zA}\ \theta_{xB}\ \theta_{yB}\ \theta_{zB} \rangle^T$$

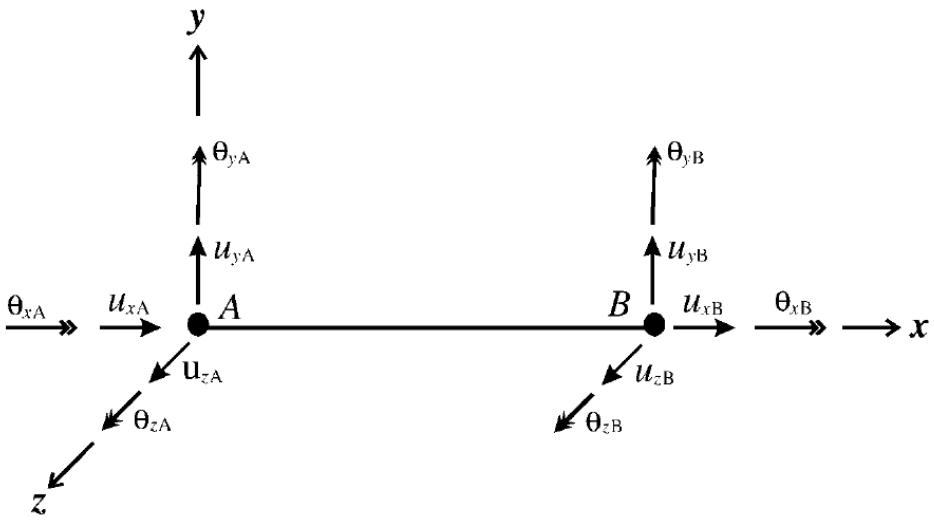

Figure 2-1 Nodal DOFs of three-dimensional beam element

The mass matrix $[\boldsymbol{m_b}]$ is:

$$[\boldsymbol{m_b}] = \frac{\boldsymbol{mL_{el}}}{\boldsymbol{420}}\begin{bmatrix} \boldsymbol{M_1} & (\boldsymbol{M_2})^T \\ \boldsymbol{M_2} & \boldsymbol{M_3} \end{bmatrix} \tag{2.5}$$

Where $\boldsymbol{L_{el}}$ is the length of the element and $\boldsymbol{m}$ is the mass per unit length. The submatrices of Eq (2.5) are:

$$\boldsymbol{M_1} = \begin{bmatrix} \boldsymbol{140} & \boldsymbol{0} & \boldsymbol{0} & \boldsymbol{0} & \boldsymbol{0} & \boldsymbol{0} \\ \boldsymbol{0} & \boldsymbol{156} & \boldsymbol{0} & \boldsymbol{0} & \boldsymbol{0} & \boldsymbol{22L_{el}} \\ \boldsymbol{0} & \boldsymbol{0} & \boldsymbol{156} & \boldsymbol{0} & \boldsymbol{-22L_{el}} & \boldsymbol{0} \\ \boldsymbol{0} & \boldsymbol{0} & \boldsymbol{0} & \boldsymbol{\frac{140I_p}{A}} & \boldsymbol{0} & \boldsymbol{0} \\ \boldsymbol{0} & \boldsymbol{0} & \boldsymbol{-22L_{el}} & \boldsymbol{0} & \boldsymbol{4L_{el}^2} & \boldsymbol{0} \\ \boldsymbol{0} & \boldsymbol{22L_{el}} & \boldsymbol{0} & \boldsymbol{0} & \boldsymbol{0} & \boldsymbol{4L_{el}^2} \end{bmatrix}$$

$$\boldsymbol{M_2} = \begin{bmatrix} \boldsymbol{70} & \boldsymbol{0} & \boldsymbol{0} & \boldsymbol{0} & \boldsymbol{0} & \boldsymbol{0} \\ \boldsymbol{0} & \boldsymbol{54} & \boldsymbol{0} & \boldsymbol{0} & \boldsymbol{0} & \boldsymbol{13L_{el}} \\ \boldsymbol{0} & \boldsymbol{0} & \boldsymbol{50} & \boldsymbol{0} & \boldsymbol{-13L_{el}} & \boldsymbol{0} \\ \boldsymbol{0} & \boldsymbol{0} & \boldsymbol{0} & \boldsymbol{\frac{70I_p}{A}} & \boldsymbol{0} & \boldsymbol{0} \\ \boldsymbol{0} & \boldsymbol{0} & \boldsymbol{13L_{el}} & \boldsymbol{0} & \boldsymbol{-3L_{el}^2} & \boldsymbol{0} \\ \boldsymbol{0} & \boldsymbol{-13L_{el}} & \boldsymbol{0} & \boldsymbol{0} & \boldsymbol{0} & \boldsymbol{-3L_{el}^2} \end{bmatrix}$$

$$M_3 = \begin{bmatrix} 140 & 0 & 0 & 0 & 0 & 0 \\ 0 & 156 & 0 & 0 & 0 & -22L_{el} \\ 0 & 0 & 156 & 0 & 22L_{el} & 0 \\ 0 & 0 & 0 & \frac{140I_p}{A} & 0 & 0 \\ 0 & 0 & 22L_{el} & 0 & 4L_{el}^2 & 0 \\ 0 & -22L_{el} & 0 & 0 & 0 & 4L_{el}^2 \end{bmatrix}$$

Where A denotes the cross area and I_p the polar moment of inertia of the beam.

The stiffness matrix $[k_b]$ is:

$$[k_b] = \begin{bmatrix} K_1 & (K_2)^T \\ K_2 & K_3 \end{bmatrix} \tag{2.6}$$

The submatrices of Eq (2.6) are:

$$K_1 = \begin{bmatrix} \frac{EA}{L_{el}} & 0 & 0 & 0 & 0 & 0 \\ 0 & \frac{12EI_z}{{L_{el}}^3} & 0 & 0 & 0 & \frac{6EI_Z}{{L_{el}}^2} \\ 0 & 0 & \frac{12EI_y}{{L_{el}}^3} & 0 & \frac{-6EI_y}{{L_{el}}^2} & 0 \\ 0 & 0 & 0 & \frac{GI_x}{L_{el}} & 0 & 0 \\ 0 & 0 & \frac{6EI_y}{{L_{el}}^2} & 0 & \frac{4EI_y}{L_{el}} & 0 \\ 0 & \frac{6EI_z}{{L_{el}}^2} & 0 & 0 & 0 & \frac{4EI_z}{L_{el}} \end{bmatrix}$$

$$K_2 = \begin{bmatrix} -\frac{EA}{L_{el}} & 0 & 0 & 0 & 0 & 0 \\ 0 & -\frac{12EI_z}{{L_{el}}^3} & 0 & 0 & 0 & -\frac{6EI_Z}{{L_{el}}^2} \\ 0 & 0 & -\frac{12EI_y}{{L_{el}}^3} & 0 & \frac{6EI_y}{{L_{el}}^2} & 0 \\ 0 & 0 & 0 & -\frac{GI_x}{L_{el}} & 0 & 0 \\ 0 & 0 & -\frac{6EI_y}{{L_{el}}^2} & 0 & \frac{2EI_y}{L_{el}} & 0 \\ 0 & \frac{6EI_z}{{L_{el}}^2} & 0 & 0 & 0 & \frac{2EI_z}{L_{el}} \end{bmatrix}$$

$$K_3 = \begin{bmatrix} \frac{EA}{L_{el}} & 0 & 0 & 0 & 0 & 0 \\ 0 & \frac{12EI_z}{{L_{el}}^3} & 0 & 0 & 0 & -\frac{6EI_Z}{{L_{el}}^2} \\ 0 & 0 & \frac{12EI_y}{{L_{el}}^3} & 0 & \frac{6EI_y}{{L_{el}}^2} & 0 \\ 0 & 0 & 0 & \frac{GI_x}{L_{el}} & 0 & 0 \\ 0 & 0 & \frac{6EI_y}{{L_{el}}^2} & 0 & \frac{4EI_y}{L_{el}} & 0 \\ 0 & -\frac{6EI_z}{{L_{el}}^2} & 0 & 0 & 0 & \frac{4EI_z}{L_{el}} \end{bmatrix}$$

Where ***E*** and ***G*** denote the elastic and shear modulus respectively, ***J*** the torsional constant, and I_y and I_z respectively the moments of inertia about the y– and z–axes of the element.

Last, before defining the damping matrix $[c_b]$, it should be noted that the damping of structures can appear in various forms [2]. By classical damping, means that the damping matrix of structure can be expressed as some linear combination of the mass and stiffness matrices of the structure. In most cases, it is impractical to consider all the vibration modes and damping ratios, so in this study Rayleigh damping is considered. Assuming Rayleigh damping, only the first two modes of the structure are considered and the damping matrix c^b of the structure can be expressed in a general form as a combination of the mass matrix m^b and stiffness matrix k^b, as:

$$[c^b] = a_0[m^b] + a_1[k^b] \tag{2.7}$$

The Rayleigh coefficients a_0 and a_1 can be determined only if the damping ratios ζ_i, ζ_j and frequencies ω_i, ω_j are given for any two vibration modes, as:

$$\begin{Bmatrix} a_0 \\ a_1 \end{Bmatrix} = 2 \begin{bmatrix} {\omega_i}^{-1} & \omega_i \\ {\omega_j}^{-1} & \omega_j \end{bmatrix}^{-1} \begin{Bmatrix} \zeta_i \\ \zeta_j \end{Bmatrix} \tag{2.8}$$

For the case when the frequencies of vibration of the first two modes, i.e., $i = 1$ and $i = 2$, are given and the damping ratios for the two modes are assumed to be the same, i.e., $\zeta_1 = \zeta_2 = \zeta$, the preceding equation reduces to:

$$\begin{Bmatrix} a_0 \\ a_1 \end{Bmatrix} = \frac{2\zeta}{\omega_1 + \omega_2} \begin{Bmatrix} \omega_1\omega_2 \\ 1 \end{Bmatrix} \tag{2.9}$$

Chapter 3

3 Solving methods

3.1 Introduction

The dynamics of VBI is a topic of special interest in bridge and vehicle engineering. The prediction of the vehicle's response, the monitoring of the bridge's structural health, the vehicle's structural health as also the passenger's comfort, all require solving the VBI system. For this reason, many analytical and numerical methods have proposed throughout the years, depending on the complexity of the system and the field of interest. Lagrange and EMBS methods are two methods proposed by [3] and [4] in order to investigate the VBI problem.

3.2 A localized Lagrange multipliers method to solve the VBI problem

3.2.1 Introduction

The localized Lagrange multipliers method is a numerical analysis presented in[5], [10]. This method overcomes the limitations of coupled and iterative algorithms, as it does not lead to time-dependent system matrices and does not require iterations at each time step. This method introduces artificial auxiliary points at the contact interface, with the aid of which it assigns two sets of Lagrange multipliers and states two sets of kinematic constrains between the auxiliary points and the adjacent subsystems. The herein presented localized Lagrange multipliers approach to solve the VBI problem is both accurate and computationally efficient, as it solves the vehicle and bridge subsystems separately but preserves the compatibility of the constrains at each time step.

3.2.2 Vehicle system modelling

The EOM of the vehicle subsystem presented in section 2.2 can also be written as:

$$\boldsymbol{K}_{\boldsymbol{eff}}^{\boldsymbol{v}}\boldsymbol{u}^{\boldsymbol{v}} - \boldsymbol{W}^{\boldsymbol{v}}\boldsymbol{\lambda}^{\boldsymbol{v}} = \boldsymbol{F}^{\boldsymbol{v}} \tag{3.1}$$

where, $\boldsymbol{K}_{\boldsymbol{eff}}^{\boldsymbol{v}}$ is the polynomial differential operator of the vehicle:

$$\boldsymbol{K}_{\boldsymbol{eff}}^{\boldsymbol{v}} = \boldsymbol{m}^{\boldsymbol{v}}\frac{\boldsymbol{d}^{\boldsymbol{2}}}{\boldsymbol{dt}^{\boldsymbol{2}}} + \boldsymbol{c}^{\boldsymbol{v}}\frac{\boldsymbol{d}}{\boldsymbol{dt}} + \boldsymbol{k}^{\boldsymbol{v}} \tag{3.2}$$

$\boldsymbol{m}^{\boldsymbol{v}}, \boldsymbol{c}^{\boldsymbol{v}}$ and $\boldsymbol{k}^{\boldsymbol{v}}$ are the mass, damping and stiffness matrices of the vehicle

$\frac{\boldsymbol{d}}{\boldsymbol{dt}}$: denotes time differentiation

$\boldsymbol{F}^{\boldsymbol{v}}, \boldsymbol{W}^{\boldsymbol{v}}, \boldsymbol{\lambda}^{\boldsymbol{v}}$ **:** as presented in general EOM of the vehicle (section 2.2)

3.2.3 Bridge system modelling

Likewise, the EOM of the bridge about its static equilibrium position, under its self-weight, can be written as:

$$\boldsymbol{K_{eff}^{b}u^{b} - W^{b}\lambda^{b} = F^{b}} \tag{3.3}$$

where, $\boldsymbol{K_{eff}^{b}}$ is the polynomial differential operator of the vehicle:

$$\boldsymbol{K_{eff}^{b} = m^{b}\frac{d^{2}}{dt^{2}} + c^{b}\frac{d}{dt} + k^{b}} \tag{3.4}$$

$\boldsymbol{m^{b}}$, $\boldsymbol{c^{b}}$, $\boldsymbol{k^{b}}$ and $\boldsymbol{F^{b}}$ **:** as presented in general EOM of the bridge (section 2.3)

3.2.4 Interaction solver

This study solves the VBI problem by formulation the EOMs of the vehicle and bridge separately. It is assumed that the vehicle's wheels are always in contact with the bridge and no jump occurs during the interaction. This assumption in association with the auxiliary points of the Lagrange method adds two sets of kinematic constrains and two sets of contact forces in the problem.

Kinematic constrains:

$$\boldsymbol{(W^{v})^{T}u^{v} + r_{c} = u_{g}} \tag{3.5}$$

And

$$\boldsymbol{\left(W^{b}\right)^{T}u^{b} = u_{g}} \tag{3.6}$$

where $\boldsymbol{r_{c}}$ represents the vector that contains the vertical irregularities as presented in (appendix)

For a contact to remain continuously closed for a finite duration, the partitioned boundary accelerations should be equal with the global boundary acceleration $\boldsymbol{\ddot{u}^{g}}$. By differentiating the kinematic constrains twice, with respect to time, the acceleration constrains can be formed as:

$$\boldsymbol{\frac{d^{2}}{dt^{2}}\left((W^{v})^{T}u^{v} + r_{c}\right) = (W^{v})^{T}\frac{d^{2}}{dt^{2}}u^{v} + v^{2}r_{c}'' = \ddot{u}^{g}} \tag{3.7}$$

And

$$\boldsymbol{\frac{d^{2}}{dt^{2}}\left(\left(W^{b}\right)^{T}u^{b}\right) = \left(\left(W^{b}\right)^{T}\frac{d^{2}}{dt^{2}} + 2v\left(W'^{b}\right)\frac{d}{dt} + v^{2}\left(W''^{b}\right)^{T}\right)u^{b} = \ddot{u}^{g}} \tag{3.8}$$

where ()' denotes differentiation with respect to the location of the wheel, as $\boldsymbol{W^b(x_N)}$ varies due to wheel's location.

Effectively:

$$\begin{aligned}
&\frac{\boldsymbol{d}}{\boldsymbol{dt}}\boldsymbol{W^b(x)} = \frac{\boldsymbol{d}}{\boldsymbol{dt}}\boldsymbol{W^b(vt)} = \boldsymbol{vW'^b(x)} \\
&\frac{\boldsymbol{d^2}}{\boldsymbol{dt^2}}\boldsymbol{W^b(x)} = \frac{\boldsymbol{d^2}}{\boldsymbol{dt^2}}\boldsymbol{W^b(vt)} = \boldsymbol{v^2W''^b(x)} \\
&\frac{\boldsymbol{d}}{\boldsymbol{dt}}\boldsymbol{r_c(x)} = \boldsymbol{vr_c{}'(x)} \\
&\frac{\boldsymbol{d^2}}{\boldsymbol{dt^2}}\boldsymbol{r_c(x)} = \boldsymbol{v^2r_c{}''(x)}
\end{aligned} \tag{3.9}$$

Representing the effective contact direction matrices, $\boldsymbol{W^v_{eff}}$ and $\boldsymbol{W^b_{eff}}$ are introduced:

$$\boldsymbol{\left(W^v_{eff}\right)^T} = \boldsymbol{(W^v)^T}\frac{\boldsymbol{d^2}}{\boldsymbol{dt^2}} \tag{3.10}$$

$$\boldsymbol{\left(W^b_{eff}\right)^T} = \boldsymbol{\left(W^b\right)^T}\frac{\boldsymbol{d^2}}{\boldsymbol{dt^2}} + \boldsymbol{2v\left(W'^b\right)}\frac{\boldsymbol{d}}{\boldsymbol{dt}} + \boldsymbol{v^2\left(W''^b\right)} \tag{3.11}$$

So, the two sets of kinematic constrains on the acceleration level are:

$$\boldsymbol{\left(W^v_{eff}\right)^T u^v + v^2 r_c{}''(x) = E^v \ddot{u}^g} \tag{3.12}$$

$$\boldsymbol{\left(W^b_{eff}\right)^T u^b = E^b \ddot{u}^g} \tag{3.13}$$

Lastly, due to Newton's third law, the contact forces are equal:

$$\boldsymbol{(E^v)^T \lambda^v = \left(E^b\right)^T \lambda^b} \tag{3.14}$$

Where, $\boldsymbol{E^v}$ and $\boldsymbol{E^b}$ are identity $[\boldsymbol{N\_wheels} \times \boldsymbol{N\_wheels}]$ matrices referring to the vehicle and bridge, respectively.

Collecting all equilibrium and compatibility equations of the VBI system together returns:

$$\boldsymbol{D}\ [\boldsymbol{u^v} \quad \boldsymbol{u^b} \quad \boldsymbol{\lambda^v} \quad \boldsymbol{\lambda^b} \quad \boldsymbol{\ddot{u}^g}]^T = [\boldsymbol{F^v} \quad \boldsymbol{F^b} \quad \boldsymbol{v^2 r_c{}''} \quad \boldsymbol{0} \quad \boldsymbol{0}]^T \tag{3.15}$$

where, $\boldsymbol{D}$ is a matrix differential operator defined as:

$$\boldsymbol{D}=\begin{bmatrix} \boldsymbol{K_{eff}^{v}} & \boldsymbol{0} & \boldsymbol{-W^{v}} & \boldsymbol{0} & \boldsymbol{0} \\ \boldsymbol{0} & \boldsymbol{K_{eff}^{b}} & \boldsymbol{0} & \boldsymbol{W^{b}} & \boldsymbol{0} \\ \boldsymbol{\left(-W_{eff}^{v}\right)^{T}} & \boldsymbol{0} & \boldsymbol{0} & \boldsymbol{0} & \boldsymbol{E^{v}} \\ \boldsymbol{0} & \boldsymbol{\left(W_{eff}^{v}\right)^{T}} & \boldsymbol{0} & \boldsymbol{0} & \boldsymbol{-E^{b}} \\ \boldsymbol{0} & \boldsymbol{0} & \boldsymbol{(E^{v})^{T}} & \boldsymbol{\left(-E^{b}\right)^{T}} & \boldsymbol{0} \end{bmatrix} \tag{3.16}$$

The above equation contains a system of five equations, the EOM of the vehicle and the bridge, the kinematic constrains and the compatibility condition. This system shows that the vehicle and the bridge are independent (**zero** in D_{12}, D_{21}), so the vehicle and bridge subsystems can be solved in parallel, reducing the computational cost of the analysis.
To do so, the contact forces must be estimated.

Solving Eq (3.16) as to $\boldsymbol{\lambda^{v}}$, $\boldsymbol{\lambda^{b}}$ and $\boldsymbol{\ddot{u}^{g}}$, results:

$$\begin{bmatrix} \boldsymbol{\lambda^{v}} \\ \boldsymbol{\lambda^{b}} \\ \boldsymbol{\ddot{u}^{g}} \end{bmatrix}=\begin{bmatrix} \boldsymbol{\left(W_{eff}^{v}\right)^{T}\left(K_{eff}^{v}\right)^{-1}W^{v}} & \boldsymbol{0} & \boldsymbol{-E^{v}} \\ \boldsymbol{0} & \boldsymbol{\left(W_{eff}^{b}\right)^{T}\left(K_{eff}^{b}\right)^{-1}W^{b}} & \boldsymbol{E^{b}} \\ \boldsymbol{(-E^{v})^{T}} & \boldsymbol{\left(E^{b}\right)^{T}} & \boldsymbol{0} \end{bmatrix}^{-1} \begin{bmatrix} \boldsymbol{\left(-W_{eff}^{v}\right)^{T}\left(K_{eff}^{v}\right)^{-1}F^{v}-v^{2}r_{c}''} \\ \boldsymbol{\left(W_{eff}^{b}\right)^{T}\left(K_{eff}^{b}\right)^{-1}F^{b}} \\ \boldsymbol{0} \end{bmatrix} \tag{3.17}$$

Also, from Eq (3.16), vehicle and bridge responses are:

$$\begin{bmatrix} \boldsymbol{u^{v}} \\ \boldsymbol{u^{b}} \end{bmatrix}=\begin{bmatrix} \boldsymbol{\left(K_{eff}^{v}\right)^{-1}} & \boldsymbol{0} \\ \boldsymbol{0} & \boldsymbol{\left(K_{eff}^{b}\right)^{-1}} \end{bmatrix}\left(\begin{bmatrix} \boldsymbol{F^{v}} \\ \boldsymbol{F^{b}} \end{bmatrix}-\begin{bmatrix} \boldsymbol{-W^{v}} & \boldsymbol{0} & \boldsymbol{0} \\ \boldsymbol{0} & \boldsymbol{W^{b}} & \boldsymbol{0} \end{bmatrix}\begin{bmatrix} \boldsymbol{\lambda^{v}} \\ \boldsymbol{\lambda^{b}} \\ \boldsymbol{\ddot{u}^{g}} \end{bmatrix}\right) \tag{3.18}$$

3.2.5 Time-integration

According to the Newmark-β method (Appendix), the velocities and accelerations of the vehicle and bridge at time step **t+Δt** of time integration are, respectively:

$$\boldsymbol{\ddot{u}^{v/b(t+\Delta t)}=a_{0}\left(u^{v/b(t+\Delta t)}-u^{v/b(t)}\right)-a_{2}\dot{u}^{v/b(t)}-a_{3}\ddot{u}^{v/b(t)}} \tag{3.19}$$

$$\boldsymbol{\dot{u}^{v/b(t+\Delta t)}=\dot{u}^{v/b(t)}+a_{6}\ddot{u}^{v/b(t)}+a_{7}\ddot{u}^{v/b(t+\Delta t)}} \tag{3.20}$$

Where, $\boldsymbol{\dot{u}^{v/b(t)}}$ and $\boldsymbol{\ddot{u}^{v/b(t)}}$ are the equivalent velocities and accelerations of the vehicle (superscript v) and of the bridge (superscript b) at current time step $\boldsymbol{t}$. The parameters $\boldsymbol{a_0}$ *to* $\boldsymbol{a_7}$ are the Newmark-β coefficients as presented in the Appendix.

Utilizing Eqs (3.2), (3.4), (3.19) and (3.20), the products $\boldsymbol{K_{eff}^{v}u^{v\,(t+\Delta t)}}$ and $\boldsymbol{K_{eff}^{b}u^{b\,(t+\Delta t)}}$ of Eqs (3.1) and (3.3) at time $\boldsymbol{t+\Delta t}$ become:

$$\left(\boldsymbol{m^v}\frac{\boldsymbol{d^2}}{\boldsymbol{dt^2}}+\boldsymbol{c^v}\frac{\boldsymbol{d}}{\boldsymbol{dt}}+\boldsymbol{k^v}\right)\boldsymbol{u^{v\,(t+\Delta t)}}=\bar{\boldsymbol{K}}^{\boldsymbol{v}}\boldsymbol{u^{v\,(t+\Delta t)}}-\boldsymbol{c^v}\bar{\ddot{\boldsymbol{u}}}^{\boldsymbol{v}\,(t)}-\boldsymbol{m^v}\bar{\ddot{\boldsymbol{u}}}^{\boldsymbol{v}\,(t)} \tag{3.21}$$

$$\left(\boldsymbol{m^b}\frac{\boldsymbol{d^2}}{\boldsymbol{dt^2}}+\boldsymbol{c^b}\frac{\boldsymbol{d}}{\boldsymbol{dt}}+\boldsymbol{k^b}\right)\boldsymbol{u^{b\,(t+\Delta t)}}=\bar{\boldsymbol{K}}^{\boldsymbol{b}}\boldsymbol{u^{b\,(t+\Delta t)}}-\boldsymbol{c^b}\bar{\ddot{\boldsymbol{u}}}^{\boldsymbol{b}\,(t)}-\boldsymbol{m^b}\bar{\ddot{\boldsymbol{u}}}^{\boldsymbol{b}\,(t)} \tag{3.22}$$

Where,

$$\bar{\dot{\boldsymbol{u}}}^{\boldsymbol{v/b\,(t)}}=\boldsymbol{a_1u^{v/b\,(t)}}+\boldsymbol{a_4}\dot{\boldsymbol{u}}^{\boldsymbol{v/b\,(t)}}+\boldsymbol{a_5}\ddot{\boldsymbol{u}}^{\boldsymbol{v/b\,(t)}} \tag{3.23}$$

$$\bar{\ddot{\boldsymbol{u}}}^{\boldsymbol{v/b\,(t)}}=\boldsymbol{a_0u^{v/b\,(t)}}+\boldsymbol{a_2}\dot{\boldsymbol{u}}^{\boldsymbol{v/b\,(t)}}+\boldsymbol{a_3}\ddot{\boldsymbol{u}}^{\boldsymbol{v/b\,(t)}} \tag{3.24}$$

And

$$\bar{\boldsymbol{K}}^{\boldsymbol{v}}=\boldsymbol{a_0m^v}+\boldsymbol{a_1c^v}+\boldsymbol{k^v} \tag{3.25}$$
$$\bar{\boldsymbol{K}}^{\boldsymbol{b}}=\boldsymbol{a_0m^b}+\boldsymbol{a_1c^b}+\boldsymbol{k^b} \tag{3.26}$$

$\bar{\boldsymbol{K}}^{\boldsymbol{v}}$ and $\bar{\boldsymbol{K}}^{\boldsymbol{b}}$ are the equivalent stiffness matrices during time-integration

The last two products of Eqs. (3.21) and (3.22) are considered as additional force vectors. As they refer to the current time $\boldsymbol{t}$, they can be considered as known for the next time step $\boldsymbol{t}+\boldsymbol{\Delta t}$. So, they are shifted to the right-hand side of Eq. (3.18) together with the force vectors $\boldsymbol{F^{v\,(t+\Delta t)}}$ and $\boldsymbol{F^{b\,(t+\Delta t)}}$, forming the equivalent force vectors $\bar{\boldsymbol{F}}^{\boldsymbol{v\,(t+\Delta t)}}$ and $\bar{\boldsymbol{F}}^{\boldsymbol{b\,(t+\Delta t)}}$:

$$\bar{\boldsymbol{F}}^{\boldsymbol{v\,(t+\Delta t)}}=\boldsymbol{F^{v\,(t+\Delta t)}}+\boldsymbol{c^v}\bar{\ddot{\boldsymbol{u}}}^{\boldsymbol{v}\,(t)}+\boldsymbol{m^v}\bar{\ddot{\boldsymbol{u}}}^{\boldsymbol{v}\,(t)}, \tag{3.27}$$

$$\bar{\boldsymbol{F}}^{\boldsymbol{v\,(t+\Delta t)}}=\boldsymbol{F^{v\,(t+\Delta t)}}+\boldsymbol{c^v}\bar{\ddot{\boldsymbol{u}}}^{\boldsymbol{v}\,(t)}+\boldsymbol{m^v}\bar{\ddot{\boldsymbol{u}}}^{\boldsymbol{v}\,(t)} \tag{3.28}$$

Employing Eq. (3.19) to (3.22), becomes:

$$\begin{bmatrix}\boldsymbol{u^v}\\ \boldsymbol{u^b}\end{bmatrix}^{(t+\Delta t)}=\begin{bmatrix}(\bar{\boldsymbol{K}}^{\boldsymbol{v}})^{-1} & \boldsymbol{0}\\ \boldsymbol{0} & (\bar{\boldsymbol{K}}^{\boldsymbol{b}})^{-1}\end{bmatrix}\left(\begin{bmatrix}\bar{\boldsymbol{F}}^{\boldsymbol{v}}\\ \bar{\boldsymbol{F}}^{\boldsymbol{b}}\end{bmatrix}^{(t+\Delta t)}-\begin{bmatrix}-\boldsymbol{W^v} & \boldsymbol{0} & \boldsymbol{0}\\ \boldsymbol{0} & \boldsymbol{W^{b\,(t+\Delta t)}} & \boldsymbol{0}\end{bmatrix}\begin{bmatrix}\boldsymbol{\lambda^v}\\ \boldsymbol{\lambda^b}\\ \ddot{\boldsymbol{u}}^{\boldsymbol{g}}\end{bmatrix}^{(t+\Delta t)}\right) \tag{3.29}$$

Similarly, the products $\left(\boldsymbol{W^v_{eff}}\right)^{\boldsymbol{T}}\boldsymbol{u^{v\,(t+\Delta t)}}$ and $\left(\boldsymbol{W^b_{eff}}\right)^{\boldsymbol{T}}\boldsymbol{u^{b\,(t+\Delta t)}}$ of Eqs. (3.12) and (3.13) at time step $\boldsymbol{t}+\boldsymbol{\Delta t}$ become:

$$\left(\boldsymbol{W^v_{eff}}\right)^{\boldsymbol{T}}\boldsymbol{u^{v\,(t+\Delta t)}}=(\bar{\boldsymbol{W}}^{\boldsymbol{v}})^{\boldsymbol{T}}\boldsymbol{u^{v\,(t+\Delta t)}}-(\boldsymbol{W^v})^{\boldsymbol{T}}\bar{\ddot{\boldsymbol{u}}}^{\boldsymbol{v}\,(t)}, \tag{3.30}$$

$$\left(\boldsymbol{W^b_{eff}}\right)^{\boldsymbol{T}}\boldsymbol{u^{b\,(t+\Delta t)}}=\left(\bar{\boldsymbol{W}}^{\boldsymbol{b}}\right)^{\boldsymbol{T}}\boldsymbol{u^{b\,(t+\Delta t)}}-\left(\boldsymbol{W^b}\right)^{\boldsymbol{T}}\bar{\ddot{\boldsymbol{u}}}^{\boldsymbol{b}\,(t)} \tag{3.31}$$

Where, $\bar{\boldsymbol{W}}^{\boldsymbol{v}}$ and $\bar{\boldsymbol{W}}^{\boldsymbol{b}}$ are the equivalent contact direction matrices during the integration of the system:

$$\overline{\boldsymbol{W}}^{\boldsymbol{v}} = \boldsymbol{a_0}\boldsymbol{W}^{\boldsymbol{v}},$$
$$\overline{\boldsymbol{W}}^{\boldsymbol{b}} = \boldsymbol{a_0}\boldsymbol{W}^{\boldsymbol{b}} + \boldsymbol{a_1}\boldsymbol{2v}\boldsymbol{W}'^{\boldsymbol{b}} + \boldsymbol{v}^{\boldsymbol{2}}\boldsymbol{W}''^{\boldsymbol{b}} \quad (3.32)$$

Finally, Eq (3.17) becomes:

$$\begin{bmatrix} \boldsymbol{\lambda}^{\boldsymbol{v}} \\ \boldsymbol{\lambda}^{\boldsymbol{b}} \\ \ddot{\boldsymbol{u}}^{\boldsymbol{g}} \end{bmatrix}^{(t+\Delta t)} = \begin{bmatrix} (\overline{\boldsymbol{W}}^{\boldsymbol{v}})^{\boldsymbol{T}}(\overline{\boldsymbol{K}}^{\boldsymbol{v}})^{-\boldsymbol{1}}\boldsymbol{W}^{\boldsymbol{v}} & \boldsymbol{0} & -\boldsymbol{E}^{\boldsymbol{v}} \\ \boldsymbol{0} & \left(\overline{\boldsymbol{W}}^{\boldsymbol{b}}\right)^{\boldsymbol{T}(t+\Delta t)}\left(\overline{\boldsymbol{K}}^{\boldsymbol{b}}\right)^{-\boldsymbol{1}}\boldsymbol{W}^{\boldsymbol{b}(t+\Delta t)} & \boldsymbol{E}^{\boldsymbol{b}} \\ (-\boldsymbol{E}^{\boldsymbol{v}})^{\boldsymbol{T}} & \left(\boldsymbol{E}^{\boldsymbol{b}}\right)^{\boldsymbol{T}} & \boldsymbol{0} \end{bmatrix}^{-\boldsymbol{1}}$$
$$\begin{bmatrix} (-\overline{\boldsymbol{W}}^{\boldsymbol{v}})^{\boldsymbol{T}}(\overline{\boldsymbol{K}}^{\boldsymbol{v}})^{-\boldsymbol{1}}\overline{\boldsymbol{F}}^{\boldsymbol{v}} + \overline{\boldsymbol{w}}^{\boldsymbol{v}} \\ \left(\overline{\boldsymbol{W}}^{\boldsymbol{b}}\right)^{\boldsymbol{T}(t+\Delta t)}\left(\overline{\boldsymbol{K}}^{\boldsymbol{b}}\right)^{-\boldsymbol{1}}\overline{\boldsymbol{F}}^{\boldsymbol{b}} + \overline{\boldsymbol{w}}^{\boldsymbol{b}} \\ \boldsymbol{0} \end{bmatrix} \quad (3.33)$$

Where vectors $\overline{\boldsymbol{w}}^{\boldsymbol{v}}$ and $\overline{\boldsymbol{w}}^{\boldsymbol{b}}$ contain additional terms produced during the time-integration:

$$\overline{\boldsymbol{w}}^{\boldsymbol{v}} = (-\boldsymbol{W}^{\boldsymbol{v}})^{\boldsymbol{T}}\left(-\ddot{\overline{\boldsymbol{u}}}^{\boldsymbol{v}(t)}\right) - \boldsymbol{v}^{\boldsymbol{2}}\boldsymbol{r_c}''$$
$$\overline{\boldsymbol{w}}^{\boldsymbol{b}} = \left(\boldsymbol{W}^{\boldsymbol{b}}\right)^{\boldsymbol{T}}\left(-\ddot{\overline{\boldsymbol{u}}}^{\boldsymbol{b}(t)}\right) + \boldsymbol{2v}\left(\boldsymbol{W}'^{\boldsymbol{b}}\right)^{\boldsymbol{T}}\left(-\dot{\boldsymbol{u}}^{\boldsymbol{b}(t)}\right) \quad (3.34)$$

3.3 Extended Modified Bridge System method to decouple railway bridges

3.3.1 Introduction

This section relies on the work [6]. The goal is to examine the dynamics of the vehicle-bridge systems in the vertical plane and break down the coupling mechanisms of VBI of MDOF vehicle-MDOF bridge systems. The decoupling of the adopted MDOF configuration relies on an asymptotic expansion analysis of the response of the coupled system in the vertical plane. Based on the asymptotic expansion analysis of the coupled system response, the study [6] brings forward the dominant coupling parameters and their relative importance on the bridge response. The proposed decoupling EMBS method solves the bridge independently of the vehicle by changing its mechanical system via additional damping, stiffness and loading terms. The proposed decoupling formulations are applicable to any bridge type.

3.3.2 Vehicle-Bridge interaction: problem formulation

This section formulates the equations of motion of an MDOF vehicle traversing a generic MDOF bridge. As with Lagrange method, the goal is to examine the dynamics of vehicle-bridge systems in the vertical plane and break down the coupling mechanisms of VBI of MDOF vehicle-MDOF bridge systems.

3.3.3 Description of the VBI problem

Vehicle subsystem

As presented in section 2.2 the EOM of the vehicle corresponds to Eq. (2.1). In EMBS method in order to facilitate the decoupling of the vehicle-bridge system, the EOM of the MDOF vehicle is partitioned into the upper part (DOFs not in contact with the bridge) and the wheel's part (DOFs in contact with the bridge). The EOM of the vehicle is considered about its statically deformed configuration under its self-weight.

So, Eq (2.1) becomes:

$$\begin{bmatrix} \boldsymbol{m^u} & \boldsymbol{0} \\ \boldsymbol{0} & \boldsymbol{m^w} \end{bmatrix} \begin{bmatrix} \ddot{\boldsymbol{u}}^{\boldsymbol{u}} \\ \ddot{\boldsymbol{u}}^{\boldsymbol{w}} \end{bmatrix} + \begin{bmatrix} \boldsymbol{c^u} & \boldsymbol{c^{u,w}} \\ (\boldsymbol{c^{u,w}})^{\boldsymbol{T}} & \boldsymbol{c^w} \end{bmatrix} \begin{bmatrix} \dot{\boldsymbol{u}}^{\boldsymbol{u}} \\ \dot{\boldsymbol{u}}^{\boldsymbol{w}} \end{bmatrix} + \begin{bmatrix} \boldsymbol{k^u} & \boldsymbol{k^{u,w}} \\ (\boldsymbol{k^{u,w}})^{\boldsymbol{T}} & \boldsymbol{k^w} \end{bmatrix} \begin{bmatrix} \boldsymbol{u}^{\boldsymbol{u}} \\ \boldsymbol{u}^{\boldsymbol{w}} \end{bmatrix} - \begin{bmatrix} \boldsymbol{0} \\ \boldsymbol{W^w} \end{bmatrix} \boldsymbol{\lambda} = \begin{bmatrix} \boldsymbol{F^u} \\ \boldsymbol{F^w} \end{bmatrix} \tag{3.35}$$

Where **m, c** and **k** denote the mass, damping and stiffness matrices of the upper part (subscript $()^u$) and of the wheels part (subscript $()^w$) of the vehicle, and the coupling submatrices between the two parts (subscripts $()^{u,w}$ and $()^{w,u}$).

$\boldsymbol{\lambda(t)}$ is the vector of the contact forces between the vehicle and bridge subsystems

$\boldsymbol{W^w}$ is the contact direction matrix (of the wheels part), associating the contact forces with the DOFs of the vehicle. Note that from eq (2.1) $\boldsymbol{W^v} = \begin{bmatrix} \boldsymbol{0} \\ \boldsymbol{W^w} \end{bmatrix}$.

$\boldsymbol{F^u}$ and $\boldsymbol{F^W}$ are the external force vectors of the two parts of the vehicle, thus no external excitation is considered and the vectors $\boldsymbol{F^u}$ and $\boldsymbol{F^W}$ are henceforth zero vectors.

Bridge subsystem

As presented in section (2.3) for the general model of a bridge subsystem, the EOM of the bridge is:

$$[\boldsymbol{m_b}]\{\ddot{\boldsymbol{u}}_{\boldsymbol{b}}\} + [\boldsymbol{c_b}]\{\dot{\boldsymbol{u}}_{\boldsymbol{b}}\} + [\boldsymbol{k_b}]\{\boldsymbol{u}_{\boldsymbol{b}}\} + \left[\boldsymbol{W^b}\right]\{\boldsymbol{\lambda}_{\boldsymbol{N}}\} = \{\boldsymbol{F}_{\boldsymbol{b}}\} \tag{3.36}$$

All terms are already presented in section (2.3)

At this point it is essential to point out that the overdot indicates differentiation with respect to the dimensional time $\boldsymbol{t}$, while prime denotes differentiation with respect to the dimensional location of the vehicle $\boldsymbol{x}$.

Coupled VBI system

The EOM of the coupled vehicle-bridge system is:

$$\boldsymbol{m\ddot{u} + c\dot{u} + ku - W\lambda = F} \tag{3.37}$$

Where $\boldsymbol{m}, \boldsymbol{c}\ and\ \boldsymbol{k}$ are the corresponding mass, damping and stiffness matrices of the entire system and $\boldsymbol{u}(\boldsymbol{t})$ is the displacement vector of the coupled system:

$$\boldsymbol{m} = \begin{bmatrix} \begin{bmatrix} \boldsymbol{m}^{\boldsymbol{u}} & \boldsymbol{0} \\ \boldsymbol{0} & \boldsymbol{m}^{\boldsymbol{w}} \end{bmatrix} & \boldsymbol{0} \\ \boldsymbol{0} & \boldsymbol{m}^{\boldsymbol{b}} \end{bmatrix}, \quad \boldsymbol{c} = \begin{bmatrix} \begin{bmatrix} \boldsymbol{c}^{\boldsymbol{u}} & \boldsymbol{c}^{\boldsymbol{u},\boldsymbol{w}} \\ \boldsymbol{c}^{\boldsymbol{w},\boldsymbol{u}} & \boldsymbol{c}^{\boldsymbol{w}} \end{bmatrix} & \boldsymbol{0} \\ \boldsymbol{0} & \boldsymbol{c}^{\boldsymbol{b}} \end{bmatrix},$$
$$\boldsymbol{k} = \begin{bmatrix} \begin{bmatrix} \boldsymbol{k}^{\boldsymbol{u}} & \boldsymbol{k}^{\boldsymbol{u},\boldsymbol{w}} \\ \boldsymbol{k}^{\boldsymbol{w},\boldsymbol{u}} & \boldsymbol{k}^{\boldsymbol{w}} \end{bmatrix} & \boldsymbol{0} \\ \boldsymbol{0} & \boldsymbol{k}^{\boldsymbol{b}} \end{bmatrix}, \tag{3.38}$$

$$\boldsymbol{u} = \begin{bmatrix} \begin{bmatrix} \boldsymbol{u}^{\boldsymbol{u}} \\ \boldsymbol{u}^{\boldsymbol{w}} \end{bmatrix} \\ \boldsymbol{u}^{\boldsymbol{b}} \end{bmatrix} \tag{3.39}$$

In this study a 2D vehicle (see applications (4.2), (4.3)) is considered where $\boldsymbol{u}^{\boldsymbol{w}}$ contains only translational DOFs along the vertical direction, thus $\boldsymbol{W}^{\boldsymbol{w}}$**=E** where **E** is the identity matrix.

$$\boldsymbol{W} = \begin{bmatrix} \begin{bmatrix} \boldsymbol{0} \\ \boldsymbol{E} \end{bmatrix} \\ -\boldsymbol{W}^{\boldsymbol{b}} \end{bmatrix} \text{ and } \boldsymbol{F} = \begin{bmatrix} \begin{bmatrix} \boldsymbol{0} \\ \boldsymbol{0} \end{bmatrix} \\ \boldsymbol{F}^{\boldsymbol{b}} \end{bmatrix} \tag{3.40}$$

To estimate the contact force $\boldsymbol{\lambda}$, as in Lagrange method, the study assumes "rigid contact" between the wheels and the bridge. This assumption implies continuous contact, and subsequently zero relative displacement/acceleration $\boldsymbol{g}_{\boldsymbol{N}}(\boldsymbol{x}, \boldsymbol{t}) = \ddot{\boldsymbol{g}}_{\boldsymbol{N}}(\boldsymbol{x}, \boldsymbol{t}) = \boldsymbol{0}$, between the wheels and the bridge. The relative displacement between the two subsystems is:

$$\boldsymbol{g}_{\boldsymbol{N}} = \boldsymbol{W}^{\boldsymbol{T}}\boldsymbol{u} - \boldsymbol{r}_{\boldsymbol{c}} = \boldsymbol{u}^{\boldsymbol{w}} - \left(\boldsymbol{W}^{\boldsymbol{b}}\right)^{\boldsymbol{T}}\boldsymbol{u}^{\boldsymbol{b}} - \boldsymbol{r}_{\boldsymbol{c}} \tag{3.41}$$

Where $\boldsymbol{r}_{\boldsymbol{c}}(\boldsymbol{x})$ is the irregularities vector, consisting of the irregularities $\boldsymbol{r}_{\boldsymbol{c}}(\boldsymbol{x}_{\boldsymbol{i}})$ at each point. The irregularities, as in Lagrange method, are simulated as presented in the (Appendix). The relative velocity $\dot{\boldsymbol{g}}_{\boldsymbol{N}}(\boldsymbol{x}, \boldsymbol{t})$ results by differentiating the relative displacement vector with respect to time $\boldsymbol{t}$:

$$\dot{\boldsymbol{g}}_{\boldsymbol{N}} = \boldsymbol{W}^{\boldsymbol{T}}\dot{\boldsymbol{u}} + \boldsymbol{v}\boldsymbol{W}'^{\boldsymbol{T}}\boldsymbol{u} - \boldsymbol{v}\boldsymbol{r}_{\boldsymbol{c}}' = \dot{\boldsymbol{u}}^{\boldsymbol{w}} - \boldsymbol{v}\left(\boldsymbol{W}^{\boldsymbol{b}}\right)'^{\boldsymbol{T}}\boldsymbol{u}^{\boldsymbol{b}} - \left(\boldsymbol{W}^{\boldsymbol{b}}\right)^{\boldsymbol{T}}\dot{\boldsymbol{u}}^{\boldsymbol{b}} - \boldsymbol{v}\boldsymbol{r}_{\boldsymbol{c}}' \tag{3.42}$$

Accordingly, the relative acceleration is:

$$\ddot{\boldsymbol{g}}_{\boldsymbol{N}} = \boldsymbol{W}^{\boldsymbol{T}}\ddot{\boldsymbol{u}} + \boldsymbol{2}\boldsymbol{v}\boldsymbol{W}'^{\boldsymbol{T}}\dot{\boldsymbol{u}} + \boldsymbol{v}^{\boldsymbol{2}}\boldsymbol{W}''^{\boldsymbol{T}}\boldsymbol{u} - \boldsymbol{v}^{\boldsymbol{2}}\boldsymbol{r}_{\boldsymbol{c}}'' \tag{3.43}$$

Applying the kinematic constrain on the acceleration level $\ddot{\boldsymbol{g}}_{\boldsymbol{N}} = \boldsymbol{0}$ and substituting $\ddot{\boldsymbol{u}}$ into the system's EOM gives the contact force:

$$\boldsymbol{\lambda} = -\boldsymbol{G}^{-1}\begin{bmatrix} \boldsymbol{W}^{T}\boldsymbol{m}^{-1}(\boldsymbol{F} - \boldsymbol{c}\dot{\boldsymbol{u}} - \boldsymbol{k}\boldsymbol{u}) \\ +2v\boldsymbol{W}'^{T}\dot{\boldsymbol{u}}\, v^{2}\boldsymbol{W}''^{T}\boldsymbol{u} - v^{2}\boldsymbol{r}_{c}'' \end{bmatrix} \tag{3.44}$$

where $\boldsymbol{G}^{-1}$ is the mass participating in the contact interaction between the wheels and the bridge.

$$\boldsymbol{G} = \boldsymbol{W}^{T}\boldsymbol{m}^{-1}\boldsymbol{W} = (\boldsymbol{m}^{w})^{-1} + \left(\boldsymbol{W}^{b}\right)^{T}\left(\boldsymbol{m}^{b}\right)^{-1}\left(\boldsymbol{W}^{b}\right) \tag{3.45}$$

Substituting the system matrices **u, m, c, k, W** and **F**, as well as the wheels response $\boldsymbol{u}^{w}$ the contact force **λ** becomes:

$$\begin{aligned} \boldsymbol{\lambda} = {} & \boldsymbol{G}^{-1}(\boldsymbol{m}^{w})^{-1}\left(\boldsymbol{c}^{w,u}\dot{\boldsymbol{u}}^{u} + \boldsymbol{c}^{w}\left(\boldsymbol{W}^{b}\right)^{T}\dot{\boldsymbol{u}}^{b} + v\boldsymbol{c}^{w}\left(\boldsymbol{W}^{b}\right)'^{T}\boldsymbol{u}^{b} + v\boldsymbol{c}^{w}\boldsymbol{r}_{c}'\right) \\ & + \boldsymbol{G}^{-1}(\boldsymbol{m}^{w})^{-1}\left(\boldsymbol{k}^{w,u}\boldsymbol{u}^{u} + \boldsymbol{k}^{w}\left(\boldsymbol{W}^{b}\right)^{T}\boldsymbol{u}^{b} + \boldsymbol{k}^{w}\boldsymbol{r}_{c}\right) \\ & + \boldsymbol{G}^{-1}\left(\boldsymbol{W}^{b}\right)^{T}\left(\boldsymbol{m}^{b}\right)^{-1}\left(\boldsymbol{F}^{b} - \boldsymbol{c}^{b}\dot{\boldsymbol{u}}^{b} - \boldsymbol{k}^{b}\boldsymbol{u}^{b}\right) \\ & + \boldsymbol{G}^{-1}\left(2v\left(\boldsymbol{W}^{b}\right)'^{T}\dot{\boldsymbol{u}}^{b} + v^{2}\left(\boldsymbol{W}^{b}\right)''^{T}\boldsymbol{u}^{b} + v^{2}\boldsymbol{r}_{c}''\right) \end{aligned} \tag{3.46}$$

Subsequently, substituting $\boldsymbol{\lambda}$ into Eq. (3.36) the bridge's EOM becomes:

$$\begin{aligned} & \boldsymbol{m}^{b}\ddot{\boldsymbol{u}}^{b} + \Big[\boldsymbol{c}^{b} + \boldsymbol{W}^{b}\boldsymbol{G}^{-1}(\boldsymbol{m}^{w})^{-1}\boldsymbol{c}^{w}\left(\boldsymbol{W}^{b}\right)^{T} \\ & \qquad + \boldsymbol{W}^{b}\boldsymbol{G}^{-1}\left(2v\left(\boldsymbol{W}^{b}\right)'^{T} - \left(\boldsymbol{W}^{b}\right)^{T}\left(\boldsymbol{m}^{b}\right)^{-1}\boldsymbol{c}^{b}\right)\Big]\dot{\boldsymbol{u}}^{b} \\ & \Big[+\boldsymbol{k}^{b} + \boldsymbol{W}^{b}\boldsymbol{G}^{-1}(\boldsymbol{m}^{w})^{-1}\left(v\boldsymbol{c}^{w}\left(\boldsymbol{W}^{b}\right)'^{T} + \boldsymbol{k}^{w}\left(\boldsymbol{W}^{b}\right)^{T}\right) \\ & \qquad + \boldsymbol{W}^{b}\boldsymbol{G}^{-1}\left(v^{2}\left(\boldsymbol{W}^{b}\right)''^{T} - \left(\boldsymbol{W}^{b}\right)^{T}\left(\boldsymbol{m}^{b}\right)^{-1}\boldsymbol{k}^{b}\right)\Big]\boldsymbol{u}^{b} \\ & = \boldsymbol{F}^{b} - \boldsymbol{W}^{b}\boldsymbol{G}^{-1}\left(\left(\boldsymbol{W}^{b}\right)^{T}\left(\boldsymbol{m}^{b}\right)^{-1}\boldsymbol{F}^{b} + v^{2}\boldsymbol{r}_{c}''\right) \\ & \qquad - \boldsymbol{W}^{b}\boldsymbol{G}^{-1}(\boldsymbol{m}^{w})^{-1}(\boldsymbol{k}^{w,u}\boldsymbol{u}^{u} + \boldsymbol{c}^{w,u}\dot{\boldsymbol{u}}^{u} + \boldsymbol{k}^{w}\boldsymbol{r}_{c} + v\boldsymbol{c}^{w}\boldsymbol{r}_{c}') \end{aligned} \tag{3.47}$$

Dimensionless description

To identify the constituent mechanisms of the VBI on the mechanical system of the bridge, this section formulates the EOMs of the vehicle and bridge subsystems in dimensionless terms, as proposed by the authors [6]. As the interest is mainly on the bridge subsystem, the dimensionless equations are expressed with reference to the length $\boldsymbol{L}$, eigenfrequency $\boldsymbol{\omega}^{b}$ and generalized mass $\boldsymbol{gm}^{b}$ of the first mode of the bridge.

The dimensionless contact force is:

$$\begin{aligned}\tilde{\boldsymbol{\lambda}} = &\frac{\mathbf{1}}{\boldsymbol{g m^b \omega^b}}\boldsymbol{G^{-1}}(\boldsymbol{m^w})^{-1}\Big(\boldsymbol{c^{w,u}\dot{\tilde{u}}^u} + \boldsymbol{c^w}\big(\boldsymbol{W^b}\big)^{\boldsymbol{T}}\boldsymbol{\dot{\tilde{u}}^b} + \boldsymbol{S_v c^w}\big(\boldsymbol{W^b}\big)^{\boldsymbol{'T}}\boldsymbol{\tilde{u}^b}\\ &+ \boldsymbol{S_v c^w R_c}^{\boldsymbol{'}}\Big)\\ +&\frac{\mathbf{1}}{\boldsymbol{g m^b (\omega^b)^2}}\boldsymbol{G^{-1}}(\boldsymbol{m^w})^{-1}\Big(\boldsymbol{k^{w,u}\tilde{u}^u} + \boldsymbol{k^w}\big(\boldsymbol{W^b}\big)^{\boldsymbol{T}}\boldsymbol{\tilde{u}^b} + \boldsymbol{k^w R_c}\Big)\\ +&\frac{\mathbf{1}}{\boldsymbol{g m^b \omega^b}}\boldsymbol{G^{-1}}\big(\boldsymbol{W^b}\big)^{\boldsymbol{T}}\big(\boldsymbol{m^b}\big)^{-1}\Big(\frac{\mathbf{1}}{\boldsymbol{(\omega^b)^2 L}}\boldsymbol{\tilde{F}^b} - \boldsymbol{c^b\dot{\tilde{u}}^b} - \frac{\mathbf{1}}{\boldsymbol{\omega^b}}\boldsymbol{k^b\tilde{u}^b}\Big)\\ &+\frac{\mathbf{1}}{\boldsymbol{g m^b}}\ \boldsymbol{G^{-1}}\Big(\boldsymbol{2S_v}\big(\boldsymbol{W^b}\big)^{\boldsymbol{'T}}\boldsymbol{\dot{\tilde{u}}^b} + \boldsymbol{S_v}^{\boldsymbol{2}}\big(\boldsymbol{W^b}\big)^{\boldsymbol{''T}}\boldsymbol{\tilde{u}^b} + \boldsymbol{S_v}^{\boldsymbol{2}}\boldsymbol{R_c}^{\boldsymbol{''}}\Big)\end{aligned} \tag{3.48}$$

Consisting of the dimensionless contact forces $\tilde{\boldsymbol{\lambda}}_{\boldsymbol{i}} = \frac{\boldsymbol{\lambda_i}}{\boldsymbol{g m^b (\omega^b)^2 L}}$ at each point i

$\tilde{\boldsymbol{u}}^{\boldsymbol{b}} = \frac{\mathbf{1}}{\boldsymbol{L}}\boldsymbol{u^b}$, $\tilde{\boldsymbol{u}}^{\boldsymbol{u}} = \frac{\mathbf{1}}{\boldsymbol{L}}\boldsymbol{u^u}$ are the (dimensionless) displacement vectors of the bridge and of the vehicle's upper part, respectively, both scaled with respect to the bridge length ***L*** (Table 3-1).

Assume $\boldsymbol{k_p^v}$ is the stiffness and $\boldsymbol{c_p^v}$ is the damping of the primary suspension system of the generic vehicle. Introducing the contact matrix $\boldsymbol{W^*}$, of the upper and wheels part of the system, the coupling $\boldsymbol{k^{u,w}}$ and $\boldsymbol{c^{u,w}}$ submatrices can be written as:

$$\boldsymbol{k^{u,w}} = \boldsymbol{k_p^v W^*} \text{ and } \boldsymbol{c^{u,w}} = \boldsymbol{c_p^v W^*} \tag{3.49}$$

Where $\boldsymbol{W^*}$ matrix varies according to the vehicle model. See sections (4.2) and (4.3) for quarter car model and 10-Dof vehicle.

Substituting the matrices $\boldsymbol{m^w}$, $\boldsymbol{k^w}$, $\boldsymbol{c^w}$ and $\boldsymbol{k^{u,w}}$, $\boldsymbol{c^{u,w}}$ the dimensionless contact force becomes:

$$\begin{aligned}\tilde{\boldsymbol{\lambda}} = &\frac{\boldsymbol{C}}{\boldsymbol{m^w}}\boldsymbol{G^{-1}}\Big(\boldsymbol{W^*\tilde{u}^u} + \big(\boldsymbol{W^b}\big)^{\boldsymbol{T}}\boldsymbol{\dot{\tilde{u}}^b} + \boldsymbol{S_v}\big(\boldsymbol{W^b}\big)^{\boldsymbol{'T}}\boldsymbol{\tilde{u}^b} + \boldsymbol{S_v R_c'}\Big)\\ &+\frac{\boldsymbol{K}}{\boldsymbol{m^w}}\boldsymbol{G^{-1}}\Big(\boldsymbol{W^*\tilde{u}^u} + \big(\boldsymbol{W^b}\big)^{\boldsymbol{T}}\boldsymbol{\tilde{u}^b} + \boldsymbol{R_c}\Big)\\ &+\frac{\mathbf{1}}{\boldsymbol{g m^b \omega^b}}\boldsymbol{G^{-1}}\big(\boldsymbol{W^b}\big)^{\boldsymbol{T}}\big(\boldsymbol{m^b}\big)^{-1}\Big(\frac{\mathbf{1}}{\boldsymbol{\omega^b L}}\boldsymbol{\tilde{F}^b} - \boldsymbol{c^b\dot{\tilde{u}}^b} - \frac{\mathbf{1}}{\boldsymbol{\omega^b}}\boldsymbol{k^b\tilde{u}^b}\Big)\\ &+\frac{\mathbf{1}}{\boldsymbol{g m^b}}\boldsymbol{G^{-1}}\Big(\boldsymbol{2S_v}\big(\boldsymbol{W^b}\big)^{\boldsymbol{'T}}\boldsymbol{\dot{\tilde{u}}^b} + \boldsymbol{S_v^2}\big(\boldsymbol{W^b}\big)^{\boldsymbol{''T}}\boldsymbol{\tilde{u}^b} + \boldsymbol{S_v^2 R_c'}\Big)\end{aligned} \tag{3.50}$$

As shown on Table (3-1), ***C*** is the impedance ratio of the primary suspension system of the vehicle, where $\boldsymbol{g m^b \omega^b}$ is the bridge's mechanical impedance, denoting the resistance of the bridge to vibrations because of its mass. ***K*** represents the stiffness ratio of the primary suspension system of the vehicle with respect to the stiffness of the fundamental mode of the bridge. It can be noticed from eq (3.50) that the contact force depends solely on the primary suspension system of the vehicle, connecting the bogies and the wheels, and includes the response of the bridge and of the vehicle's upper part $\boldsymbol{u^u}$ (but not the response of the wheels part $\boldsymbol{u^w}$).

Table 3-1 Dimensionless groups of the coupled vehicle-bridge system

group	description	group	description
$\tilde{u}^u = \frac{1}{L}u^u$	Dimensionless vehicle displacement vector	$M = \frac{m^V}{gm^b}$	Mass ratio
$\tilde{u}^b = \frac{1}{L}u^b$	Dimensionless bridge displacement vector	$K = \frac{k_p^V}{gm^b(\omega^b)^2}$	Stiffness ratio
$M^b = \frac{1}{gm^b}m^b$	Scaled bridge mass matrix	$C = \frac{C_p^V}{gm^b\omega^b}$	Impedance ratio
$C^b = \frac{1}{gm^b\omega^B}c^b$	Scaled bridge damping matrix	$\Omega = \frac{\omega^P}{\omega^b}$	Eigenfrequency ratio
$K^b = \frac{1}{gm^b(\omega^b)^{\mathbf{2}}}k^b$	Scaled bridge stiffness matrix	$\zeta^P = \frac{C_p^V}{2m^V\omega^P}$	Damping ratio of vehicle's primary suspension system
$\tilde{F}^b = \frac{1}{gm^b(\omega^b)^{\mathbf{2}}}F^b$	Scaled bridge force vector	$M^W = \frac{m^W}{gm^b}$	Mass ratio of vehicle wheels
$R_c = \frac{1}{L}r_c$	Scaled irregularities vector	$\tau = m^B t$	Dimensionless time
$R_c{}' = r_c{}'$	Scaled slope of irregularities vector	$S_V = \frac{V}{\omega^b L}$	Speed parameter
$\boldsymbol{R_c}'' = \boldsymbol{Lr_c}''$	Scaled curvature of irregularities vector		

Accordingly, the dimensionless EOM of the bridge becomes:

$$\begin{aligned} \boldsymbol{M^b}\ddot{\widetilde{\boldsymbol{u}}}^{\boldsymbol{b}} + \Big(\boldsymbol{C^b} + \boldsymbol{C}\boldsymbol{W}^{\boldsymbol{w}}_{\boldsymbol{eff}} + \boldsymbol{2S_v}\boldsymbol{W}^{\boldsymbol{b'}}_{\boldsymbol{eff}} - \frac{\boldsymbol{1}}{\boldsymbol{\omega^b}}\boldsymbol{W}^{\boldsymbol{b}}_{\boldsymbol{eff}}\big(\boldsymbol{m^b}\big)^{-\boldsymbol{1}}\boldsymbol{c^b}\Big)\dot{\widetilde{\boldsymbol{u}}}^{\boldsymbol{b}} \\ + \Big(\boldsymbol{K^b} + \boldsymbol{C}\boldsymbol{S_v}\boldsymbol{W}^{\boldsymbol{w'}}_{\boldsymbol{eff}} + \boldsymbol{K}\boldsymbol{W}^{\boldsymbol{w}}_{\boldsymbol{eff}} + \boldsymbol{S_v^2}\boldsymbol{W}^{\boldsymbol{b''}}_{\boldsymbol{eff}} \\ - \frac{\boldsymbol{1}}{(\hat{\boldsymbol{\omega}}\boldsymbol{\omega^b})^{\boldsymbol{2}}}\boldsymbol{W}^{\boldsymbol{b}}_{\boldsymbol{eff}}\big(\boldsymbol{m^b}\big)^{-\boldsymbol{1}}\boldsymbol{k^b}\Big)\widetilde{\boldsymbol{u}}^{\boldsymbol{b}} \\ = \widetilde{\boldsymbol{F}}^{\boldsymbol{b}} - \boldsymbol{W^b}\boldsymbol{G^{-1}}\left(\frac{\boldsymbol{K}}{\boldsymbol{m^w}}\boldsymbol{R_c} + \frac{\boldsymbol{CS_v}}{\boldsymbol{m^w}}\boldsymbol{R_c'} + \frac{\boldsymbol{S_v^2}}{\boldsymbol{m^b}}\boldsymbol{R_c''}\right) \\ - \frac{\boldsymbol{1}}{(\hat{\boldsymbol{\omega}}\boldsymbol{\omega^b})^{\boldsymbol{2}}}\boldsymbol{W}^{\boldsymbol{b}}_{\boldsymbol{eff}}\big(\boldsymbol{m^b}\big)^{-\boldsymbol{1}}\boldsymbol{F^b} - \boldsymbol{W}^{\boldsymbol{w*}}_{\boldsymbol{eff}}\big(\boldsymbol{K}\widetilde{\boldsymbol{u}}^{\boldsymbol{u}} + \boldsymbol{C}\dot{\widetilde{\boldsymbol{u}}}^{\boldsymbol{u}}\big) \end{aligned} \tag{3.51}$$

Where $\boldsymbol{M^b}$, $\boldsymbol{C^b}$ and $\boldsymbol{K^b}$ are the dimensionless (scaled) mass, damping and stiffness matrices of the bridge, and $\boldsymbol{F^b}$ is the dimensionless force vector acting on the bridge due to the vehicle's self-weight. For brevity reasons, the following dimensionless matrices are introduced:

$$\begin{aligned} \boldsymbol{W}^{\boldsymbol{b}}_{\boldsymbol{eff}} &= \frac{\boldsymbol{1}}{\boldsymbol{gm^b}}\boldsymbol{W^b}\boldsymbol{G^{-1}}\big(\boldsymbol{W^b}\big)^{\boldsymbol{T}} \\ \boldsymbol{W}^{\boldsymbol{b'}}_{\boldsymbol{eff}} &= \frac{\boldsymbol{1}}{\boldsymbol{gm^b}}\boldsymbol{W^b}\boldsymbol{G^{-1}}\boldsymbol{L}\big(\boldsymbol{W^b}\big)^{\boldsymbol{'T}} \\ \boldsymbol{W}^{\boldsymbol{b''}}_{\boldsymbol{eff}} &= \frac{\boldsymbol{1}}{\boldsymbol{gm^b}}\boldsymbol{W^b}\boldsymbol{G^{-1}}\boldsymbol{L^2}\big(\boldsymbol{W^b}\big)^{\boldsymbol{''T}} \\ \boldsymbol{W}^{\boldsymbol{w}}_{\boldsymbol{eff}} &= \frac{\boldsymbol{1}}{\boldsymbol{m^w}}\boldsymbol{W^b}\boldsymbol{G^{-1}}\big(\boldsymbol{W^b}\big)^{\boldsymbol{T}} \\ \boldsymbol{W}^{\boldsymbol{w'}}_{\boldsymbol{eff}} &= \frac{\boldsymbol{1}}{\boldsymbol{m^w}}\boldsymbol{W^b}\boldsymbol{G^{-1}}\boldsymbol{L}\big(\boldsymbol{W^b}\big)^{\boldsymbol{'T}} \\ \boldsymbol{W}^{\boldsymbol{w*}}_{\boldsymbol{eff}} &= \frac{\boldsymbol{1}}{\boldsymbol{m^w}}\boldsymbol{W^b}\boldsymbol{G^{-1}}\boldsymbol{W^*} \end{aligned} \tag{3.52}$$

The dimensionless EOM of the vehicle's upper part is:

$$\begin{aligned} \frac{\boldsymbol{1}}{\boldsymbol{gm^b}}\boldsymbol{m^u}\ddot{\widetilde{\boldsymbol{u}}}^{\boldsymbol{u}} + \frac{\boldsymbol{1}}{\boldsymbol{gm^b\omega^b}}\boldsymbol{c^u}\dot{\widetilde{\boldsymbol{u}}}^{\boldsymbol{u}} + \frac{\boldsymbol{1}}{\boldsymbol{gm^b}(\boldsymbol{\omega^b})^{\boldsymbol{2}}}\boldsymbol{k^u}\widetilde{\boldsymbol{u}}^{\boldsymbol{u}} \\ = -\boldsymbol{C}(\boldsymbol{W^*})^{\boldsymbol{T}}\left(\big(\boldsymbol{W^b}\big)^{\boldsymbol{T}}\dot{\widetilde{\boldsymbol{u}}}^{\boldsymbol{b}} + \boldsymbol{S_v}\big(\boldsymbol{W^b}\big)^{\boldsymbol{'T}}\widetilde{\boldsymbol{u}}^{\boldsymbol{b}} + \boldsymbol{S_v}\boldsymbol{R_c'}\right) \\ - \boldsymbol{K}(\boldsymbol{W^*})^{\boldsymbol{T}}\left(\big(\boldsymbol{W^b}\big)^{\boldsymbol{T}}\widetilde{\boldsymbol{u}}^{\boldsymbol{b}} + \boldsymbol{R_c}\right) \end{aligned} \tag{3.53}$$

The EOM of the bridge can be written as:

$$\boldsymbol{M^b}\ddot{\widetilde{\boldsymbol{u}}}^{\boldsymbol{b}} + \Big(\boldsymbol{C^b} + \boldsymbol{C_I}(\boldsymbol{x}, \boldsymbol{S_v})\Big)\dot{\widetilde{\boldsymbol{u}}}^{\boldsymbol{b}} + \Big(\boldsymbol{K^b} + \boldsymbol{K_I}(\boldsymbol{x}, \boldsymbol{S_v})\Big)\widetilde{\boldsymbol{u}}^{\boldsymbol{b}} = \boldsymbol{F^b} + \boldsymbol{F_I}\big(\widetilde{\boldsymbol{u}}^{\boldsymbol{u}}, \dot{\widetilde{\boldsymbol{u}}}^{\boldsymbol{u}}\big) \tag{3.54}$$

Eq (3.54) shows that the effect of VBI on the bridge can be expressed via three terms: an additional damping matrix term $\boldsymbol{C_I(x, S_v)}$, an additional stiffness matrix term $\boldsymbol{K_I(x, S_v)}$ and an additional loading vector term $\boldsymbol{F_I(\tilde{u}^u, \dot{\tilde{u}}^u)}$.

The additional terms are:

$$\begin{aligned}
\boldsymbol{C_I(x, S_v)} &= \boldsymbol{CW_{eff}^{w} + 2S_v W_{eff}^{b'} - \frac{1}{\omega^b} W_{eff}^{b} (m^b)^{-1} c^b} \\
\boldsymbol{K_I(x, S_v)} &= \boldsymbol{CS_v W_{eff}^{w'} + KW_{eff}^{w} + S_v^2 W_{eff}^{b''} - \frac{1}{(\dot{\omega}^b)^2} W_{eff}^{b} (m^b)^{-1} k^b} \\
\boldsymbol{F_I(\tilde{u}^u, \dot{\tilde{u}}^u)} &= \boldsymbol{-W^b G^{-1} \left(\frac{K}{m^w} R_c + \frac{CS_v}{m^w} R_c' + \frac{S_v^2}{m^b} R_c'' \right)} \\
&\quad \boldsymbol{- \frac{1}{(\dot{\omega}^b)^2} W_{eff}^{b} (m^b)^{-1} f^b - W_{eff}^{w*} (K\tilde{u}^u + C\dot{\tilde{u}}^u)}
\end{aligned} \tag{3.55}$$

The additional damping term corresponds to a time-varying additional damping matrix, mainly dependent on the impedance ratio C of the primary suspension system of the suspension's system of the vehicle. The additional stiffness term is also time-varying, as it depends on the location of the vehicle on the bridge. Lastly, the additional loading vector includes additional forces acting on the bridge due to irregularities, as well as due to the response of the traversing vehicle. Note that the vehicle response appears solely in the additional loading vector**.**

Decoupling methodology

The formulation of eq (3.54) is exact and informative regarding the constituent mechanisms of the VBI on the mechanical system of the bridge. However, it still involves the fully coupled system. The present section, as presented by the researchers in [6], examines further the MDOF vehicle-MDOF bridge system and estimates the response of the bridge as an asymptotic expansion about a small dimensionless parameter $\boldsymbol{\varepsilon}$ (corresponding to a vehicle to bridge frequency ratio Ω). This allows to determine the relative importance of the constituent VBI mechanisms and decouple the vehicle-bridge system by eliminating the vehicle response from the EOM of the bridge.

Asymptotic expansion of the coupled EOMs

Consider a frequency $\boldsymbol{\omega^p}$, corresponding to the vehicle's primary suspension system, defined as:

$$\boldsymbol{\omega^p = \sqrt{\frac{k_p^v}{m^v}} \rightarrow k_p^v = m^v (\omega^p)^2} \tag{3.56}$$

Where $\boldsymbol{m^v}$ is the vehicle's total mass and $\boldsymbol{k_p^v}$ is the stiffness of the primary suspension system. Accordingly, the damping of the primary suspension system is:

$$\boldsymbol{c_p^v = 2m^v \omega^p \zeta^p \rightarrow \zeta^p = \frac{c_p^v}{2m^v \omega^p}} \tag{3.57}$$

Where $\boldsymbol{\zeta^p}$ is the corresponding damping ratio of the primary suspension system of the vehicle. Note that $\boldsymbol{\omega^p}$ does not necessarily correspond to any of the natural frequencies of the vehicle. Let $\boldsymbol{M = m^v/gm^b}$ denote the vehicle to bridge mass ratio and $\boldsymbol{\Omega = \omega^p/\omega^b}$ the eigenfrequency ratio. With the aid of $\boldsymbol{\zeta^p}$, $\boldsymbol{M}$ and $\boldsymbol{\Omega}$, and considering that $\boldsymbol{C = 2M\Omega\zeta^p}$ and $\boldsymbol{K = M\Omega^2}$, the EOM of the bridge becomes:

$$\begin{aligned} \boldsymbol{M^b\ddot{\tilde{u}}^b} &+ \left(\boldsymbol{C^b + 2M\Omega\zeta^p W^w_{eff} + 2S_v W^{b'}_{eff} - \frac{1}{\omega^b} W^b_{eff}\left(m^b\right)^{-1} c^b}\right)\boldsymbol{\dot{\tilde{u}}^b} \\ &+ \left(\boldsymbol{K^b + 2M\Omega\zeta^p S_v W^{w'}_{eff} + M\Omega^2 W^w_{eff} + S_v^2 W^{b''}_{eff}}\right. \\ &\left.\boldsymbol{- \frac{1}{(\omega^b)^2} W^b_{eff}\left(m^b\right)^{-1} k^b}\right)\boldsymbol{\tilde{u}^b} \\ &= \boldsymbol{\tilde{F}^b - W^b G^{-1}\left(\frac{M\Omega^2}{m^w} R_c + \frac{2M\Omega\zeta^p S_v}{m^w} R'_c + \frac{S_v^2}{m^b} R''_c\right)} \\ &\boldsymbol{- \frac{1}{(\omega^b)^2} W^b_{eff}\left(m^b\right)^{-1} F^b - W^{w*}_{eff}\left(M\Omega^2\tilde{u}^u + 2M\Omega\zeta^p\dot{\tilde{u}}^u\right)} \end{aligned} \tag{3.58}$$

Accordingly, the EOM of the vehicle's upper part is:

$$\begin{aligned} \boldsymbol{\frac{1}{gm^b} m^u\ddot{\tilde{u}}^u + \frac{1}{m^b\omega^b} c^u\dot{\tilde{u}}^u + \frac{1}{m^b(\omega^b)^2} k^u\tilde{u}^u} \\ \boldsymbol{= -2M\Omega\zeta^p (W^*)^T\left(W^b\right)^T\dot{\tilde{u}}^b} \\ \boldsymbol{- M\Omega(W^*)^T\left(\left(W^b\right)'^T\tilde{u}^b + R'_c\right)[2\zeta^p S_v + \Omega]} \end{aligned} \tag{3.59}$$

In practice, the frequency ratio $\boldsymbol{\Omega}$ of the vehicle's primary suspension system with respect to the fundamental frequency of the bridge obtains small values. That converts the original VBI problem into a perturbation problem with small parameter $\boldsymbol{\varepsilon=\Omega}$. For $\boldsymbol{0 < \varepsilon \ll 1}$, assume that the bridge response from eq (3.58) has an asymptotic expansion of the form:

$$\begin{aligned} \boldsymbol{\tilde{u}^b} &= \boldsymbol{\tilde{u}^b_0 + \varepsilon\tilde{u}^b_1 + \varepsilon^2\tilde{u}^b_2 + O(\varepsilon^3)} \\ \boldsymbol{\dot{\tilde{u}}^b} &= \boldsymbol{\dot{\tilde{u}}^b_0 + \varepsilon\dot{\tilde{u}}^b_1 + \varepsilon^2\dot{\tilde{u}}^b_2 + O(\varepsilon^3)} \\ \boldsymbol{\ddot{\tilde{u}}^b} &= \boldsymbol{\ddot{\tilde{u}}^b_0 + \varepsilon\ddot{\tilde{u}}^b_1 + \varepsilon^2\ddot{\tilde{u}}^b_2 + O(\varepsilon^3)} \end{aligned} \tag{3.60}$$

Substituting eq (3.60) into the bridge's EOM and keeping only the zero-order terms in $\boldsymbol{\varepsilon}$, the zero-order EOM of the bridge is:

$$\begin{aligned} \boldsymbol{M^b\ddot{\tilde{u}}^b_0} &+ \left(\boldsymbol{C^b + 2S_v W^{b'}_{eff} - \frac{1}{\omega^b} W^b_{eff}\left(m^b\right)^{-1} c^b}\right)\boldsymbol{\dot{\tilde{u}}^b_0} \\ &+ \left(\boldsymbol{K^b + S_v^2 W^{b''}_{eff} - \frac{1}{(\omega^b)^2} W^b_{eff}\left(m^b\right)^{-1} k^b}\right)\boldsymbol{\tilde{u}^b_0} \\ &= \boldsymbol{\tilde{F}^b - W^b G^{-1}\left(\frac{S_v^2}{m^b} R''_c\right) - \frac{1}{(\omega^b)^2} W^b_{eff}\left(m^b\right)^{-1} F^b} \end{aligned} \tag{3.61}$$

Which includes the external forces acting on the bridge due to the vehicle's self-weight $\boldsymbol{F^b}$, neglecting though other dynamic characteristics of the vehicle, such us the stiffness and impedance ratios and the vehicle's response. In conclusion, the only vehicle parameters that affect the zero-order response of the bridge are the vehicle's mass and moving speed. Likewise, the zero-order response of the vehicle's upper part is:

$$\frac{\mathbf{1}}{\boldsymbol{gm^b}}\boldsymbol{m^u}\ddot{\tilde{\boldsymbol{u}}}_{\mathbf{0}}^{\boldsymbol{u}}+\frac{\mathbf{1}}{\boldsymbol{m^b\omega^b}}\boldsymbol{c^u}\dot{\tilde{\boldsymbol{u}}}_{\mathbf{0}}^{\boldsymbol{u}}+\frac{\mathbf{1}}{\boldsymbol{m^b(\omega^b)^2}}\boldsymbol{k^u}\tilde{\boldsymbol{u}}_{\mathbf{0}}^{\boldsymbol{u}}=\mathbf{0} \tag{3.62}$$

For small mass of the wheels $\boldsymbol{m^w}$ with respect to the generalized mass of the bridge $\boldsymbol{gm^b}$ $\left(\boldsymbol{M^w}=\boldsymbol{m^w/gm^b}\ll\mathbf{1}\right)$, the dimensionless mass participating in the contact $\left(\mathbf{1}/\boldsymbol{gm^b}\right)\boldsymbol{G^{-1}}$ converges to the dimensionless mass of the wheels, therefore:

$$\frac{\mathbf{1}}{\boldsymbol{gm^b}}\boldsymbol{G^{-1}}=\frac{\mathbf{1}}{\boldsymbol{gm^b}}\left((\boldsymbol{m^w})^{-\mathbf{1}}+\left(\boldsymbol{W^b}\right)^{\boldsymbol{T}}\left(\boldsymbol{m^b}\right)^{-\mathbf{1}}\boldsymbol{W^b}\right)^{-\mathbf{1}}\approx\boldsymbol{M^wE} \tag{3.63}$$

Where E is the identity matrix. Subsequently, the EOM of the bridge reduces to:

$$\boldsymbol{M^b}\ddot{\tilde{\boldsymbol{u}}}_{\mathbf{0}}^{\boldsymbol{b}}+\boldsymbol{C^b}\dot{\tilde{\boldsymbol{u}}}_{\mathbf{0}}^{\boldsymbol{b}}+\boldsymbol{K^b}\tilde{\boldsymbol{u}}_{\mathbf{0}}^{\boldsymbol{b}}=\boldsymbol{F^b} \tag{3.64}$$

Which solely depends on $\boldsymbol{F^b}$, as the terms associated with the dimensionless contact mass $\left(\mathbf{1}/\boldsymbol{gm^b}\right)\boldsymbol{G^{-1}}$ vanish from eq (3.61). This expression corresponds to the well-known moving load method [1]. So, eq (3.64) shows that the moving load method is a zero-order approximation of the bridge response (for small stiffness and impedance C ratios of the primary suspension system of the vehicle), under the additional assumption of small, normalized mass of the wheels with respect to the bridge's generalized mass ($\boldsymbol{M^w}=\boldsymbol{m^w/gm^b}\ll\mathbf{1}$) . In other words, the moving load method is valid under assumptions, which often are not satisfied.

The first order in $\boldsymbol{\varepsilon}$ bridge's EOM is:

$$\begin{aligned}\boldsymbol{M^b}\ddot{\tilde{\boldsymbol{u}}}_{\mathbf{1}}^{\boldsymbol{b}}+\left(\boldsymbol{C^b}+\mathbf{2}\boldsymbol{S_v}\boldsymbol{W_{eff}^{b'}}-\frac{\mathbf{1}}{\boldsymbol{\omega^b}}\boldsymbol{W_{eff}^b}\left(\boldsymbol{m^b}\right)^{-\mathbf{1}}\boldsymbol{c^b}\right)\dot{\tilde{\boldsymbol{u}}}_{\mathbf{1}}^{\boldsymbol{b}}\\+\left(\boldsymbol{K^b}+\boldsymbol{S_v^2}\boldsymbol{W_{eff}^{b''}}-\frac{\mathbf{1}}{(\check{}\boldsymbol{\omega^b})^2}\boldsymbol{W_{eff}^b}\left(\boldsymbol{m^b}\right)^{-\mathbf{1}}\boldsymbol{k^b}\right)\tilde{\boldsymbol{u}}_{\mathbf{1}}^{\boldsymbol{b}}\\=-\mathbf{2}\boldsymbol{M\zeta^p}\left(\boldsymbol{W_{eff}^{w*}}\dot{\tilde{\boldsymbol{u}}}_{\mathbf{0}}^{\boldsymbol{b}}+\boldsymbol{S_v}\boldsymbol{W_{eff}^{w'}}\tilde{\boldsymbol{u}}_{\mathbf{0}}^{\boldsymbol{b}}+\boldsymbol{W_{eff}^{w*}}\dot{\tilde{\boldsymbol{u}}}_{\mathbf{0}}^{\boldsymbol{u}}\right.\\\left.+\boldsymbol{W^bG^{-1}}\frac{\boldsymbol{S_v}}{\boldsymbol{m^w}}\boldsymbol{R_c'}\right)\end{aligned} \tag{3.65}$$

The vehicle's upper part first-order response is:

$$\frac{\mathbf{1}}{\boldsymbol{gm^b}}\boldsymbol{m^u}\ddot{\tilde{\boldsymbol{u}}}_{\mathbf{1}}^{\boldsymbol{u}}+\frac{\mathbf{1}}{\boldsymbol{m^b\omega^b}}\boldsymbol{c^u}\dot{\tilde{\boldsymbol{u}}}_{\mathbf{1}}^{\boldsymbol{u}}+\frac{\mathbf{1}}{\boldsymbol{m^b(\omega^b)^2}}\boldsymbol{k^u}\tilde{\boldsymbol{u}}_{\mathbf{1}}^{\boldsymbol{u}} = -\mathbf{2}\boldsymbol{M\zeta^p}(\boldsymbol{W^*})^{\boldsymbol{T}}\left(\left(\boldsymbol{W^b}\right)^{\boldsymbol{T}}\dot{\tilde{\boldsymbol{u}}}_{\mathbf{0}}^{\boldsymbol{b}}-\boldsymbol{S_v}\left(\boldsymbol{W^b}\right)'^{\boldsymbol{T}}\tilde{\boldsymbol{u}}_{\mathbf{0}}^{\boldsymbol{b}}+\boldsymbol{S_vR_c'}\right) \tag{3.66}$$

Lastly, the second order in $\boldsymbol{\varepsilon}$ response of the bridge is:

$$\begin{aligned}\boldsymbol{M^b}\ddot{\tilde{\boldsymbol{u}}}_{\mathbf{2}}^{\boldsymbol{b}}+\left(\boldsymbol{C^b}+\mathbf{2}\boldsymbol{S_v}\boldsymbol{W_{eff}^{b'}}-\frac{\mathbf{1}}{\boldsymbol{\omega^b}}\boldsymbol{W_{eff}^b}\left(\boldsymbol{m^b}\right)^{-\mathbf{1}}\boldsymbol{c^b}\right)\dot{\tilde{\boldsymbol{u}}}_{\mathbf{2}}^{\boldsymbol{b}}\\ +\left(\boldsymbol{K^b}+\boldsymbol{S_v^2}\boldsymbol{W_{eff}^{b''}}-\frac{\mathbf{1}}{(\ddot{\boldsymbol{\omega}}\boldsymbol{\omega^b})^{\mathbf{2}}}\boldsymbol{W_{eff}^b}\left(\boldsymbol{m^b}\right)^{-\mathbf{1}}\boldsymbol{k^b}\right)\tilde{\boldsymbol{u}}_{\mathbf{2}}^{\boldsymbol{b}}\\ =\mathbf{2}\boldsymbol{M\zeta^p}\left(\boldsymbol{W_{eff}^{w*}}\dot{\tilde{\boldsymbol{u}}}_{\mathbf{1}}^{\boldsymbol{b}}+\boldsymbol{S_v}\boldsymbol{W_{eff}^{w'}}\tilde{\boldsymbol{u}}_{\mathbf{1}}^{\boldsymbol{b}}+\boldsymbol{W_{eff}^{w*}}\dot{\tilde{\boldsymbol{u}}}_{\mathbf{1}}^{\boldsymbol{u}}\right)\\ -\boldsymbol{M}\left(\boldsymbol{W_{eff}^{w}}\tilde{\boldsymbol{u}}_{\mathbf{0}}^{\boldsymbol{b}}+\frac{\mathbf{1}}{\boldsymbol{m^w}}\boldsymbol{W^bG^{-1}R_c}\right)\end{aligned} \tag{3.67}$$

To demonstrate the effect of different orders of $\boldsymbol{\varepsilon}$ on bridge response, the authors of [5] have examined the response of a Skidtrask bridge traversed by a one-vehicle Pioneer passenger train (Figure 3-1). By doing so they concluded that smaller orders of the bridge response have a higher effect on the total response of the bridge and that the first two orders $\left(\tilde{\boldsymbol{u}}_{\mathbf{0}}^{\boldsymbol{b}}+\boldsymbol{\varepsilon}\tilde{\boldsymbol{u}}_{\mathbf{1}}^{\boldsymbol{b}}\right)$ of the bridge response provide a very good approximation of the solution.

3.3.4 Extended Modified Bridge System (EMBS) method

As mentioned above, the asymptotic expansion analysis about the small dimensionless parameter **ε=Ω** reveals the terms that should be included in the EOM of the bridge. As shown in the Figure (3-1) at least all terms up to first order in $\boldsymbol{\varepsilon}$ should be considered. This allows to eliminate the vehicle response from the EOM of the bridge. Based on the expressions of the zero and first order response of the bridge and neglecting higher order terms with minor influence on the bridge response, the writers [6] proposed a decoupled MDOF EOM for the bridge system. The proposed formula depends on the self-weight of the vehicle (acting on the bridge) $\boldsymbol{F^b}$, the impedance ratio of the vehicle's primary suspension system $\boldsymbol{C}$, the normalized mass of the wheels $\boldsymbol{M_w}$ and the speed parameter $\boldsymbol{S_v}$, neglecting terms associated with the stiffness ratio $\boldsymbol{K}$ and vehicle's response.

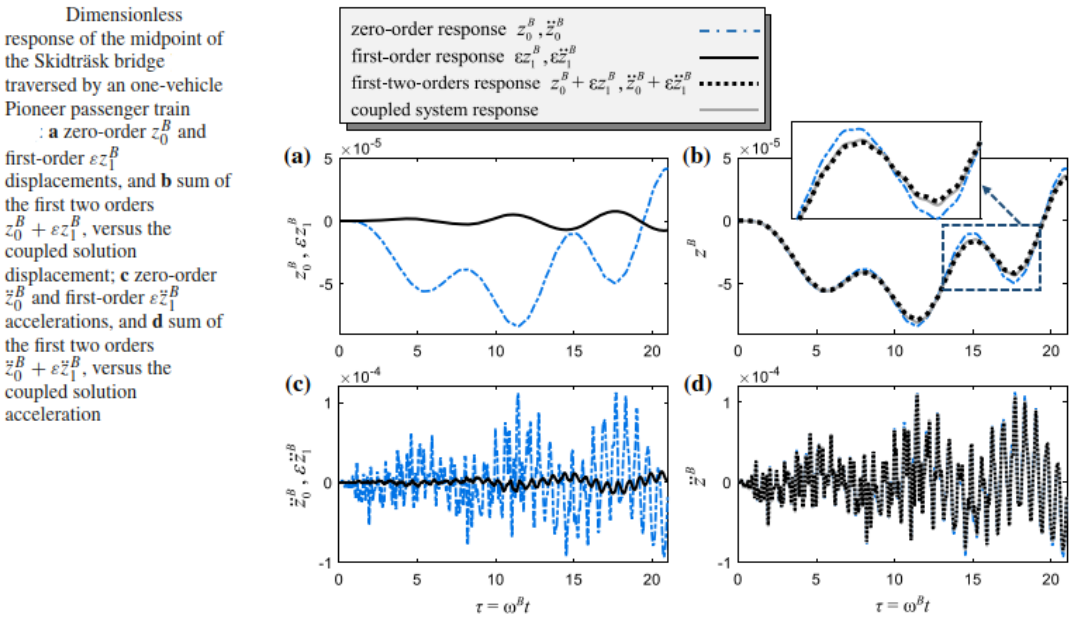

Dimensionless response of the midpoint of the Skidträsk bridge traversed by an one-vehicle Pioneer passenger train : **a** zero-order z_0^B and first-order εz_1^B displacements, and **b** sum of the first two orders $z_0^B + \varepsilon z_1^B$, versus the coupled solution displacement; **c** zero-order $\ddot{z}_0^B$ and first-order $\varepsilon \ddot{z}_1^B$ accelerations, and **d** sum of the first two orders $\ddot{z}_0^B + \varepsilon \ddot{z}_1^B$, versus the coupled solution acceleration

Figure 3-1 Validation of the proposed method [6]

The EOM of the bridge with the EMBS method becomes:

$$\boldsymbol{M^b\ddot{u}^b + \left(C^b + C_{EMBS}\right)\dot{u}^b + \left(K^b + K_{EMBS}\right)u^b = F^b + F_{EMBS}} \tag{3.68}$$

Where,

$$\begin{aligned}
&\boldsymbol{C_{EMBS} = CW_{eff}^{w} + 2S_v W_{eff}^{b'} - \frac{1}{\breve{\omega}^b} W_{eff}^{b}\left(m^b\right)^{-1} c^b} \text{ , additional damping matrix} \\
&\boldsymbol{K_{EMBS} = CS_v W_{eff}^{w'} + S_v^2 W_{eff}^{b''} - \frac{1}{\left(\breve{\omega}^b\right)^2} W_{eff}^{b}\left(m^b\right)^{-1} k^b} \text{ , additional stiffness matrix} \\
&\boldsymbol{F_{EMBS} = -\frac{1}{\left(\breve{\omega}^b\right)^2 L} W_{eff}^{b}\left(m^b\right)^{-1} F^b - W^b G^{-1}\left(\frac{CS_v}{m^w} R_c' + \frac{S_v^2}{g m^b} R_c''\right)} \text{ , additional load vector}
\end{aligned} \tag{3.69}$$

Time-integration

As in Lagrange method (section 3.2.5), in order to estimate the response of the vehicle-bridge system Newmark-β method is being used. According to (Appendix B):

$$\boldsymbol{\left[K_{eff}\right] = a_0[M] + a_1[C] + [K],} \tag{3.70}$$

$$\begin{aligned}
\boldsymbol{\left\{P_{eff}\right\}_{t+\Delta t}} = &\boldsymbol{\{P\}_{t+\Delta t} + [M]\left(a_0\{U\}_t + a_2\{\dot{U}\}_t + a_3\{\ddot{U}\}_t\right)} \\
&\boldsymbol{+ [C]\left(a_1\{U\}_t + a_4\{\dot{U}\}_t + a_5\{\ddot{U}\}_t\right)}
\end{aligned} \tag{3.71}$$

$$\{\boldsymbol{U}\}_{\boldsymbol{t+\Delta t}} = \left[\boldsymbol{K}_{\boldsymbol{eff}}\right]^{-1}\left\{\boldsymbol{P}_{\boldsymbol{eff}}\right\}_{\boldsymbol{t+\Delta t}} \tag{3.72}$$

Where according to eq (3.68),

$$[\boldsymbol{M}] = \boldsymbol{M}^{\boldsymbol{b}}, [\boldsymbol{C}] = \boldsymbol{C}^{\boldsymbol{b}} + \boldsymbol{C}_{\boldsymbol{EMBS}}, [\boldsymbol{K}] = \boldsymbol{K}^{\boldsymbol{b}} + \boldsymbol{K}_{\boldsymbol{EMBS}}, \{\boldsymbol{P}\} = \boldsymbol{F}^{\boldsymbol{b}} + \boldsymbol{F}_{\boldsymbol{EMBS}} \tag{3.73}$$

During the time-integration the time dependent above matrices (3.69) are formed as:

$$\begin{aligned}
\boldsymbol{C}_{\boldsymbol{EMBS}} &= \boldsymbol{C}\boldsymbol{W}_{\boldsymbol{eff}}^{\boldsymbol{w}\,(\boldsymbol{t+\Delta t})} + 2\boldsymbol{S}_{\boldsymbol{v}}\boldsymbol{W}_{\boldsymbol{eff}}^{\boldsymbol{b'}\,(\boldsymbol{t+\Delta t})} - \frac{\mathbf{1}}{\boldsymbol{\omega}^{\boldsymbol{b}}}\boldsymbol{W}_{\boldsymbol{eff}}^{\boldsymbol{b}\,(\boldsymbol{t+\Delta t})}\left(\boldsymbol{m}^{\boldsymbol{b}}\right)^{-1}\boldsymbol{c}^{\boldsymbol{b}} \\
\boldsymbol{K}_{\boldsymbol{EMBS}} &= \boldsymbol{C}\boldsymbol{S}_{\boldsymbol{v}}\boldsymbol{W}_{\boldsymbol{eff}}^{\boldsymbol{w'}\,(\boldsymbol{t+\Delta t})} + \boldsymbol{S}_{\boldsymbol{v}}^{\mathbf{2}}\boldsymbol{W}_{\boldsymbol{eff}}^{\boldsymbol{b''}\,(\boldsymbol{t+\Delta t})} - \frac{\mathbf{1}}{(\boldsymbol{\omega}^{\boldsymbol{b}})^{\mathbf{2}}}\boldsymbol{W}_{\boldsymbol{eff}}^{\boldsymbol{b}\,(\boldsymbol{t+\Delta t})}\left(\boldsymbol{m}^{\boldsymbol{b}}\right)^{-1}\boldsymbol{k}^{\boldsymbol{b}} \\
\boldsymbol{F}_{\boldsymbol{EMBS}} &= -\frac{\mathbf{1}}{(\boldsymbol{\omega}^{\boldsymbol{b}})^{\mathbf{2}}\boldsymbol{L}}\boldsymbol{W}_{\boldsymbol{eff}}^{\boldsymbol{b}\,(\boldsymbol{t+\Delta t})}\left(\boldsymbol{m}^{\boldsymbol{b}}\right)^{-1}\boldsymbol{F}^{\boldsymbol{b}\,(\boldsymbol{t+\Delta t})} \\
&\quad - \boldsymbol{W}^{\boldsymbol{b}\,(\boldsymbol{t+\Delta t})}\boldsymbol{G}^{-\mathbf{1}}\left(\frac{\boldsymbol{C}\boldsymbol{S}_{\boldsymbol{v}}}{\boldsymbol{m}^{\boldsymbol{w}}}\boldsymbol{R}_{\boldsymbol{c}}' + \frac{\boldsymbol{S}_{\boldsymbol{v}}^{\mathbf{2}}}{\boldsymbol{g}\boldsymbol{m}^{\boldsymbol{b}}}\boldsymbol{R}_{\boldsymbol{c}}''\right)
\end{aligned} \tag{3.74}$$

All the parameters from Eqs. (3.70)~(3.73) are now fully defined and the dynamic response of the system can be estimated using Newmark-β (Appendix B).

Chapter 4

4 Applications and MATLAB simulation

4.1 Introduction

The procedure of the simulation of the VBI system can be summarized as detailed bellow. Firstly, the vehicle model is introduced in MATLAB, constructing the matrices m_v, k_v, c_v and W^v in the form of eqs (3.1) and (3.54) for Lagrange and EMBS solving methods. Then the bridge model is designed in COMSOL Multiphysics software where the user can choose from a variety of structural elements (beams, trusses, etc.)[7] , define the geometry and the structural features and built the final structure model. Afterwards, the mass, stiffness, damping m_b, k_b, c_b matrices, along with several other information for the bridge subsystem, are exported from COMSOL to MATLAB. The VBI system is now fully defined and the time-integration of the simulation follows the Newmark-β method, leading to the dynamic response of the system.

4.2 Sprung mass model

This model represents an undamped quarter car model with 2 degrees of freedom including body mass bouncing and wheel/axle mass bouncing (Figure 4-1). The kinetic equilibrium function of the vehicle for all degrees of freedom, according to the Newton's 2nd law, is:

$Equation\ of\ motion\ for\ the\ wheel$:

$$\boldsymbol{m^w\ddot{u}_1 + c_v(\dot{u}_1 - \dot{u}_2) + k_v(u_1 - u_2) = F_v} \tag{4.1}$$

$Car\ body\ bounce\ motion$:

$$\boldsymbol{M^v\ddot{u}_2 + c_v(\dot{u}_2 - \dot{u}_1) + k_v(u_2 - u_1) = 0} \tag{4.2}$$

Corresponding to the general form (2.1) for the vehicle subsystem, Eqs. (4.1) and (4.2) become:

$$\begin{bmatrix} \boldsymbol{m^w} & \boldsymbol{0} \\ \boldsymbol{0} & \boldsymbol{M^v} \end{bmatrix} \begin{Bmatrix} \ddot{\boldsymbol{u}}_1 \\ \ddot{\boldsymbol{u}}_2 \end{Bmatrix} + \begin{bmatrix} \boldsymbol{c_v} & \boldsymbol{-c_v} \\ \boldsymbol{-c_v} & \boldsymbol{c_v} \end{bmatrix} \begin{Bmatrix} \dot{\boldsymbol{u}}_1 \\ \dot{\boldsymbol{u}}_2 \end{Bmatrix} + \begin{bmatrix} \boldsymbol{k_v} & \boldsymbol{-k_v} \\ \boldsymbol{-k_v} & \boldsymbol{k_v} \end{bmatrix} \begin{Bmatrix} \boldsymbol{u}_1 \\ \boldsymbol{u}_2 \end{Bmatrix} = \begin{Bmatrix} \boldsymbol{F_{self} - \lambda_1} \\ \boldsymbol{0} \end{Bmatrix} \tag{4.3}$$

where,

$\boldsymbol{F_v = F_{self} + \lambda_1}$,

$\boldsymbol{F_{self} = M_{self} g}$ is the force vector corresponding to self-weight of the vehicle

$\boldsymbol{M_{self} = (M^v + m^w)}$ is the self-weight of the sprung mass system

$\boldsymbol{g = 9.81} \left[\frac{\boldsymbol{m}}{\boldsymbol{s^2}}\right]$ is the acceleration of gravity

$\boldsymbol{u_1}$, $\boldsymbol{u_2}$: vertical displacements for the wheel and the car body

Note that for only 1-wheel $\boldsymbol{W^v} = \begin{bmatrix}\mathbf{1}\\ \mathbf{0}\end{bmatrix}$ and $\{\boldsymbol{\lambda_N}\} = \boldsymbol{\lambda_1}$

so $\boldsymbol{W^v\lambda_N} = \begin{bmatrix}\boldsymbol{\lambda_1}\\ \mathbf{0}\end{bmatrix}$ (see eq (2.1)), where $\boldsymbol{W^v\lambda_N}$ is already shifted in the right hand of eq (4.3)

To examine the dynamics of the above vehicle model interacting with a bridge model, using Lagrange and EMBS methods, Eq. (4.3) should be formed in the standards of Eq. (3.1) and (3.35) respectively.

So, for the Lagrange method we define:

$\boldsymbol{m^v} = \begin{bmatrix}\boldsymbol{m^w} & \mathbf{0}\\ \mathbf{0} & \boldsymbol{M^v}\end{bmatrix}$, $\boldsymbol{c^v} = \begin{bmatrix}\boldsymbol{c_v} & \boldsymbol{-c_v}\\ \boldsymbol{-c_v} & \boldsymbol{c_v}\end{bmatrix}$, $\boldsymbol{k^v} = \begin{bmatrix}\boldsymbol{k_v} & \boldsymbol{-k_v}\\ \boldsymbol{-k_v} & \boldsymbol{k_v}\end{bmatrix}$, $\boldsymbol{W^v} = \begin{bmatrix}\mathbf{1}\\ \mathbf{0}\end{bmatrix}$, $\boldsymbol{\lambda^v} = \boldsymbol{\lambda_1}$,
$\boldsymbol{F_v} = \boldsymbol{-M_{self}}$

And for the EMBS method:

$\boldsymbol{m^u} = \boldsymbol{M^v}$, $\boldsymbol{m^w} = \boldsymbol{m^w}$,
$\boldsymbol{c^u} = \boldsymbol{c^{u,w}} = \boldsymbol{c^{w,u}} = \boldsymbol{c^w} = \boldsymbol{c^v}$

$\boldsymbol{k^u} = \boldsymbol{k^{u,w}} = \boldsymbol{k^{w,u}} = \boldsymbol{k^w} = \boldsymbol{k^v}$

$\boldsymbol{W^w} = [\mathbf{1}]$
$\boldsymbol{W^*} = [\mathbf{1}] \rightarrow \textit{since there is only one wheel}$

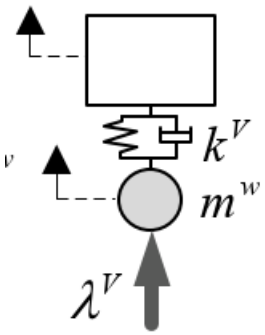

Figure 4-1 Sprung mass model

Table 4-1 Vehicle's model parameters

Car body mass $\boldsymbol{M^v}$ $\boldsymbol{(kg)}$	**Wheel mass** $\boldsymbol{m^w}$ $\boldsymbol{(kg)}$	**Suspension system stiffness** $\boldsymbol{k^v}$ $\left(\frac{\boldsymbol{kN}}{\boldsymbol{m}}\right)$	**Suspension system damping** $\boldsymbol{c^v}$ $\left(\frac{\boldsymbol{kN \cdot s}}{\boldsymbol{m}}\right)$
5750	**0.01**	**1595**	**0**

4.3 Train vehicle model

The presented vehicle model is commonly used to describe the passenger car of a train vehicle[8],[9]. The vehicle is supported on two double-axes bogies at each end and is modelled as a 10-DOF lumped mass system, comprising the vehicle body mass and its moment of inertia $(\boldsymbol{m_c, J_c})$,the two bogie masses and the associated moments of inertia $(\boldsymbol{m_t J_t})$, and four wheelset unsprung masses $(\boldsymbol{m_w})$. The bogie sideframe mass is linked with the wheel unsprung mass through the primary suspension springs $(\boldsymbol{k_{s1}, c_{s1}})$ and linked with the vehicle body mass through the secondary suspension springs $(\boldsymbol{k_{s2}, c_{s2}})$ (Figure 4-2).

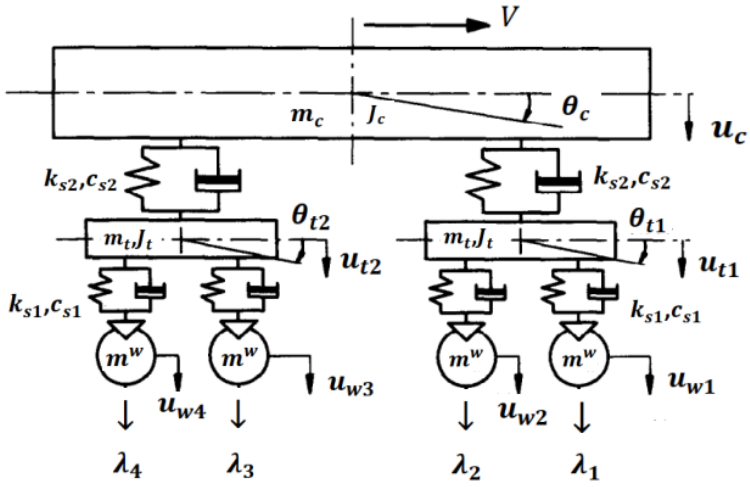

Figure 4-2 10-DOFs vehicle model

Equations of motion for the vehicle subsystem

Car body bounce

$$m_c\ddot{u}_c + 2c_{s2}\dot{u}_c + 2k_{s2}u_c - c_{s2}(\dot{u}_{t1} + \dot{u}_{t2}) - k_{s2}(u_{t1} + u_{t2}) = 0 \tag{4.4}$$

Car body pitch

$$J_c\ddot{\theta}_c + 2c_{s2}l_c^2\dot{\theta}_c + 2k_{s2}l_c^2\theta_c - c_{s2}l_c(\dot{u}_{t1} + \dot{u}_{t2}) - k_{s2}l_c(u_{t1} + u_{t2}) = 0 \tag{4.5}$$

Bogie* 1 *bounce

$$\begin{aligned} m_t\ddot{u}_{t1} + (c_{s2} + 2c_{s1})\dot{u}_{t1} + (k_{s2} + 2k_{s1})u_{t1} - c_{s1}(\dot{u}_{w1} + \dot{u}_{w2}) \\ - k_{s1}(u_{w1} + u_{w2}) - c_{s2}(\dot{u}_c + l_c\dot{\theta}_c) - k_{s2}(u_c + l_c\theta_c) = 0 \end{aligned} \tag{4.6}$$

Bogie 1 pitch

$$J_t\ddot{\theta}_{t1} + 2c_{s1}l_t^2\dot{\theta}_{t1} + 2k_{s1}l_t^2\theta_{t1} - c_{s1}l_t(\dot{u}_{w1} + \dot{u}_{w2}) - k_{s1}l_t(u_{w1} + u_{w2}) = 0 \qquad (4.7)$$

Bogie 2 bounce

$$\begin{aligned} m_t\ddot{u}_{t2} + (c_{s2} + 2c_{s1})\dot{u}_{t2} + (k_{s2} + 2k_{s1})u_{t2} - c_{s1}(\dot{u}_{w3} + \dot{u}_{w4}) \\ - k_{s1}(u_{w3} + u_{w4}) - c_{s2}\left(\dot{u}_c - l_c\dot{\theta}_c\right) - k_{s2}(u_c - l_c\theta_c) = 0 \end{aligned} \qquad (4.8)$$

Bogie 2 pitch

$$J_t\ddot{\theta}_{t2} + 2c_{s1}l_t^2\dot{\theta}_{t2} + 2k_{s1}l_t^2\theta_{t2} - c_{s1}l_t(\dot{u}_{w3} + \dot{u}_{w4}) - k_{s1}l_t(u_{w3} + u_{w4}) = 0 \qquad (4.9)$$

Wheels equations

$$\begin{aligned} &m_w\ddot{u}_{w1} + c_{s1}(\dot{u}_{w1} - \dot{u}_{t1}) + k_{s1}(u_{w1} - u_{t1}) - c_{s1}l_t\dot{\theta}_{t1} - k_{s1}l_t\theta_{t1} + \lambda_1 = F_{self} \\ &m_w\ddot{u}_{w2} + c_{s1}(\dot{u}_{w2} - \dot{u}_{t1}) + k_{s1}(u_{w2} - u_{t1}) + c_{s1}l_t\dot{\theta}_{t1} + k_{s1}l_t\theta_{t1} + \lambda_2 = F_{self} \\ &m_w\ddot{u}_{w3} + c_{s1}(\dot{u}_{w3} - \dot{u}_{t2}) + k_{s1}(u_{w3} - u_{t2}) - c_{s1}l_t\dot{\theta}_{t2} - k_{s1}l_t\theta_{t2} + \lambda_3 = F_{self} \\ &m_w\ddot{u}_{w4} + c_{s1}(\dot{u}_{w4} - \dot{u}_{t2}) + k_{s1}(u_{w4} - u_{t2}) + c_{s1}l_t\dot{\theta}_{t2} + k_{s1}l_t\theta_{t2} + \lambda_4 = F_{self} \end{aligned} \qquad (4.10)$$

Matrix form of Eqs. (4.6)~(4.12)

Vehicle mass matrix

$$\boldsymbol{m_v} = \begin{bmatrix} m_c & \mathbf{0} & \mathbf{0} & \mathbf{0} & \mathbf{0} & \mathbf{0} & \mathbf{0} & \mathbf{0} & \mathbf{0} & \mathbf{0} \\ \mathbf{0} & J_c & \mathbf{0} & \mathbf{0} & \mathbf{0} & \mathbf{0} & \mathbf{0} & \mathbf{0} & \mathbf{0} & \mathbf{0} \\ \mathbf{0} & \mathbf{0} & m_t & \mathbf{0} & \mathbf{0} & \mathbf{0} & \mathbf{0} & \mathbf{0} & \mathbf{0} & \mathbf{0} \\ \mathbf{0} & \mathbf{0} & \mathbf{0} & J_t & \mathbf{0} & \mathbf{0} & \mathbf{0} & \mathbf{0} & \mathbf{0} & \mathbf{0} \\ \mathbf{0} & \mathbf{0} & \mathbf{0} & \mathbf{0} & m_t & \mathbf{0} & \mathbf{0} & \mathbf{0} & \mathbf{0} & \mathbf{0} \\ \mathbf{0} & \mathbf{0} & \mathbf{0} & \mathbf{0} & \mathbf{0} & J_t & \mathbf{0} & \mathbf{0} & \mathbf{0} & \mathbf{0} \\ \mathbf{0} & \mathbf{0} & \mathbf{0} & \mathbf{0} & \mathbf{0} & \mathbf{0} & m_w & \mathbf{0} & \mathbf{0} & \mathbf{0} \\ \mathbf{0} & \mathbf{0} & \mathbf{0} & \mathbf{0} & \mathbf{0} & \mathbf{0} & \mathbf{0} & m_w & \mathbf{0} & \mathbf{0} \\ \mathbf{0} & \mathbf{0} & \mathbf{0} & \mathbf{0} & \mathbf{0} & \mathbf{0} & \mathbf{0} & \mathbf{0} & m_w & \mathbf{0} \\ \mathbf{0} & \mathbf{0} & \mathbf{0} & \mathbf{0} & \mathbf{0} & \mathbf{0} & \mathbf{0} & \mathbf{0} & \mathbf{0} & m_w \end{bmatrix}$$

$\boldsymbol{c_v}$

$$= \begin{bmatrix} 2c_{s2} & \mathbf{0} & -c_{s2} & \mathbf{0} & -c_{s2} & \mathbf{0} & \mathbf{0} & \mathbf{0} & \mathbf{0} & \mathbf{0} \\ \mathbf{0} & 2c_{s2}l_c^2 & -c_{s2}l_c & \mathbf{0} & c_{s2}l_c & \mathbf{0} & \mathbf{0} & \mathbf{0} & \mathbf{0} & \mathbf{0} \\ -c_{s2} & -c_{s2}l_c & c_{s2} + 2c_{s1} & \mathbf{0} & \mathbf{0} & \mathbf{0} & -c_{s1} & -c_{s1} & \mathbf{0} & \mathbf{0} \\ \mathbf{0} & \mathbf{0} & \mathbf{0} & 2c_{s1}l_t^2 & \mathbf{0} & \mathbf{0} & -c_{s1}l_t & c_{s1}l_t & \mathbf{0} & \mathbf{0} \\ -c_{s2} & c_{s2}l_c & \mathbf{0} & \mathbf{0} & c_{s2} + 2c_{s1} & \mathbf{0} & \mathbf{0} & \mathbf{0} & -c_{s1} & -c_{s1} \\ \mathbf{0} & \mathbf{0} & \mathbf{0} & \mathbf{0} & \mathbf{0} & 2c_{s1}l_t^2 & \mathbf{0} & \mathbf{0} & -c_{s1}l_t & -c_{s1}l_t \\ \mathbf{0} & \mathbf{0} & -c_{s1} & -c_{s1}l_t & \mathbf{0} & \mathbf{0} & c_{s1} & \mathbf{0} & \mathbf{0} & \mathbf{0} \\ \mathbf{0} & \mathbf{0} & -c_{s1} & c_{s1}l_t & \mathbf{0} & \mathbf{0} & \mathbf{0} & c_{s1} & \mathbf{0} & \mathbf{0} \\ \mathbf{0} & \mathbf{0} & \mathbf{0} & \mathbf{0} & -c_{s1} & -c_{s1}l_t & \mathbf{0} & \mathbf{0} & c_{s1} & \mathbf{0} \\ \mathbf{0} & \mathbf{0} & \mathbf{0} & \mathbf{0} & -c_{s1} & -c_{s1}l_t & \mathbf{0} & \mathbf{0} & \mathbf{0} & c_{s1} \end{bmatrix}$$

$$\boldsymbol{k_v} = \begin{bmatrix} 2k_{s2} & \mathbf{0} & -k_{s2} & \mathbf{0} & -k_{s2} & \mathbf{0} & \mathbf{0} & \mathbf{0} & \mathbf{0} & \mathbf{0} \\ \mathbf{0} & 2k_{s2}l_c^2 & -k_{s2}l_c & \mathbf{0} & k_{s2}l_c & \mathbf{0} & \mathbf{0} & \mathbf{0} & \mathbf{0} & \mathbf{0} \\ -k_{s2} & -k_{s2}l_c & k_{s2}+2k_{s1} & \mathbf{0} & \mathbf{0} & \mathbf{0} & -k_{s1} & -k_{s1} & \mathbf{0} & \mathbf{0} \\ \mathbf{0} & \mathbf{0} & \mathbf{0} & 2k_{s1}l_t^2 & \mathbf{0} & \mathbf{0} & -k_{s1}l_t & k_{s1}l_t & \mathbf{0} & \mathbf{0} \\ -k_{s2} & k_{s2}l_c & \mathbf{0} & \mathbf{0} & k_{s2}+2k_{s1} & \mathbf{0} & \mathbf{0} & \mathbf{0} & -k_{s1} & -k_{s1} \\ \mathbf{0} & \mathbf{0} & \mathbf{0} & \mathbf{0} & \mathbf{0} & 2k_{s1}l_t^2 & \mathbf{0} & \mathbf{0} & -k_{s1}l_t & -k_{s1}l_t \\ \mathbf{0} & \mathbf{0} & -k_{s1} & -k_{s1}l_t & \mathbf{0} & \mathbf{0} & k_{s1} & \mathbf{0} & \mathbf{0} & \mathbf{0} \\ \mathbf{0} & \mathbf{0} & -k_{s1} & k_{s1}l_t & \mathbf{0} & \mathbf{0} & \mathbf{0} & k_{s1} & \mathbf{0} & \mathbf{0} \\ \mathbf{0} & \mathbf{0} & \mathbf{0} & \mathbf{0} & -k_{s1} & -k_{s1}l_t & \mathbf{0} & \mathbf{0} & k_{s1} & \mathbf{0} \\ \mathbf{0} & \mathbf{0} & \mathbf{0} & \mathbf{0} & -k_{s1} & -k_{s1}l_t & \mathbf{0} & \mathbf{0} & \mathbf{0} & k_{s1} \end{bmatrix}$$

$$\ddot{\boldsymbol{u}}_{\boldsymbol{v}} = \begin{Bmatrix} \ddot{u}_c \\ \ddot{\theta}_c \\ \ddot{u}_{t1} \\ \ddot{\theta}_{t1} \\ \ddot{u}_{t2} \\ \ddot{\theta}_{t2} \\ \ddot{u}_{w1} \\ \ddot{u}_{w2} \\ \ddot{u}_{w3} \\ \ddot{u}_{w4} \end{Bmatrix} \qquad \dot{\boldsymbol{u}}_{\boldsymbol{v}} = \begin{Bmatrix} \dot{u}_c \\ \dot{\theta}_c \\ \dot{u}_{t1} \\ \dot{\theta}_{t1} \\ \dot{u}_{t2} \\ \dot{\theta}_{t2} \\ \dot{u}_{w1} \\ \dot{u}_{w2} \\ \dot{u}_{w3} \\ \dot{u}_{w4} \end{Bmatrix} \qquad \boldsymbol{u}_{\boldsymbol{v}} = \begin{Bmatrix} u_c \\ \theta_c \\ u_{t1} \\ \theta_{t1} \\ u_{t2} \\ \theta_{t2} \\ u_{w1} \\ u_{w2} \\ u_{w3} \\ u_{w4} \end{Bmatrix}$$

$$\boldsymbol{F_v} = \begin{Bmatrix} 0 \\ 0 \\ 0 \\ 0 \\ 0 \\ 0 \\ F_{self} - \lambda_1 \\ F_{self} - \lambda_2 \\ F_{self} - \lambda_3 \\ F_{self} - \lambda_4 \end{Bmatrix}, where\ \boldsymbol{F_{self}} = -(\boldsymbol{m_c} + \mathbf{0.5}\boldsymbol{m_t} + \mathbf{0.25}\boldsymbol{m_c})\boldsymbol{g}$$

In order to correspond to the Lagrange and EMBS methods forms (3.1) and (3.35), the above matrices should be written as presented below:

<u>Corresponding to Lagrange method</u>

$\boldsymbol{m_v}, \boldsymbol{c_v}$ and $\boldsymbol{k_v}$ matrices already correspond in the specifications, so only $\boldsymbol{W^v}, \boldsymbol{\lambda^v}\ and\ \boldsymbol{F^v}$ are clarified:

$$\boldsymbol{W^v} = \begin{bmatrix} \boldsymbol{zeros(ndofs - N\_wheels)} \\ \boldsymbol{eye(N\_wheels)} \end{bmatrix}, \boldsymbol{\lambda^v} = \begin{Bmatrix} \boldsymbol{\lambda_1} \\ \boldsymbol{\lambda_2} \\ \boldsymbol{\lambda_3} \\ \boldsymbol{\lambda_4} \end{Bmatrix} \; and \; \boldsymbol{F^v} = \begin{Bmatrix} 0 \\ 0 \\ 0 \\ 0 \\ 0 \\ 0 \\ F_{self} \\ F_{self} \\ F_{self} \\ F_{self} \end{Bmatrix}$$

And for the EMBS method the equivalent matrices are clarified as:

$$\boldsymbol{c^{uu}} = \begin{bmatrix} \boldsymbol{2c_{s2}} & \boldsymbol{0} & \boldsymbol{-c_{s2}} & \boldsymbol{0} & \boldsymbol{-c_{s2}} & \boldsymbol{0} \\ \boldsymbol{0} & \boldsymbol{2c_{s2}l_c^2} & \boldsymbol{-c_{s2}l_c} & \boldsymbol{0} & \boldsymbol{c_{s2}l_c} & \boldsymbol{0} \\ \boldsymbol{-c_{s2}} & \boldsymbol{-c_{s2}l_c} & \boldsymbol{c_{s2} + 2c_{s1}} & \boldsymbol{0} & \boldsymbol{0} & \boldsymbol{0} \\ \boldsymbol{0} & \boldsymbol{0} & \boldsymbol{0} & \boldsymbol{2c_{s1}l_t^2} & \boldsymbol{0} & \boldsymbol{0} \\ \boldsymbol{-c_{s2}} & \boldsymbol{c_{s2}l_c} & \boldsymbol{0} & \boldsymbol{0} & \boldsymbol{c_{s2} + 2c_{s1}} & \boldsymbol{0} \\ \boldsymbol{0} & \boldsymbol{0} & \boldsymbol{0} & \boldsymbol{0} & \boldsymbol{0} & \boldsymbol{2c_{s1}l_t^2} \end{bmatrix}$$

$$\boldsymbol{c^{uw}} = \boldsymbol{(c^{wu})^T} = \begin{bmatrix} \boldsymbol{0} & \boldsymbol{0} & \boldsymbol{0} & \boldsymbol{0} \\ \boldsymbol{0} & \boldsymbol{0} & \boldsymbol{0} & \boldsymbol{0} \\ \boldsymbol{-c_{s1}} & \boldsymbol{-c_{s1}} & \boldsymbol{0} & \boldsymbol{0} \\ \boldsymbol{-c_{s1}l_t} & \boldsymbol{c_{s1}l_t} & \boldsymbol{0} & \boldsymbol{0} \\ \boldsymbol{0} & \boldsymbol{0} & \boldsymbol{-c_{s1}} & \boldsymbol{-c_{s1}} \\ \boldsymbol{0} & \boldsymbol{0} & \boldsymbol{-c_{s1}l_t} & \boldsymbol{-c_{s1}l_t} \end{bmatrix}$$

$$\boldsymbol{c^{ww}} = \begin{bmatrix} \boldsymbol{c_{s1}} & \boldsymbol{0} & \boldsymbol{0} & \boldsymbol{0} \\ \boldsymbol{0} & \boldsymbol{c_{s1}} & \boldsymbol{0} & \boldsymbol{0} \\ \boldsymbol{0} & \boldsymbol{0} & \boldsymbol{c_{s1}} & \boldsymbol{0} \\ \boldsymbol{0} & \boldsymbol{0} & \boldsymbol{0} & \boldsymbol{c_{s1}} \end{bmatrix}$$

$$\boldsymbol{k^u} = \begin{bmatrix} \boldsymbol{2k_{s2}} & \boldsymbol{0} & \boldsymbol{-k_{s2}} & \boldsymbol{0} & \boldsymbol{-k_{s2}} & \boldsymbol{0} \\ \boldsymbol{0} & \boldsymbol{2k_{s2}l_c^2} & \boldsymbol{-k_{s2}l_c} & \boldsymbol{0} & \boldsymbol{k_{s2}l_c} & \boldsymbol{0} \\ \boldsymbol{-k_{s2}} & \boldsymbol{-k_{s2}l_c} & \boldsymbol{k_{s2} + 2k_{s1}} & \boldsymbol{0} & \boldsymbol{0} & \boldsymbol{0} \\ \boldsymbol{0} & \boldsymbol{0} & \boldsymbol{0} & \boldsymbol{2k_{s1}l_t^2} & \boldsymbol{0} & \boldsymbol{0} \\ \boldsymbol{-k_{s2}} & \boldsymbol{k_{s2}l_c} & \boldsymbol{0} & \boldsymbol{0} & \boldsymbol{k_{s2} + 2k_{s1}} & \boldsymbol{0} \\ \boldsymbol{0} & \boldsymbol{0} & \boldsymbol{0} & \boldsymbol{0} & \boldsymbol{0} & \boldsymbol{2k_{s1}l_t^2} \end{bmatrix}$$

$$\boldsymbol{k^{uw}} = \boldsymbol{(k^{wu})^T} = \begin{bmatrix} \boldsymbol{0} & \boldsymbol{0} & \boldsymbol{0} & \boldsymbol{0} \\ \boldsymbol{0} & \boldsymbol{0} & \boldsymbol{0} & \boldsymbol{0} \\ \boldsymbol{-k_{s1}} & \boldsymbol{-k_{s1}} & \boldsymbol{0} & \boldsymbol{0} \\ \boldsymbol{-k_{s1}l_t} & \boldsymbol{k_{s1}l_t} & \boldsymbol{0} & \boldsymbol{0} \\ \boldsymbol{0} & \boldsymbol{0} & \boldsymbol{-k_{s1}} & \boldsymbol{-k_{s1}} \\ \boldsymbol{0} & \boldsymbol{0} & \boldsymbol{-k_{s1}l_t} & \boldsymbol{-k_{s1}l_t} \end{bmatrix}$$

$$\boldsymbol{k^w} = \begin{bmatrix} \boldsymbol{k_{s1}} & \boldsymbol{0} & \boldsymbol{0} & \boldsymbol{0} \\ \boldsymbol{0} & \boldsymbol{k_{s1}} & \boldsymbol{0} & \boldsymbol{0} \\ \boldsymbol{0} & \boldsymbol{0} & \boldsymbol{k_{s1}} & \boldsymbol{0} \\ \boldsymbol{0} & \boldsymbol{0} & \boldsymbol{0} & \boldsymbol{k_{s1}} \end{bmatrix}$$

$$\boldsymbol{m^u} = \boldsymbol{diag\{m_c, J_c, m_t, J_t, m_t, J_t\}}$$

$$\boldsymbol{m^w = diag\{m_w, m_w, m_w, m_w\}}$$

$$\boldsymbol{W^* = \begin{bmatrix} 0 & 0 & -1 & l_t/L & 0 & 0 \\ 0 & 0 & -1 & -l_t/L & 0 & 0 \\ 0 & 0 & 0 & 0 & -1 & l_t/L \\ 0 & 0 & 0 & 0 & -1 & l_t/L \end{bmatrix}}$$

Table 4-2 Parameters of the 10-DOFs vehicle model

Parameter	Value
Car body mass $\boldsymbol{m_c}$	34230 (kg)
Bogie mass $\boldsymbol{m_t}$	2760 (kg)
Wheel mass $\boldsymbol{m_w}$	1583 (kg)
Car body mass inertia $\boldsymbol{J_c}$	1.624× 10^6 $(kg \cdot m^2)$
Bogie mass inertia $\boldsymbol{J_t}$	2500 $(kg \cdot m^2)$
Primary suspension stiffness $\boldsymbol{k_{s1}}$	807.5 (kN/m)
Primary suspension damping $\boldsymbol{c_{s1}}$	7.5 $(kN \cdot s/m)$
Secondary suspension stiffness $\boldsymbol{k_{s2}}$	182.7 (kN/m)
Secondary suspension damping $\boldsymbol{c_{s2}}$	16.35 $(kN \cdot s/m)$
Half-distance between bogies $\boldsymbol{l_c}$	8.875 (m)
Half wheelbase $\boldsymbol{l_t}$	1.50 (m)

4.4 Simply supported bridge model

In this study the simply supported bridge is modelled as a 2D structure (Figure 4-3) with Euler-Bernoulli beam elements (Figure 4-4). The finite element model of the bridge is developed and analyzed using COMSOL Multiphysics simulation software.

Figure 4-3 2D simply supported bridge

In the 2D bridge case, the 2D beam element consists of 2Dofs per node, one in the vertical direction $\boldsymbol{u_y}$ and one rotation $\boldsymbol{\theta_z}$ (Figure 4-4). The general form of the EOM of the bridge remains the same but the mass, stiffness and damping matrices presented in Eqs (4.11), (4.12) and (4.13) are adapted in order to serve the 2D beams properties. Subsequently, the mass matrix $[\boldsymbol{m_b}]$, the stiffness matrix $[\boldsymbol{k_b}]$ and the damping matrix $[\boldsymbol{c_b}]$ become:

$$[\boldsymbol{m_b}] = \frac{\boldsymbol{m}}{\boldsymbol{420}}\begin{bmatrix} \boldsymbol{156} & \boldsymbol{22L} & \boldsymbol{54} & \boldsymbol{-13L} \\ \boldsymbol{22L} & \boldsymbol{4L^2} & \boldsymbol{13L} & \boldsymbol{-3L^2} \\ \boldsymbol{54} & \boldsymbol{13L} & \boldsymbol{156} & \boldsymbol{-22L} \\ \boldsymbol{-13L} & \boldsymbol{-3L^2} & \boldsymbol{-22L} & \boldsymbol{4L^2} \end{bmatrix} \tag{4.11}$$

$$[\boldsymbol{k_b}] = \frac{\boldsymbol{EI}}{\boldsymbol{L^3}}\begin{bmatrix} \boldsymbol{12} & \boldsymbol{6L} & \boldsymbol{-12} & \boldsymbol{6L} \\ \boldsymbol{6L} & \boldsymbol{4L^2} & \boldsymbol{-6L} & \boldsymbol{2L^2} \\ \boldsymbol{-12} & \boldsymbol{-6L} & \boldsymbol{12} & \boldsymbol{-6L} \\ \boldsymbol{6L} & \boldsymbol{2L^2} & \boldsymbol{-6L} & \boldsymbol{4L^2} \end{bmatrix} \tag{4.12}$$

$$\left[\boldsymbol{c^b}\right] = \boldsymbol{a_0}\left[\boldsymbol{m^b}\right] + \boldsymbol{a_1}\left[\boldsymbol{k^b}\right] \tag{4.13}$$

where coefficients $\boldsymbol{a_0}$ and $\boldsymbol{a_1}$ are estimated from eq (Appendix)

The above matrices are extracted from COMSOL, for the entire bridge structure. COMSOL Multiphysics also gives the ability to extract the mesh information of the model. That information contain details about the elements, nodes and degrees of freedom of the model. The nodes position (coordinates) and the equivalent DOFs of the node, in addition to the vehicle's position, are some of the most principal parameters for the VBI system's definition.

The detection of the vehicle's position on the structure and the equivalent element that acts on, are constantly renewed and estimated.

The contact direction matrix $\left[\boldsymbol{W^b}\right]$ from eq (2.2) for the 2D simply supported bridge can be evaluated with the help of shape functions for a 2D beam element, as presented bellow.

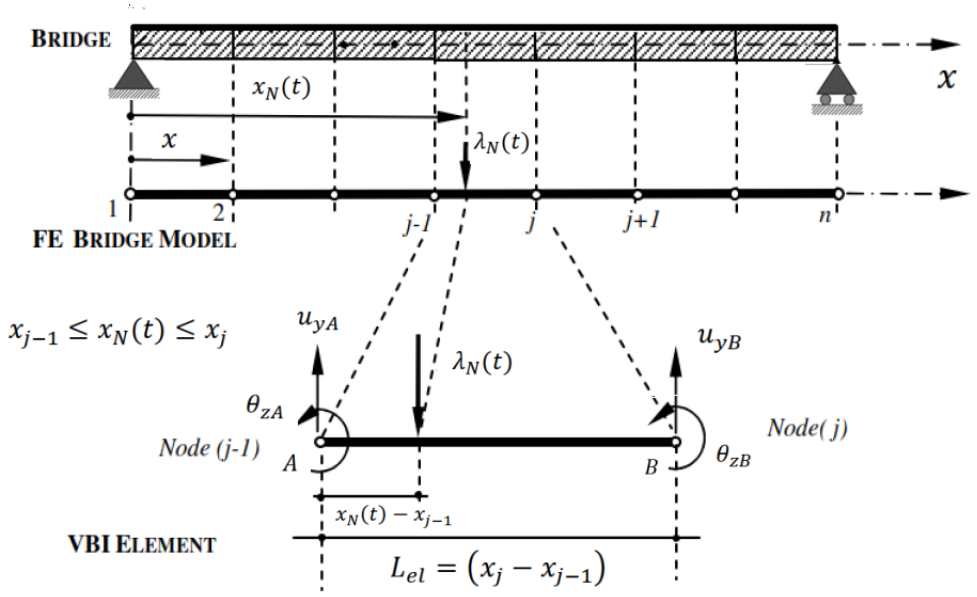

Figure 4-4 Euler-Bernoulli beam element

In the beam local system, the displacements, $\boldsymbol{u}$, and rotations, $\boldsymbol{\theta}$, are interpolated as:

$$\begin{Bmatrix} \boldsymbol{u} \\ \boldsymbol{\theta} \end{Bmatrix} = [\boldsymbol{N_3}\ \boldsymbol{N_5}\ \boldsymbol{N_4}\ \boldsymbol{N_6}] \begin{Bmatrix} \boldsymbol{u_{yA}} \\ \boldsymbol{\theta_{zA}} \\ \boldsymbol{u_{yB}} \\ \boldsymbol{\theta_{zB}} \end{Bmatrix} = [\boldsymbol{N}] \begin{Bmatrix} \boldsymbol{u_{yA}} \\ \boldsymbol{\theta_{zA}} \\ \boldsymbol{u_{yB}} \\ \boldsymbol{\theta_{zB}} \end{Bmatrix} \tag{4.14}$$

The shape functions are used to transfer the forces from the wheels to the equivalent nodes of the bridge element at each time step of the simulation. So as the vehicle's N-wheel moves through the beam elements the equivalent $\boldsymbol{\lambda_N}$ contact force acts on a specific element. To specify that element we estimate the wheel's position through eq (2.3) for time $\boldsymbol{t_i}$ and locate it to the nodes coordinates of the structure, accordingly. As the active beam element is now known, with the help of the mesh information, extracted from COMSOL Multiphysics, the degrees of freedom that correspond to the active beam element can also be specified. Through this process the $\boldsymbol{W^b}$ contact direction matrix can be estimated at each time, as:

$\boldsymbol{W^b(x_i)} = [\boldsymbol{N}] \begin{Bmatrix} \boldsymbol{u_{j-1}} \\ \boldsymbol{\theta_{j-1}} \\ \boldsymbol{u_j} \\ \boldsymbol{\theta_j} \end{Bmatrix}$, where j-1 and j denote the nodes of the active element

$\boldsymbol{W^b(x_i)}$ is a $[\boldsymbol{ndofs\_bridge} \times \boldsymbol{N\_wheels}]$ matrix where the only nonzero entries in the matrix correspond to the DOFs of the bridge deck in contact with the vehicle's wheels.

Table 4-3 Parameters of the bridge model

Span length L (m)	**Mass per unit length m** $\left(\frac{kg}{m^2}\right)$	**Moment of inertia I** (m^4)	**Young's modulus E** (GPa)	**Poisson's ratio v**
25	**2303**	**2.90**	**2.87**	**0.2**

4.5 Results

4.5.1 Sprung mass and simply supported bridge interaction

This section presents the dynamic responses of the interaction between the sprung mass model, presented in section 4.2, and the simply supported bridge, presented in section 4.4 (Figure 4-5) and examines the influence of several parameters of the model.

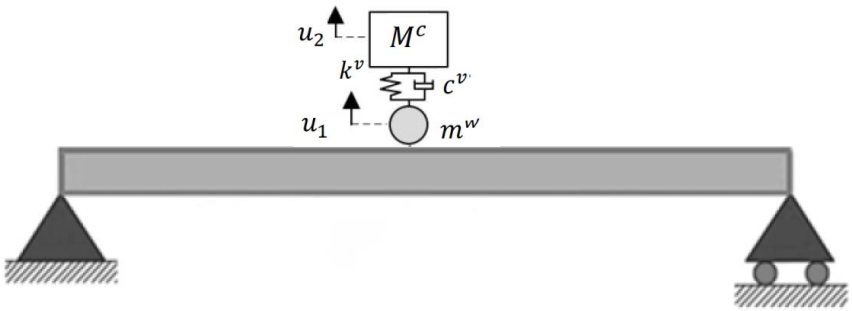

(a)

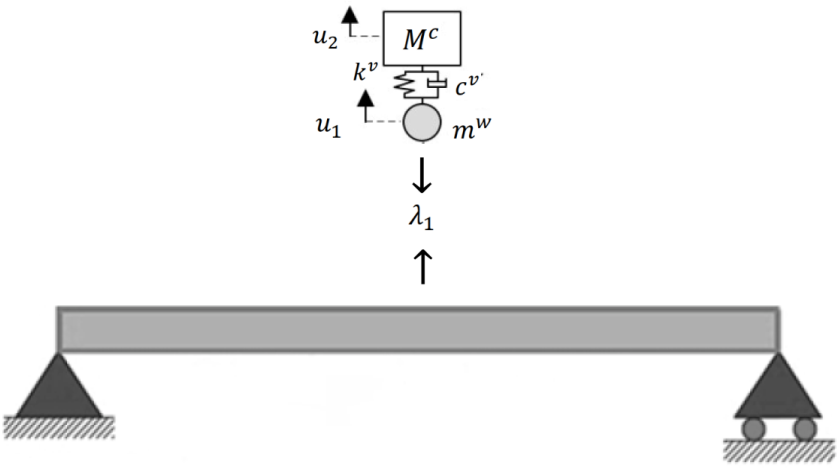

(b)

Figure 4-5 Sprung mass-bridge (a) travelling the bridge (b) interaction

The dynamic response of the sprung mass-bridge system results after simulating the VBI model in MATLAB, as mentioned in the introduction. Using the solving methods proposed in sections 3.2 and 3.3 the above results arise.

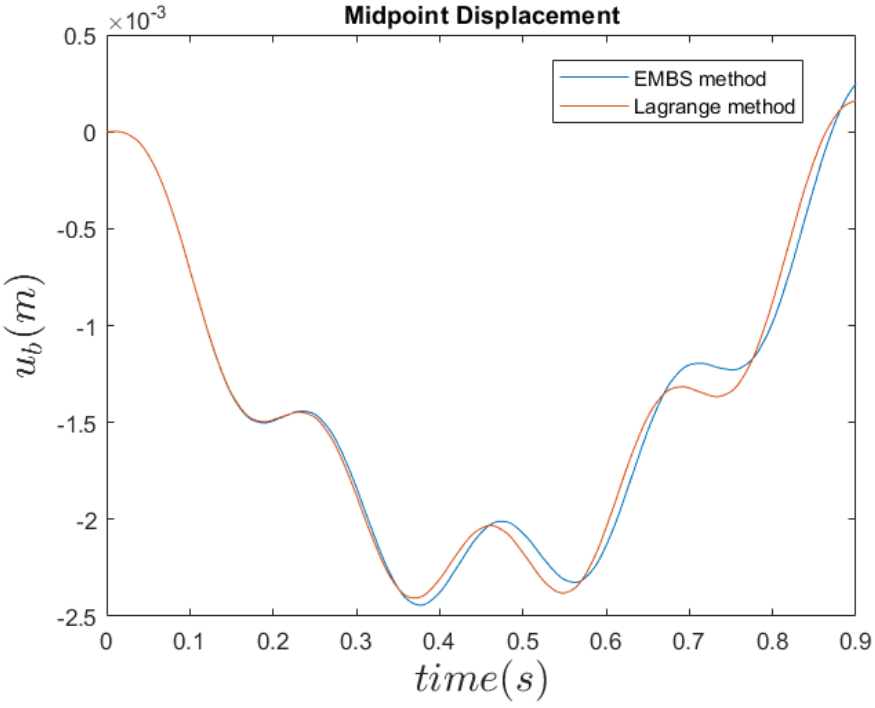

(a)

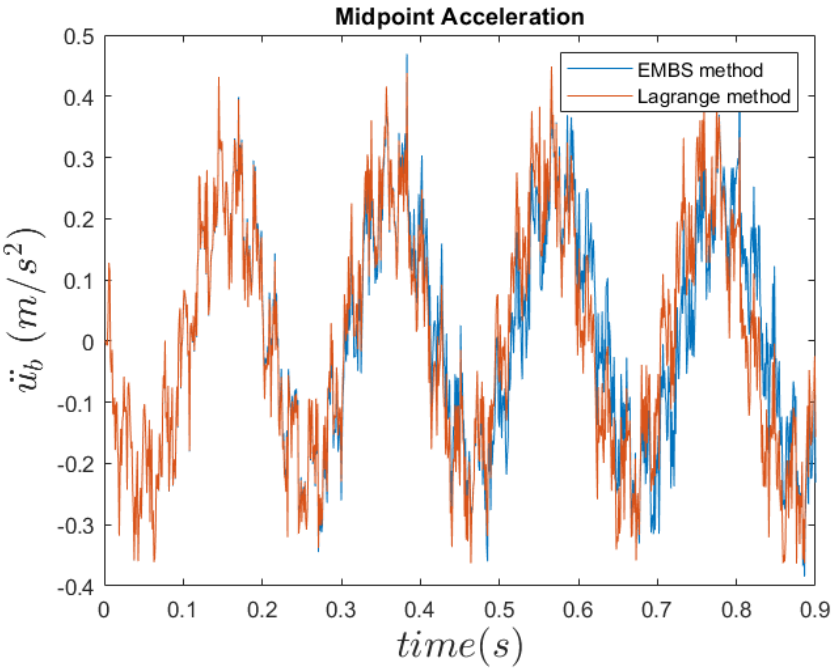

(b)

Figure 4-6 Vertical (a) displacement, (b) acceleration of the midpoint of the bridge

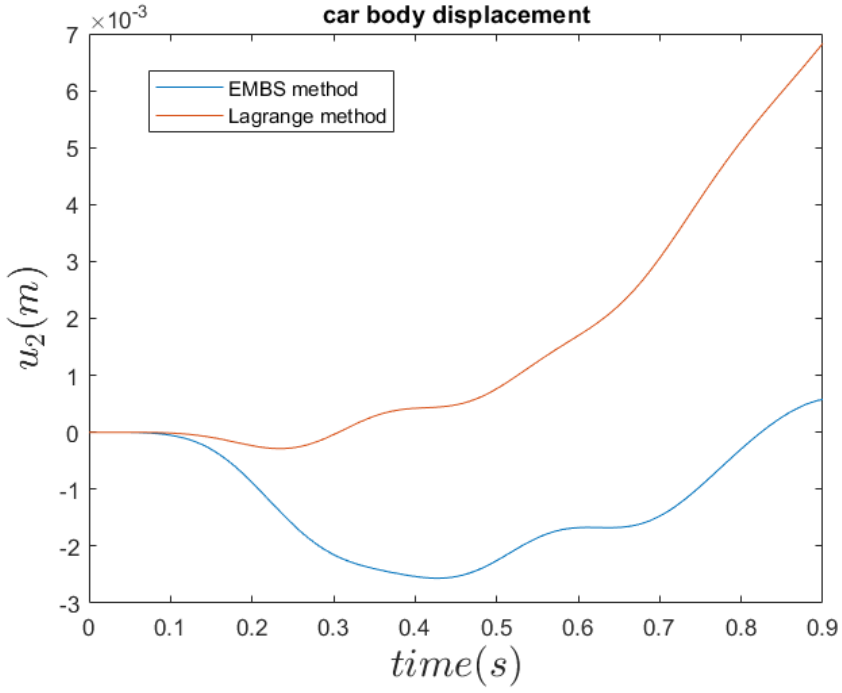

(a)

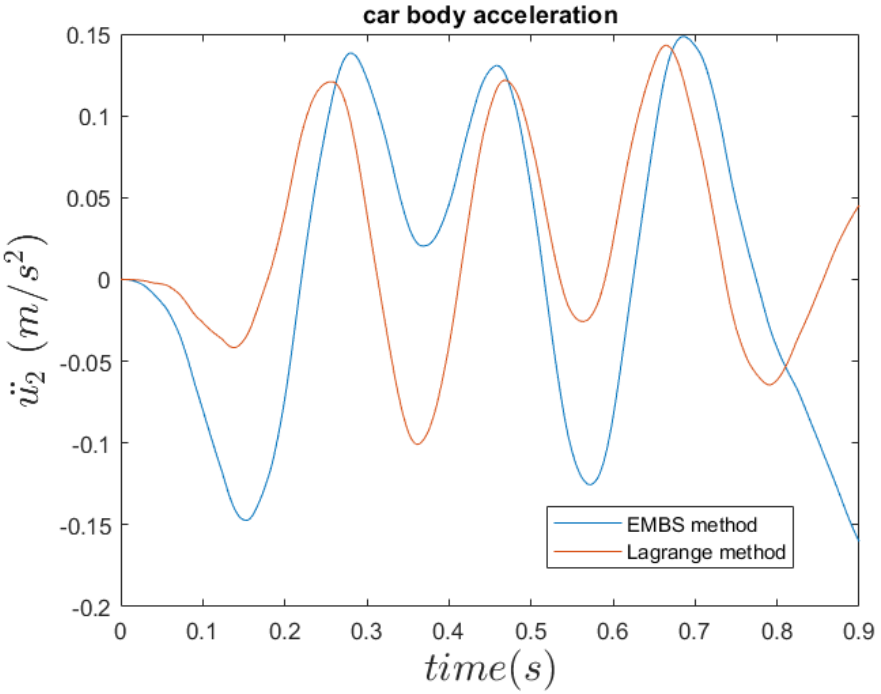

(b)

Figure 4-7 Car body vertical (a) displacement (b) acceleration

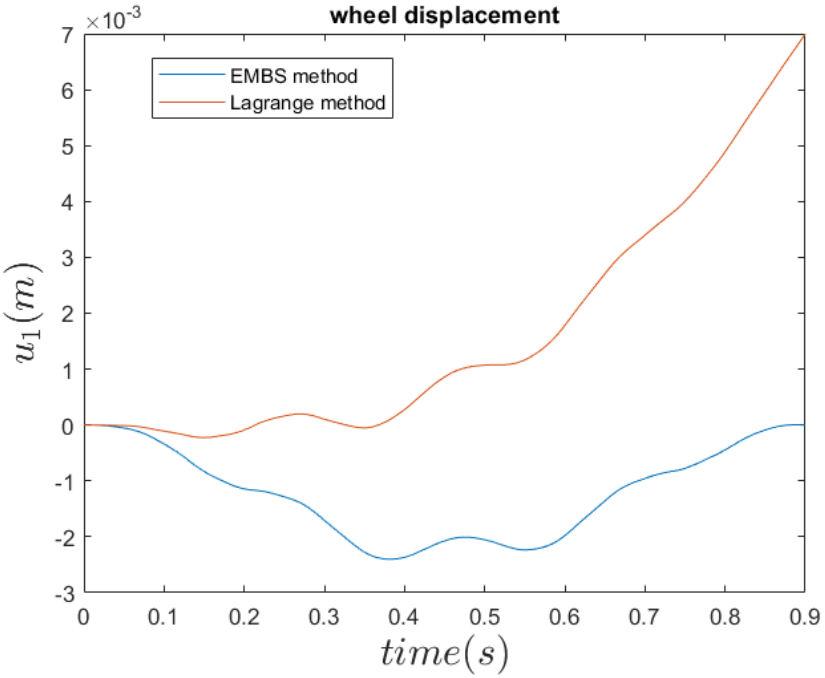

(a)

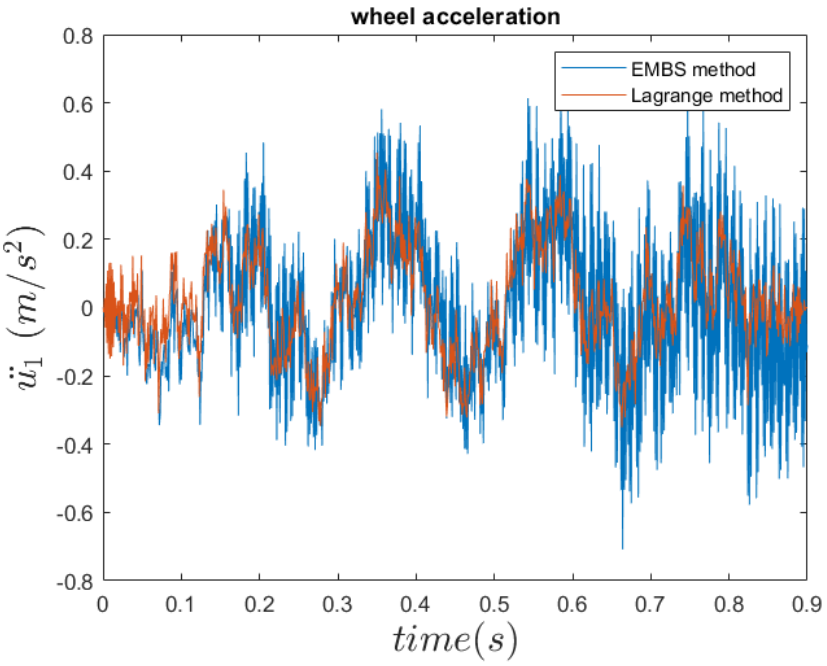

(b)

Figure 4-8 Wheel's (a) displacement (b) acceleration

As we can see in Figure (4-6) the two solving methods (EMBS and Lagrange) present quite similar results. However, in Figures (4-8(a)) we can see the results of Lagrange method diverge from those of EMBS. As it seems the response of the car body and wheel of the system in the Lagrange method tend to increase constantly, in contrast to the EMBS method where the vehicle's response seems more reasonable. Comparing the results from Figures ((4-6)~(4.8)) with those of [1],[10] for the same vehicle-bridge system we lead to the conclusion that EMBS method is more accurate

Verification

To verify the simulated responses a static calculation could be carried out. According to the Euler-Bernoulli beam theory and in the situation where a point load is on the middle of a simply supported bridge [11], we can get:

$$\frac{d^4v}{dx^4} = \frac{P}{EI}\delta\left(x - \frac{L}{2}\right) \tag{4.15}$$

By integration:

$$\frac{d^3v}{dx^3} = \frac{P}{EI}\theta\left(x - \frac{L}{2}\right) + c_1 \tag{4.16}$$

$$\frac{d^2v}{dx^2} = \frac{P}{EI}\left(x - \frac{L}{2}\right)\theta\left(x - \frac{L}{2}\right) + c_1x + c_2 \tag{4.17}$$

$$\frac{dv}{dx} = \frac{P}{EI}\frac{1}{2}\left(x - \frac{L}{2}\right)^2 \theta\left(x - \frac{L}{2}\right) + \frac{c_1}{2}x^2 + c_2 x \tag{4.18}$$

$$v(x) = \frac{P}{EI}\frac{1}{6}\left(x - \frac{L}{2}\right)^3 \theta\left(x - \frac{L}{2}\right) + \frac{c_1}{6}x^3 + \frac{c_2}{2}x^2 + c_3 x + c_4 \tag{4.19}$$

So, for the case of simply supported bridge the boundary conditions are:

$$\begin{aligned} v(0) &= v(L) = 0 \\ v''(0) &= v''(L) = 0 \end{aligned} \tag{4.20}$$

Subsequently for eq (4.8) and (4.6),

$$0 = \frac{P}{EI}\frac{1}{6}\left(0 - \frac{L}{2}\right)^3 \theta\left(0 - \frac{L}{2}\right) + \frac{c_1}{6}0^3 + \frac{c_2}{2}0^2 + c_3 0 + c_4\,, \qquad for\ v(0) = 0$$

$\rightarrow\ \boldsymbol{c_4 = 0}$ since $\theta(x) = 0\ if\ x < 0$

$$0 = \frac{P}{EI}\left(0 - \frac{L}{2}\right)\theta\left(0 - \frac{L}{2}\right) + c_1 0 + c_2, \qquad for\ v''(0) = 0$$

$\rightarrow\ \boldsymbol{c_2 = 0}$

$$0 = \frac{P}{EI}\frac{1}{6}\left(L - \frac{L}{2}\right)^3 \theta\left(L - \frac{L}{2}\right) + \frac{c_1}{6}L^3 + \frac{c_2}{2}L^2 + c_3 L + c_4, \qquad for\ v(L) = 0$$

$\rightarrow\ \boldsymbol{c_3 = \frac{PL^2}{16EI}}$ since $\theta(1) = 0$, for Euler-Bernoulli beams

$$0 = \frac{P}{EI}\left(L - \frac{L}{2}\right)\theta\left(L - \frac{L}{2}\right) + c_1 L + c_2 \ \ for\ v''(L) = 0$$

$\rightarrow\ \boldsymbol{c_1 = -\frac{P}{2EI}}$

Eventually,

$$\boldsymbol{v\left(x = \frac{L}{2}\right) = -\frac{PL^3}{48EI}} \tag{4.21}$$

Where for the quarter car model and the simply supported bridge of our model
$M^v = 5750\ [kg], m^w = 0.01\ [kg], E = 2.87\ [GPa], L = 25[m]\ and\ I = 2.9\ [m^4]$

$\boldsymbol{P} = (M^v + m^w)\boldsymbol{g}$, point load resulting from the vehicle's weight

So,

$$\boldsymbol{v\left(x = \frac{L}{2}\right) = -2.2062 \times 10^{-3}[m]}$$

In Figure (4-9) we can see the midpoint displacement of the bridge the time that the vehicle is located in the middle of the beam. The corresponding values from Lagrange and EMBS methods are $\boldsymbol{u_b = -2.05 \times 10^{-3}[m]}$ and $\boldsymbol{u_b = -2.07 \times 10^{-3}[m]}$, respectively and come to quite good agreement with the analytical solution.

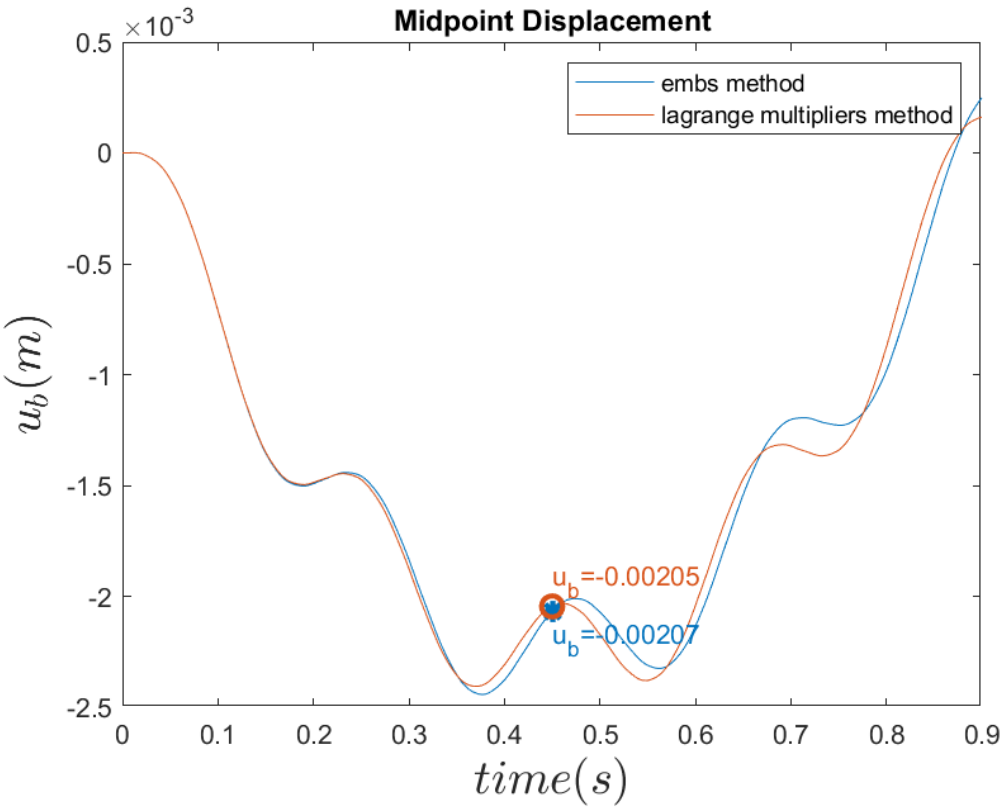

Figure 4-9 Vertical displacement of the midpoint of the bridge

Influence of speed

The bellow plots present the response of the system in case where the vehicle's speed is initially 100[km/h] and increases by a factor of 2 and 3. All the other parameters remain the same.

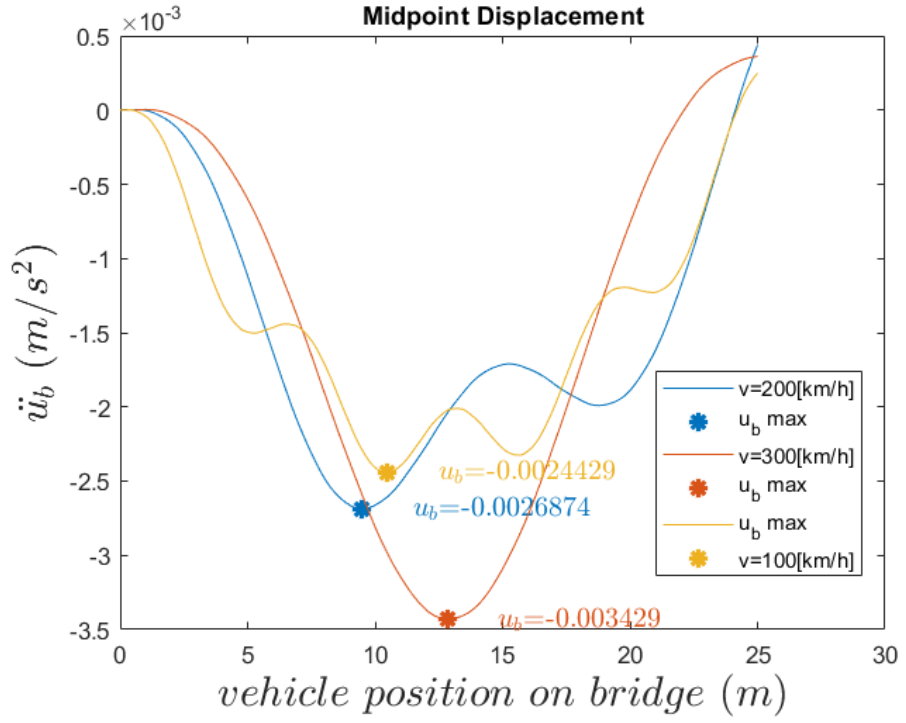

(a)

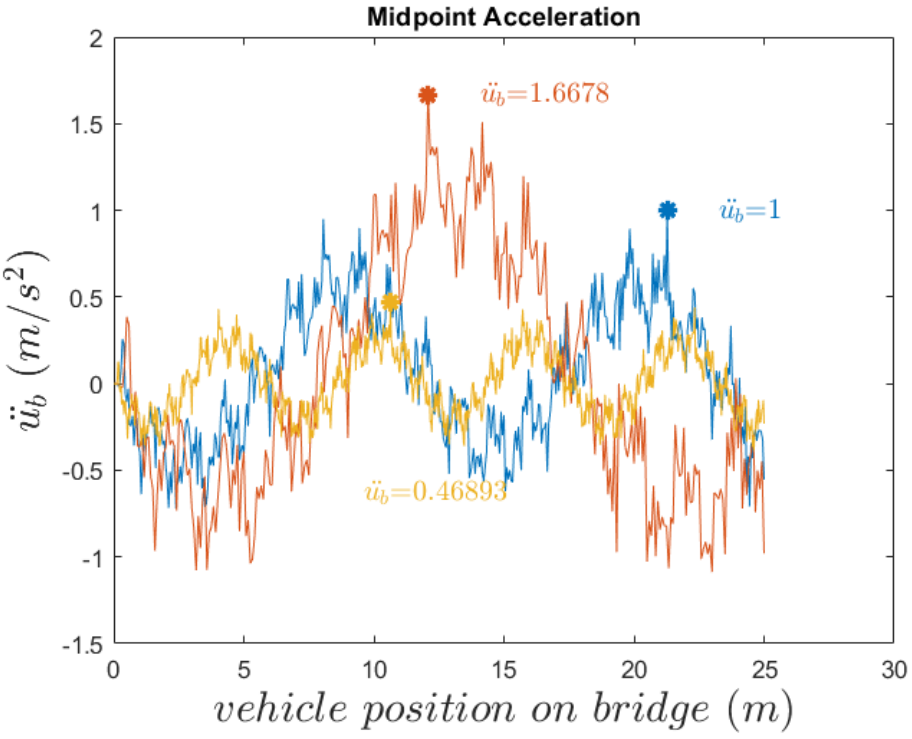

(b)

Figure 4-10 Speed influence in (a) displacement (b) acceleration of the bridge's midpoint

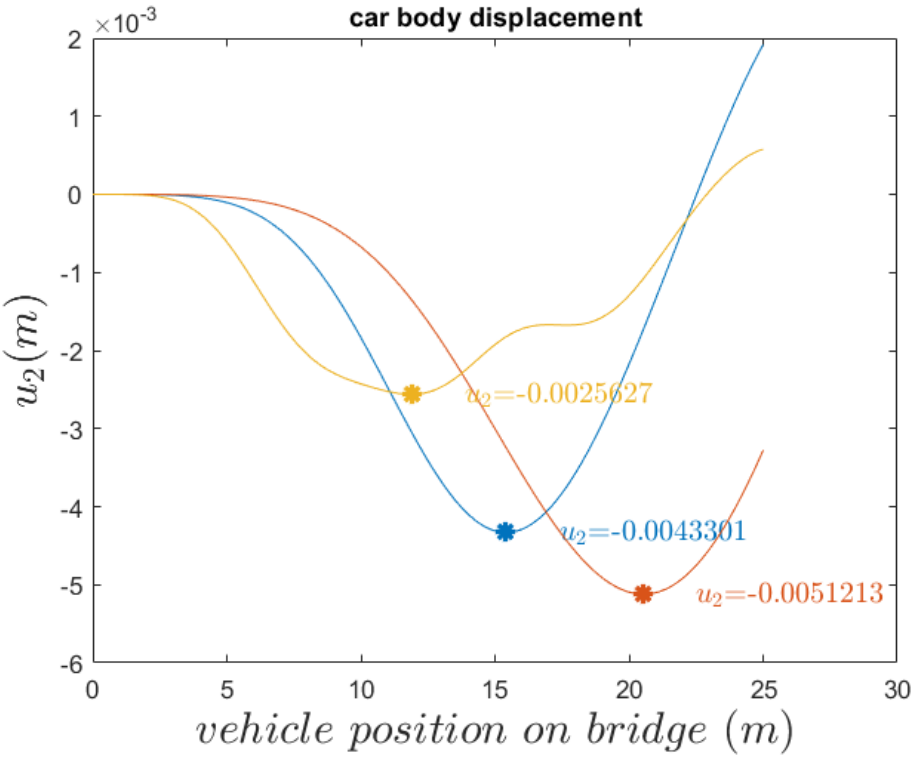

(a)

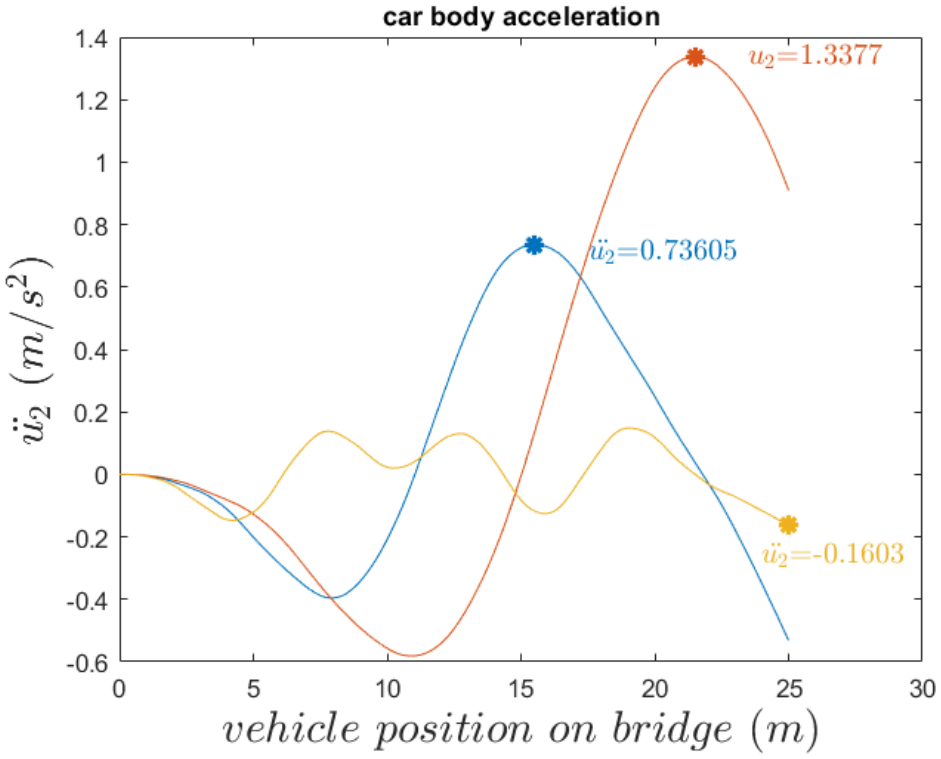

(b)

Figure 4-11 Speed influence in (a) displacement (b) acceleration of the car body

As the simulation's results show, the speed of the vehicle has a significant effect on the dynamic response of the system. Figures (4-10) show that by increasing the vehicle's speed by 2 and 3 times, the maximum value of the midpoint displacement increases by 1.1 and 1.4, respectively. An even bigger increase on the displacement response (by factors 1.69 and 2) is noted by the car body of the vehicle. The accelerations of the bridge and vehicle Figures (4-11) also increase by increasing the vehicle's speed, where the car body of the system presents the biggest variation (by factors 4.6 and 8.3).

Influence of mass

This time the vehicle's system mass is doubled and all the other parameters referring to the vehicle and the bridge remain the same.

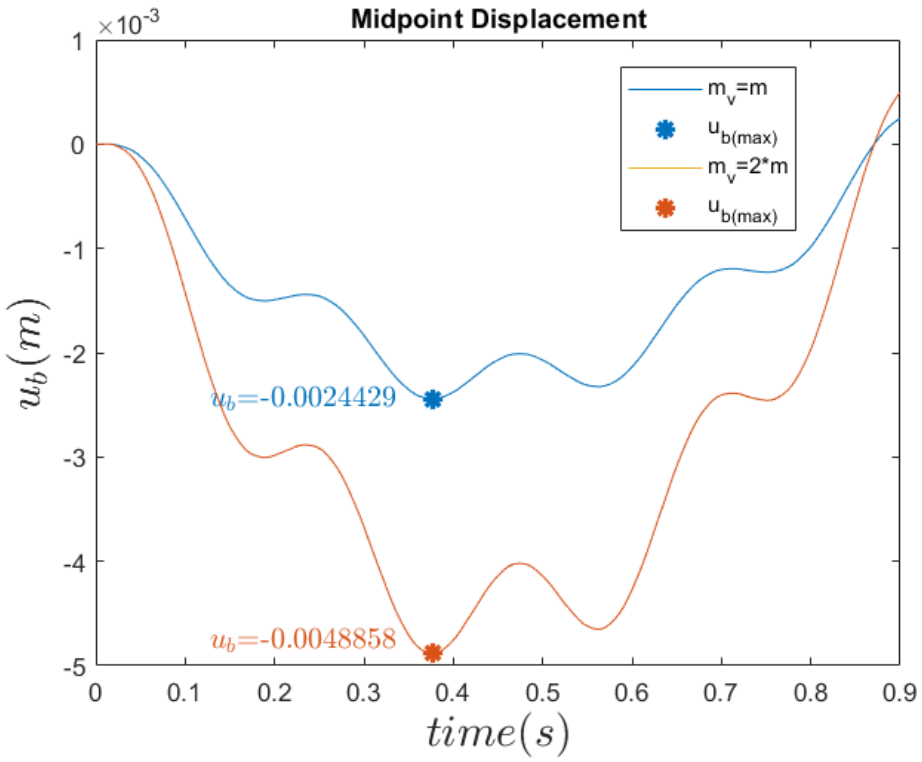

(a)

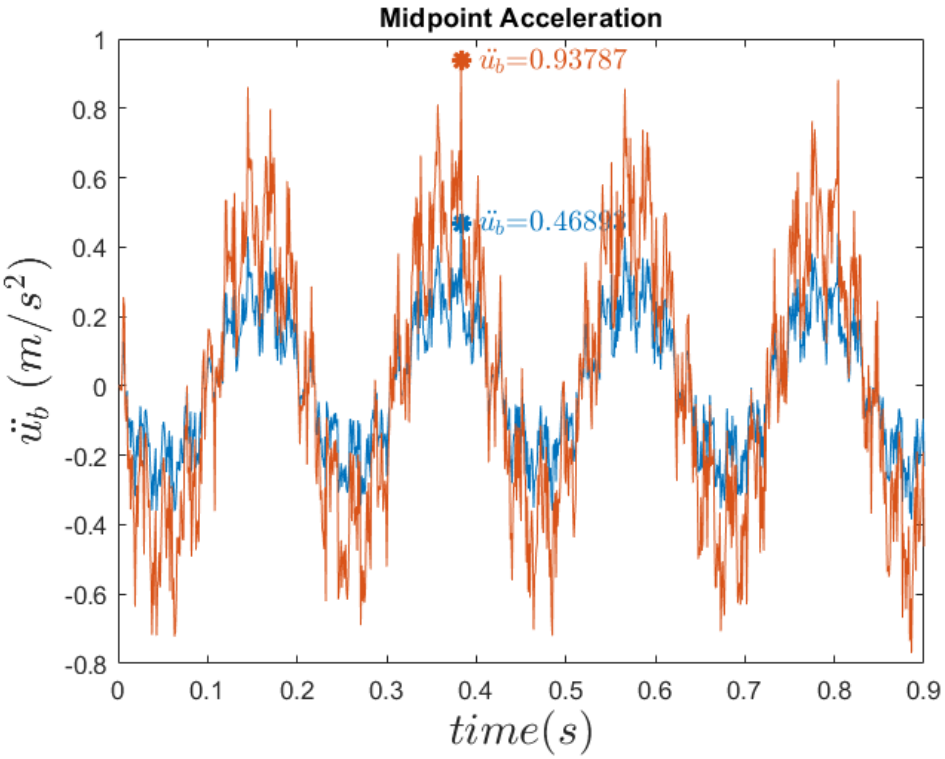

(b)

Figure 4-12 Influence of vehicle's mass in the bridge's midpoint (a) displacement (b) acceleration

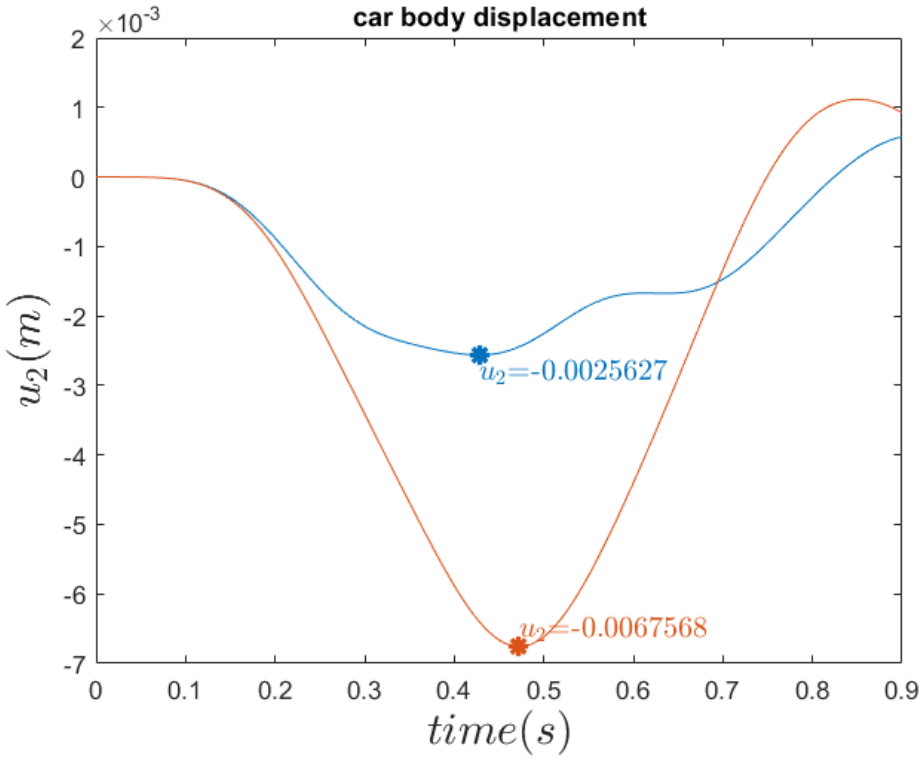

(a)

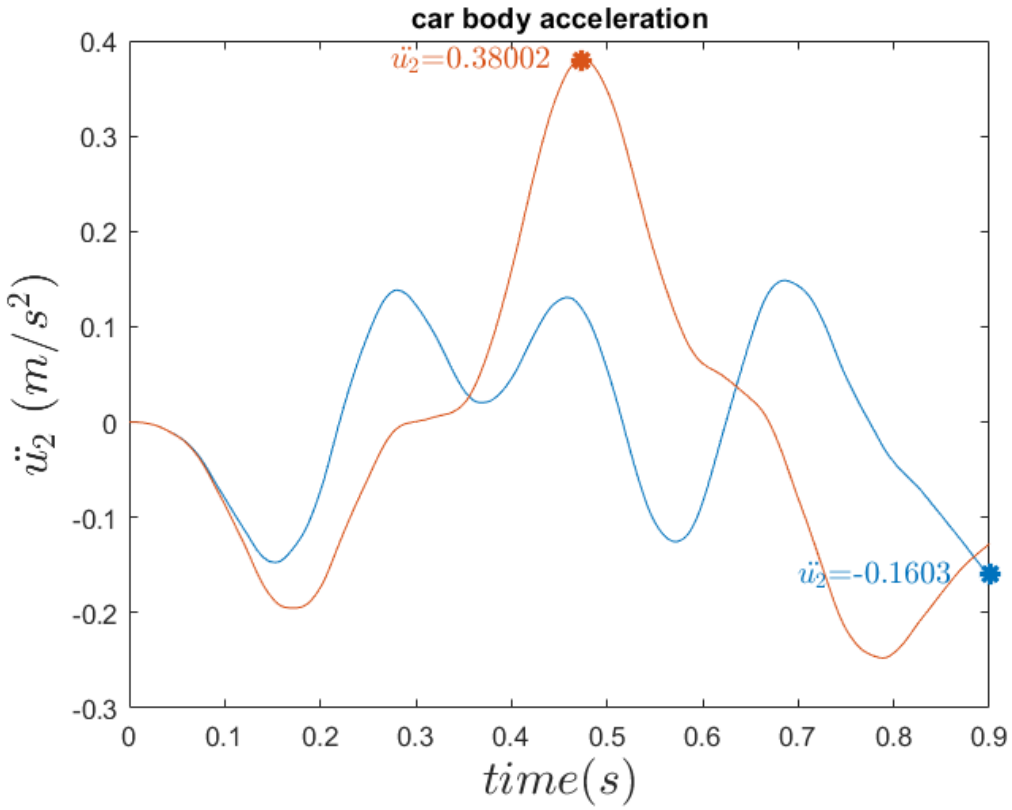

Figure 4-13 Influence of vehicle's mass in the car's body (a) displacement (b) acceleration

(b)

As expected, any change in the vehicle's mass corresponds immediately in the dynamic response of the system. By increasing the vehicle's mass, Figures (4-13),(4.14) show that both the bridge and vehicle subsystems display an increase in their responses. Specifically, it's worth mentioning that the midpoint displacement of the bridge is doubled just like the mass of the vehicle. This fact can easily be explained for the case of the sprung mass vehicle and the simply supported bridge by just observing Eq. (4.10).

Influence of vehicle's suspension stiffness

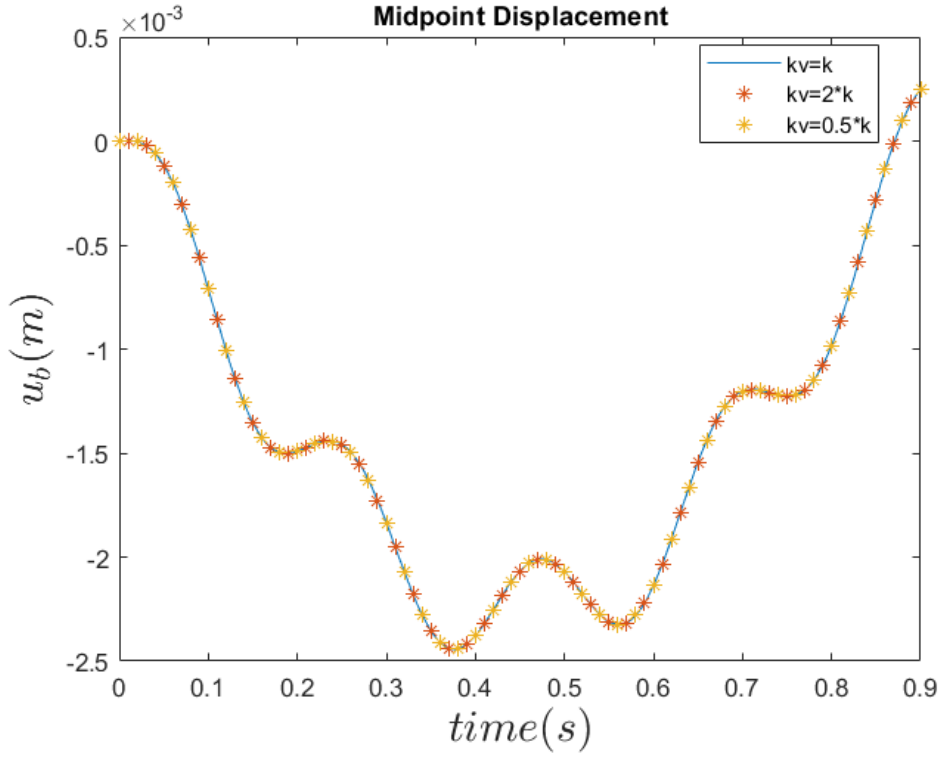

(a)

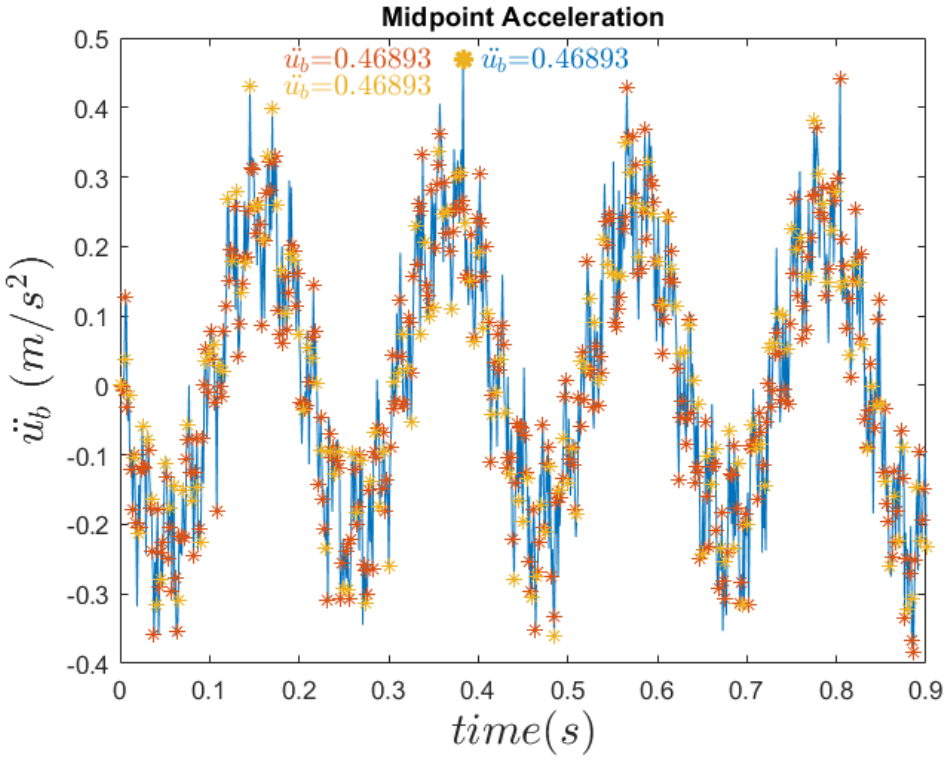

(b)

Figure 4-14 Midpoint (a) displacement (b) acceleration for different suspension stiffness

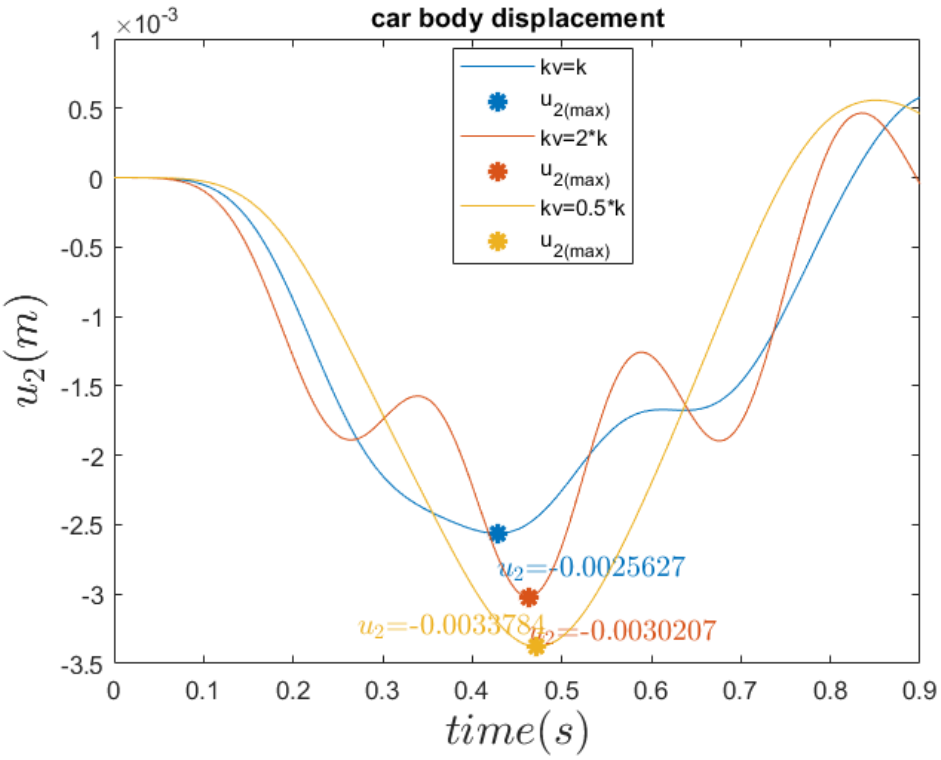

(a)

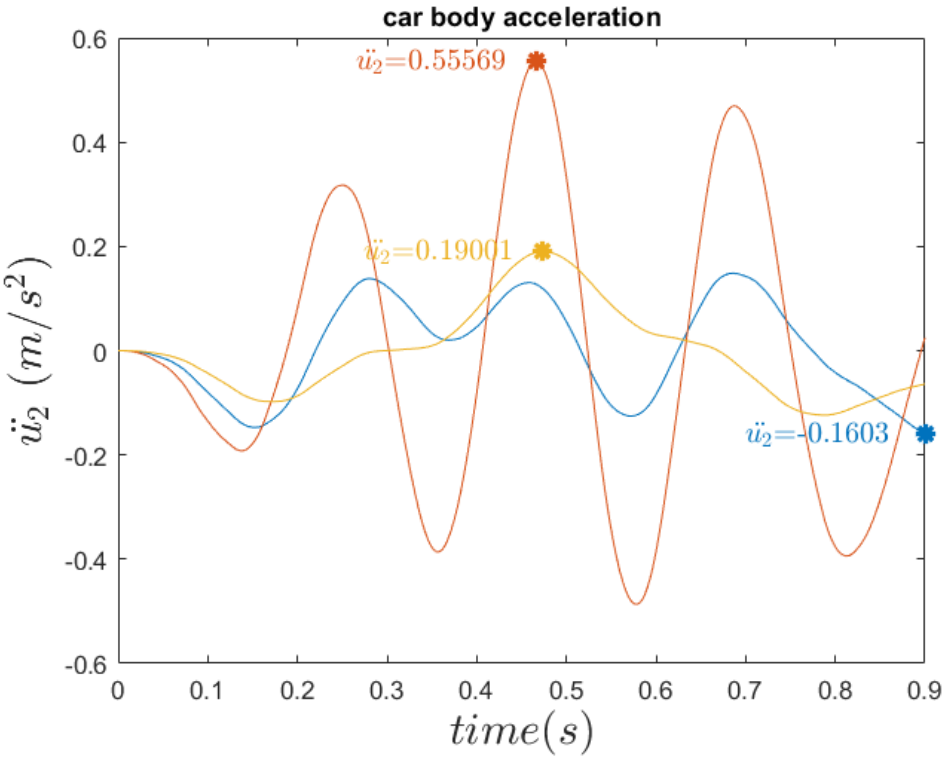

(b)

Figure 4-15 Car's body (a) displacement (b) acceleration for different suspension stiffness

As can be seen from figure (4-14) the influence of the suspension stiffness of the vehicle on the bridge response is generally quite small. Someone could even suppose that the effect of the suspension stiffness of the moving vehicle could be ignored in a practical design. Although, after examining Figure (4-15) comes to notice that by changing the vehicle's stiffness could lead to essential increase in the vertical acceleration of the car body of the vehicle, a very negative fact for the riding comfort of the passengers.

Influence of irregularities

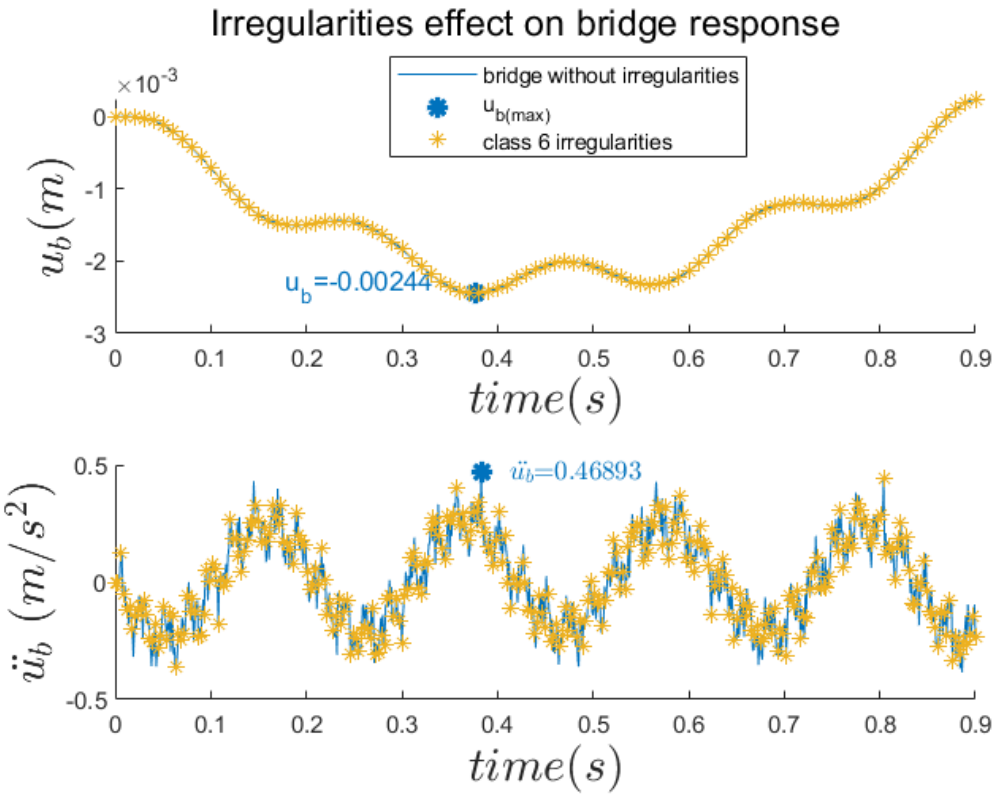

Figure 4-16 Midpoint (top) displacement, (bottom) acceleration considering road discontinuities/roughness

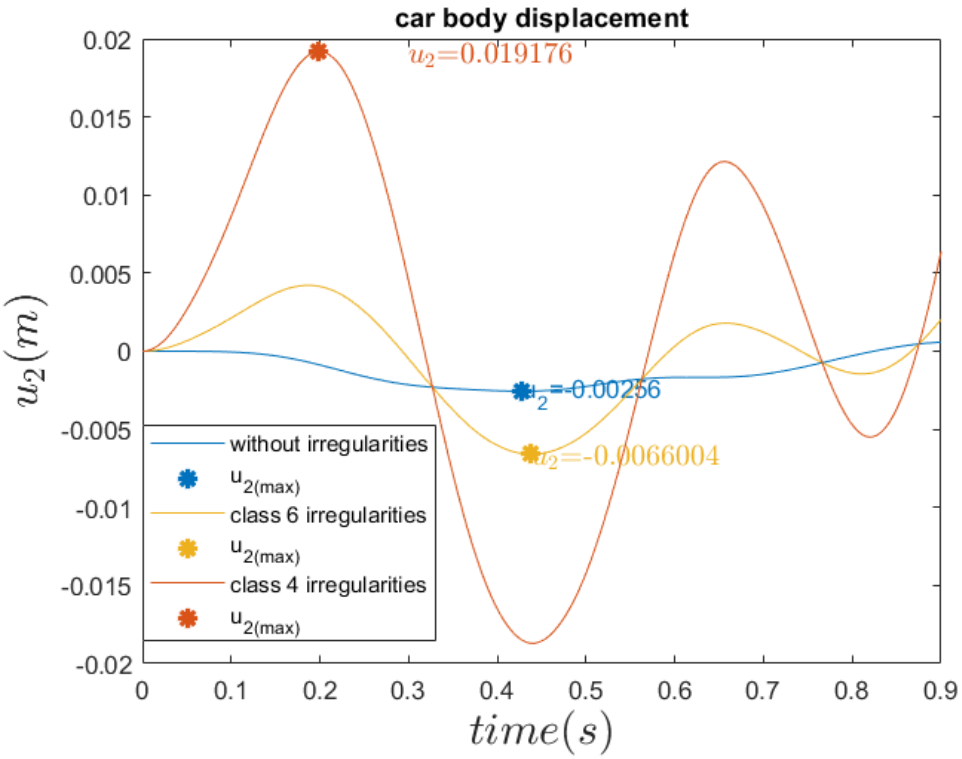

(a)

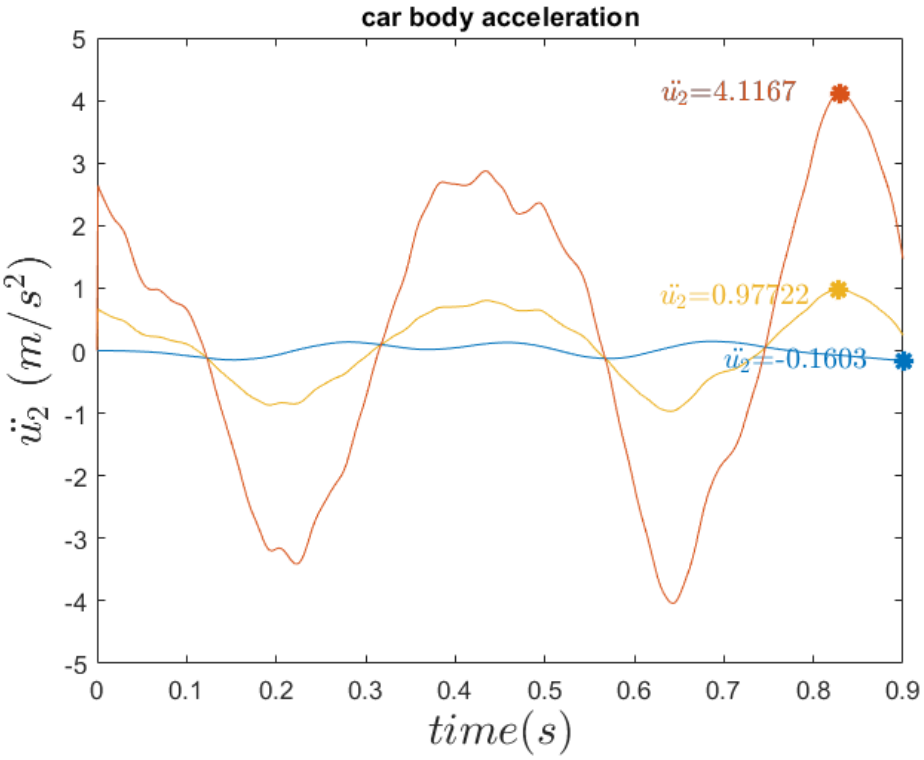

(b)

Figure 4-17 Car's body (a) displacement, (b) acceleration considering road discontinuities/roughness

From Figure (4-16) can be noticed that for the case of moderate vertical irregularities (Appendix A) the influence on the bridge response is negligible. The range and the maximum values of the bridge's midpoint displacement and acceleration Figure (4-16) remain almost the same. On the other hand, the irregularity profile of the bridge can drastically increase the level of the vibrations in the vehicle subsystem. As it can be seen in Figure (4-17) the displacement and mostly the acceleration of the car body of the vehicle present steep increase when the surface of the bridge is not smooth (class 4 and 6 irregularities). Note that those increases in the displacement and acceleration of the car body occur for discontinuities of small amplitudes (O () =10^{-3}mm), pointing out that even small discontinuities on the bridge have a major impact in the vehicle's response.

4.5.2 Train vehicle and simply supported bridge interaction

In the previous section we examined a simply (2-DOF) vehicle interacting with a simply supported bridge. In this section, a more complex model is presented for the vehicle subsystem interacting with the same bridge model (Figure 4-18).

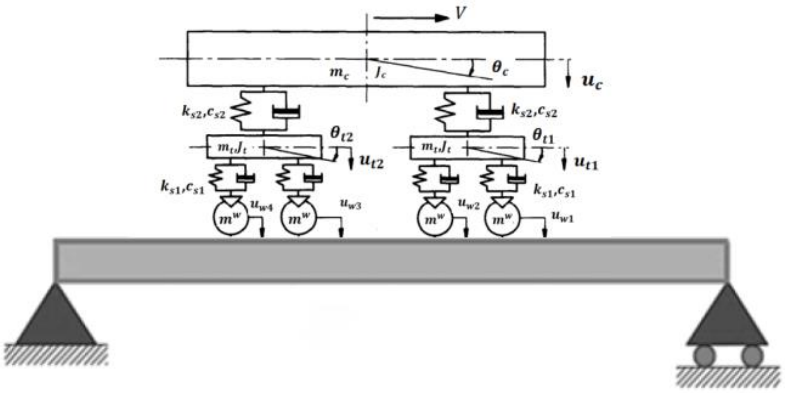

(a)

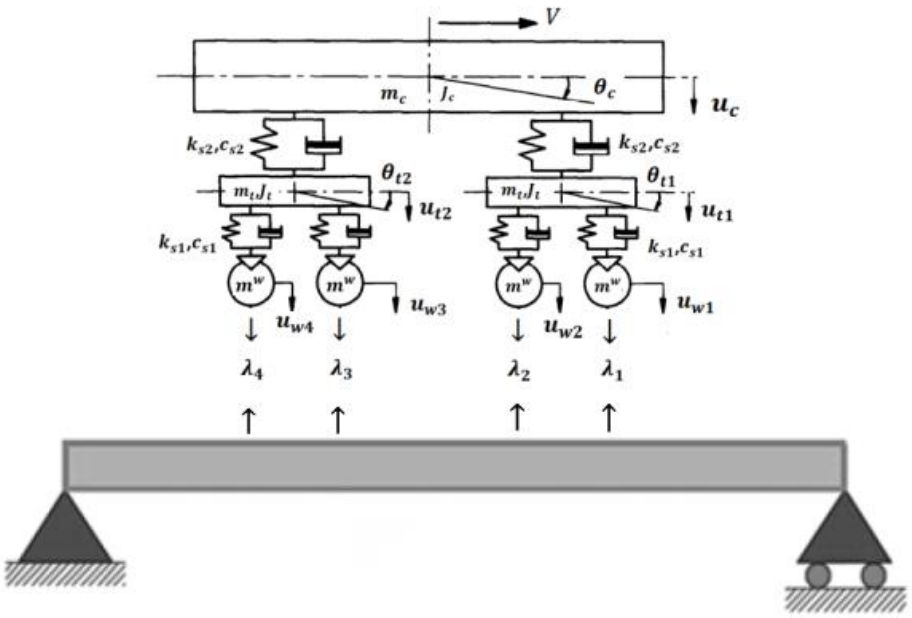

(b)

Figure 4-18 (a) train vehicle travelling a simply supported bridge (b) VBI interaction system

The following results represent the responses of the VBI system during and after the time of their interaction. The below responses correspond to the values of Table (4-3) for an undamped bridge. In figures (4-20),(4-21) we can examine the upper's part response of the vehicle where we notice that the car body of the vehicle presents smaller values than the bogies, for both vertical displacements and accelerations. It is also noticed that the bogies responses converge faster than those of the car's body. Those notifications come to an agreement with the fact that the passengers of the vehicle are placed in the car body. So, for the car body to provide both comfort and safety to the passengers, the vibration of the VBI is mainly absorbed by the primary suspension system and the bogies.

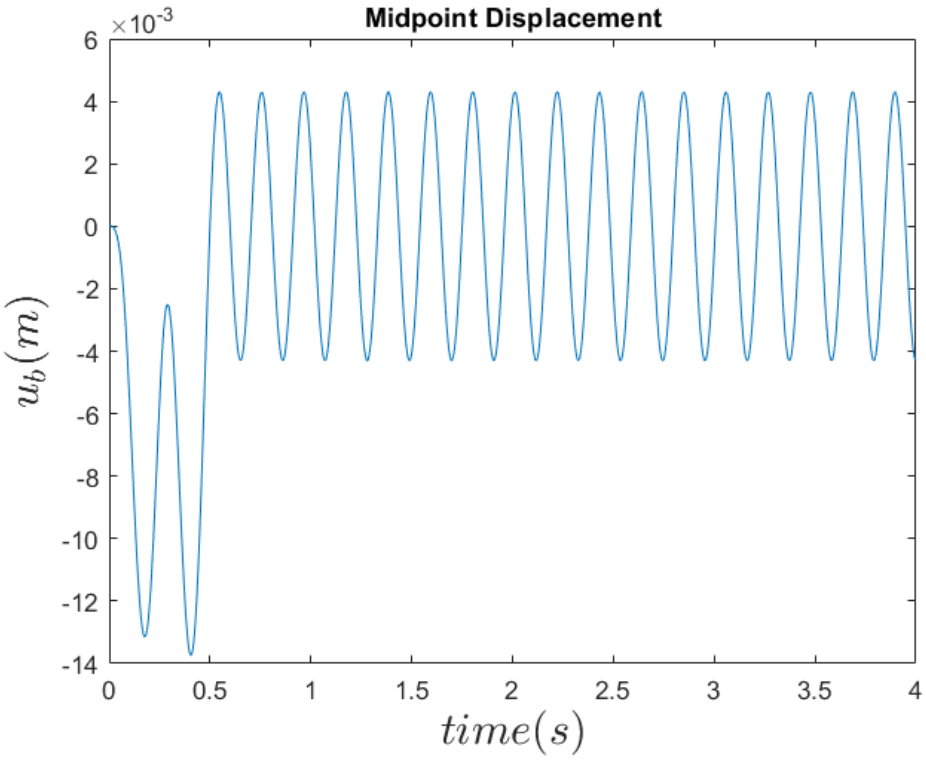

(a)

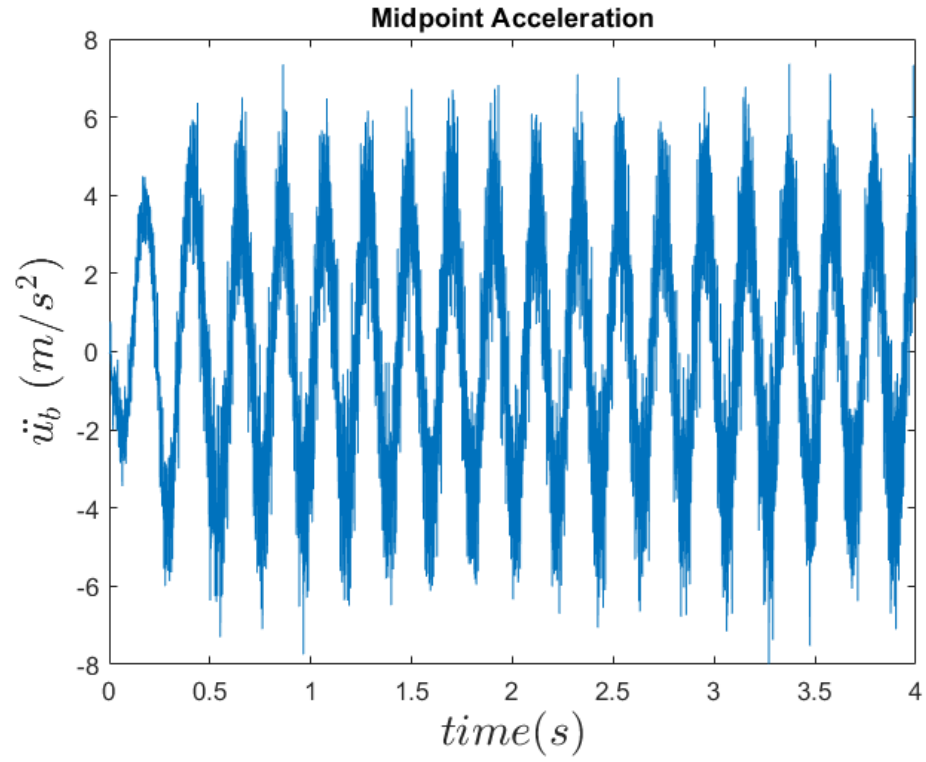

(b)

Figure 4-19 Midpoint (a) displacement (b) acceleration of the bridge

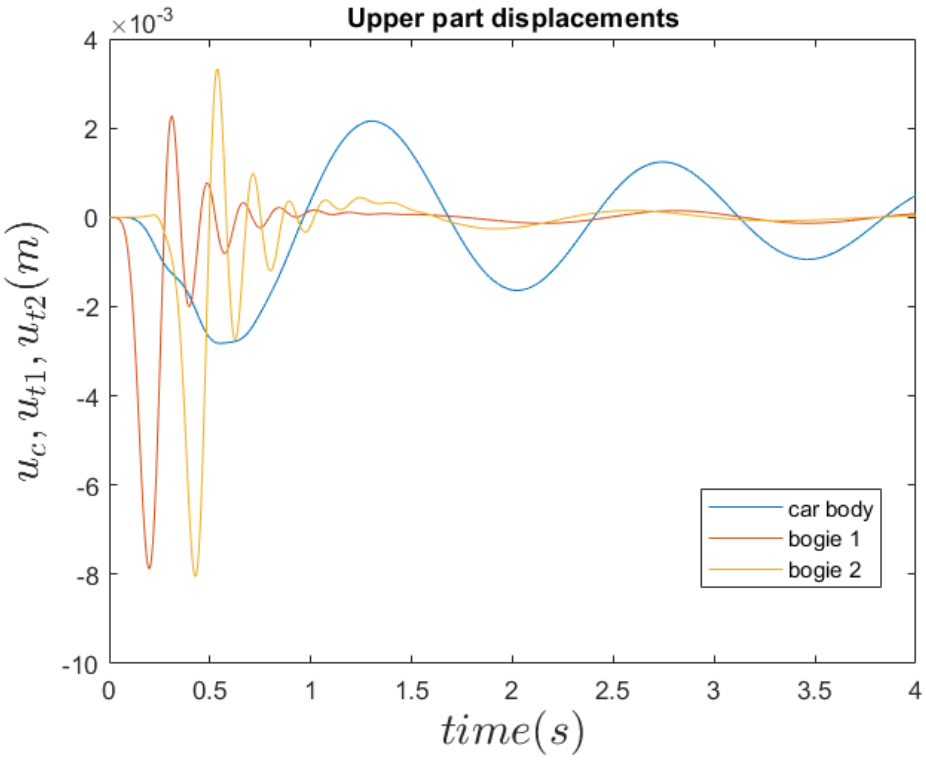

(a)

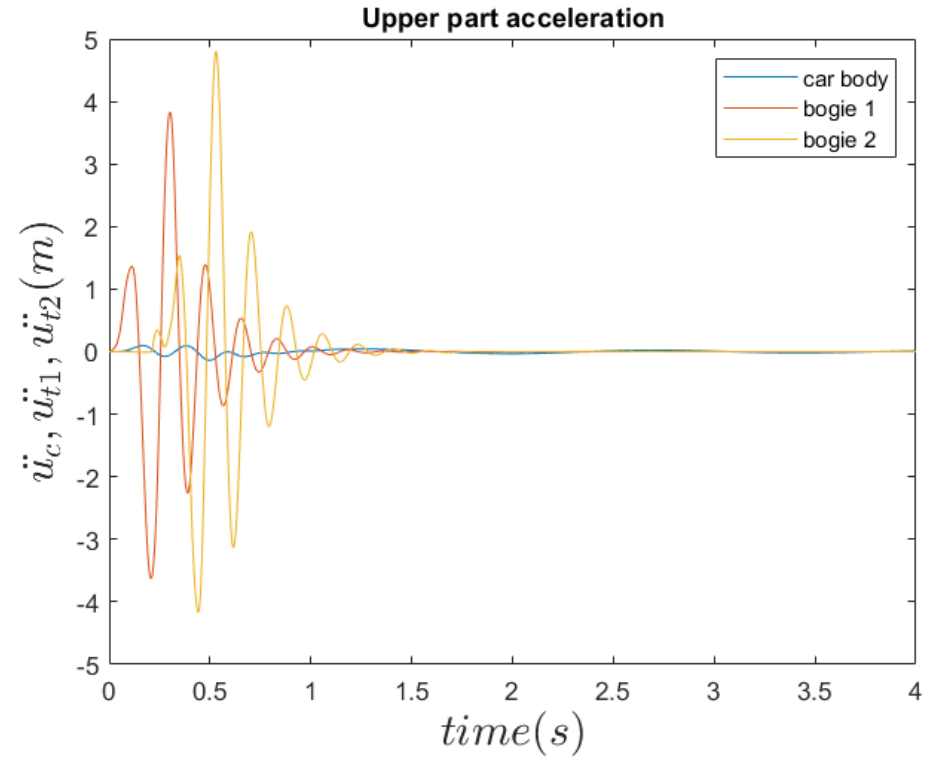

(b)

Figure 4-20 (a) displacement, (b) acceleration response for the upper part of the vehicle (car body, bogies)

(a)

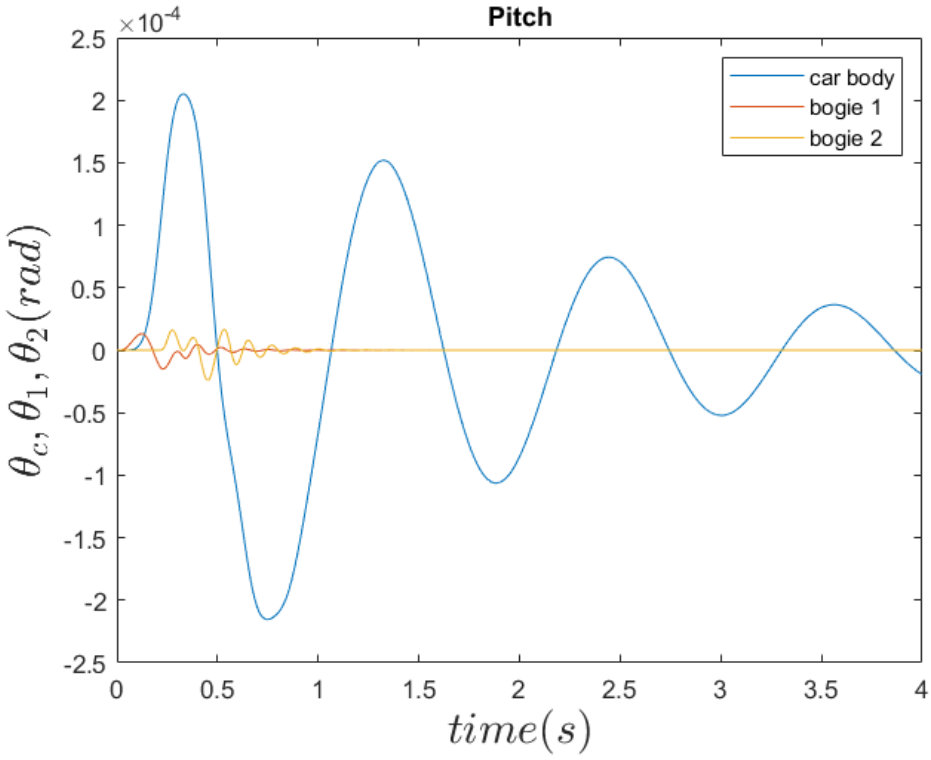

(a)

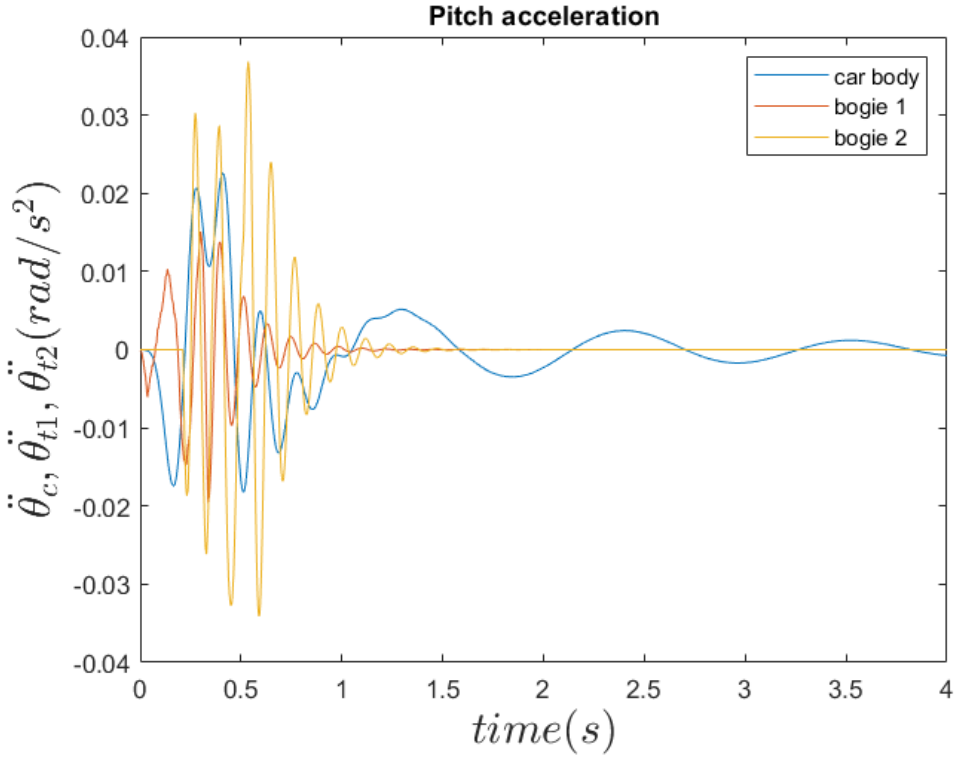

(b)

Figure 4-21 Vehicle's upper part pitch (a) rotation (b) acceleration

Influence of structural damping

The previous simulation is repeated for the case where the structural damping of the bridge is considered, as presented in section 2.3.1.

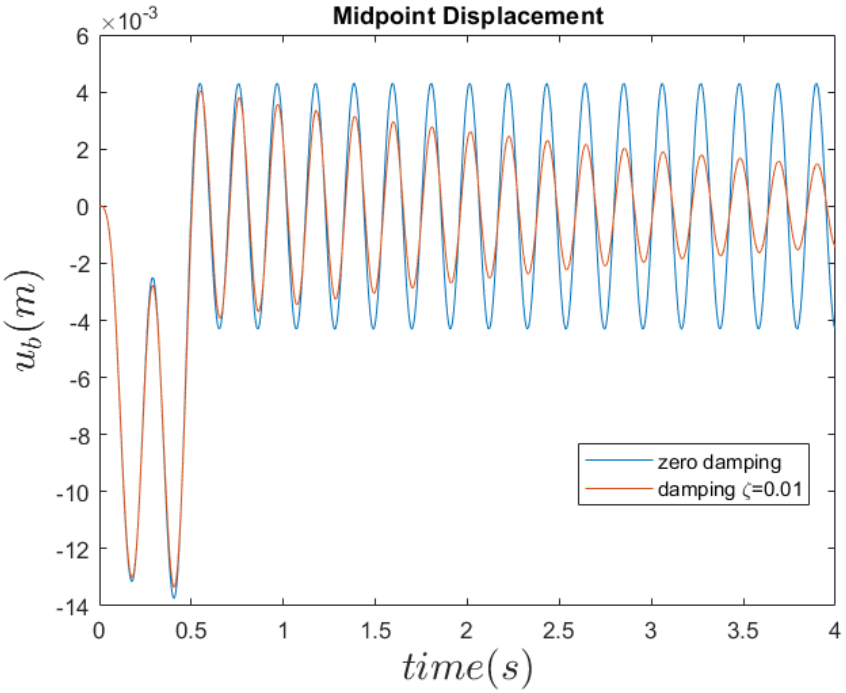

(a)

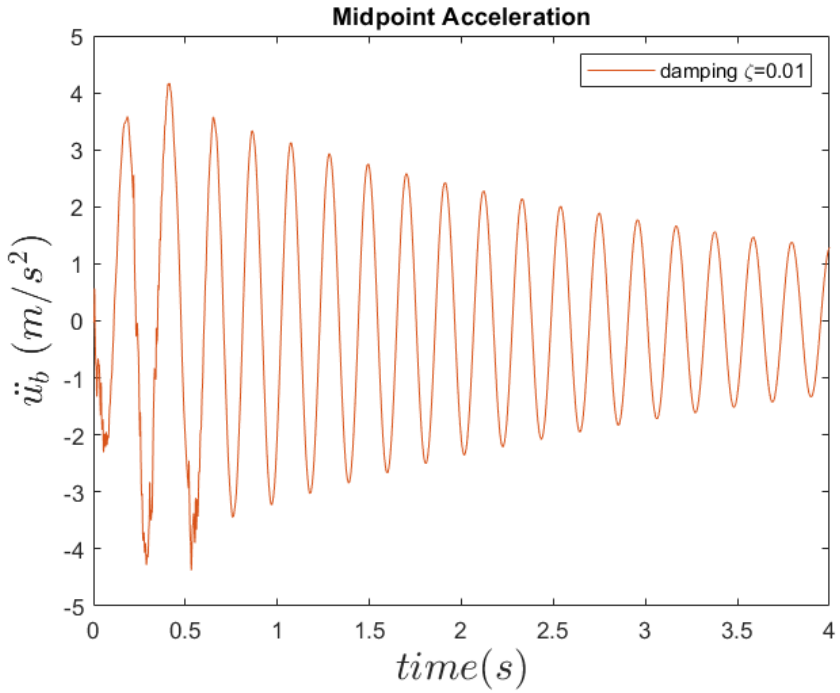

(b)

Figure 4-22 Midpoint (a) displacement (b) acceleration considering structural damping

As expected by including the structural damping of the bridge subsystem, the bridge's response is directly affected. Figure (4-22(a)) shows that the bridge's midpoint displacement is mainly affected after the departure of the vehicle, where the bridge's response constantly converges during the time of the simulation. Moreover, it is interesting to point out that the bridge's midpoint acceleration changes significantly. Comparing Figure (4-19(b)) and (4-22(b)) we notice that the bridge's midpoint acceleration amplitude is smaller and more importantly the total response is much smoother.

Influence of vehicle's suspension damping

In this case we examine the influence of the primary and secondary damping of the vehicle's suspension system. As expected from increasing the value of the primary and secondary suspension damping, the amplitude of the vehicle's displacement appears to decrease for the upper part of the vehicle (car body and bogies). At this point, we should note that the car's body response is mostly affected by the secondary suspension while the responses of the bogies are similar effected by both primary and secondary suspension changes Figure (4-23),(4-24).

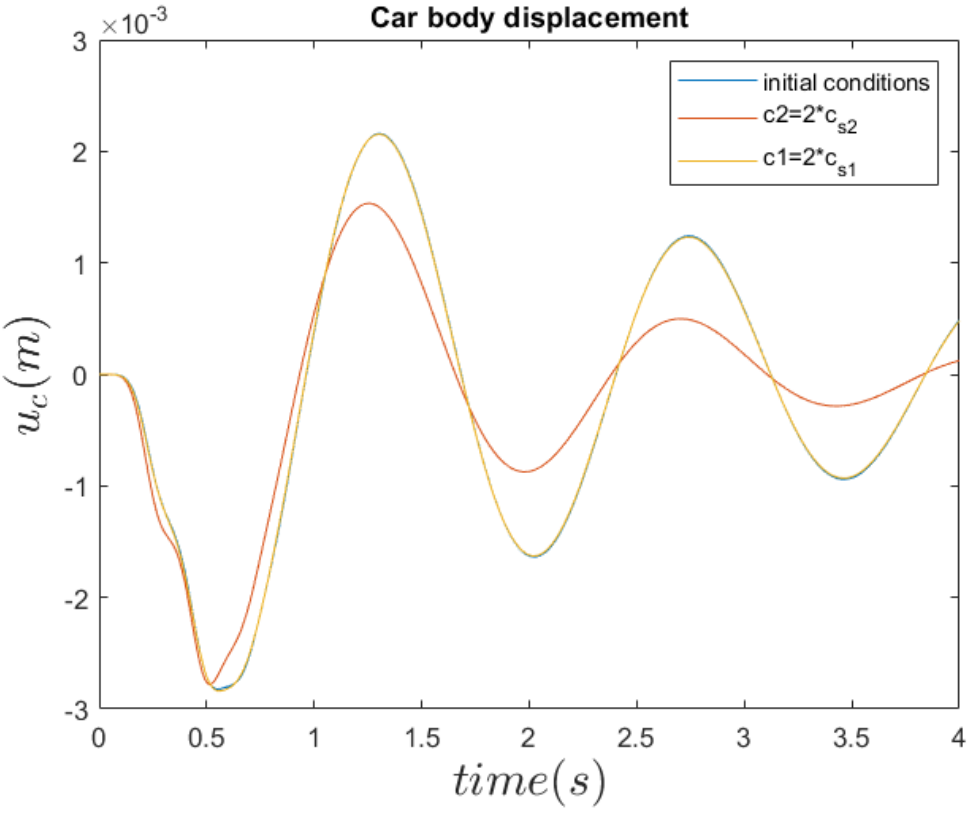

(a)

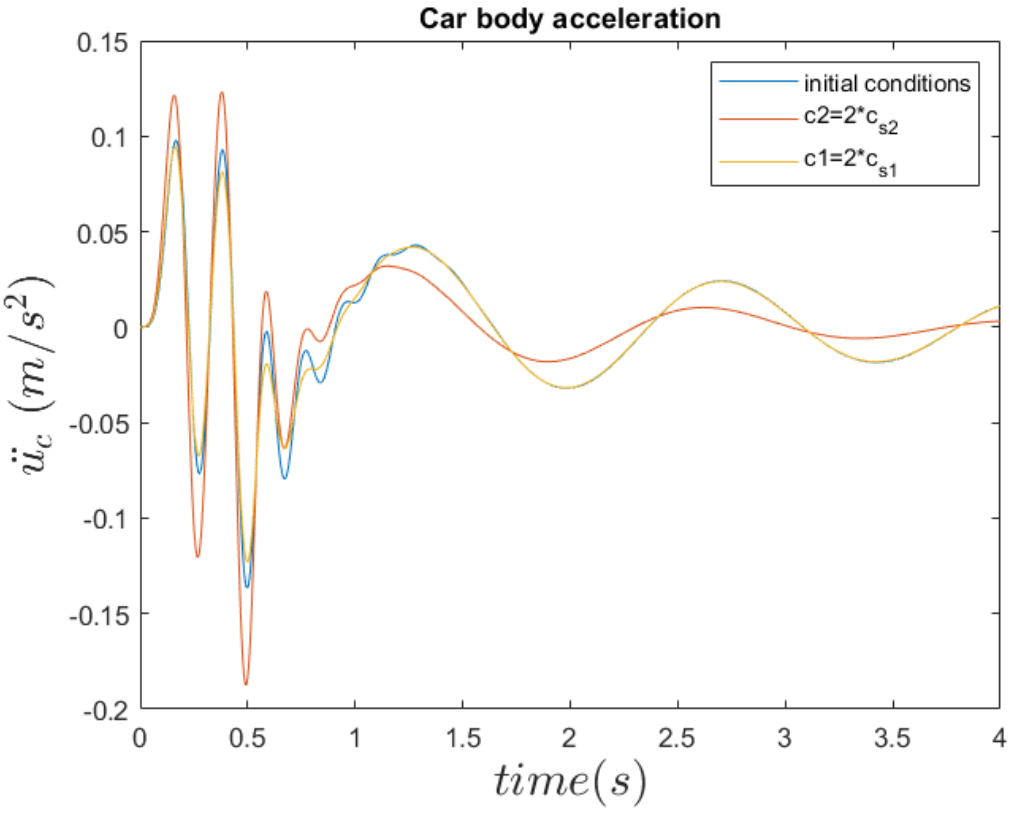

(b)

Figure 4-23 Car body (a) displacement (b) acceleration -effect of suspension damping

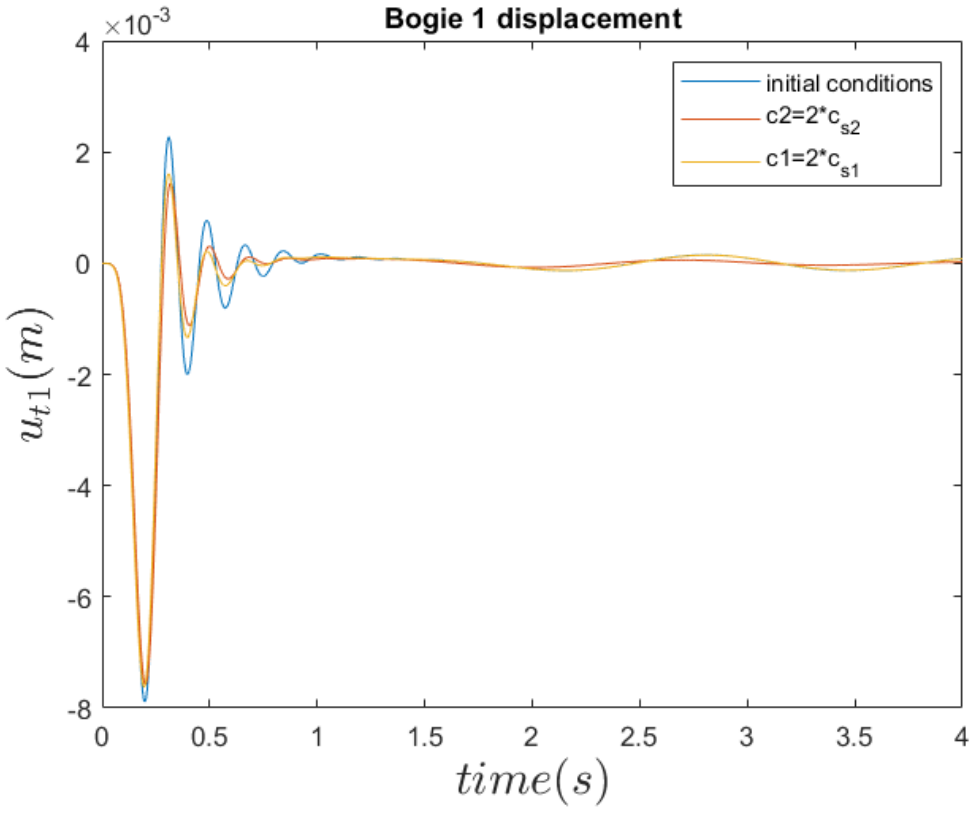

(a)

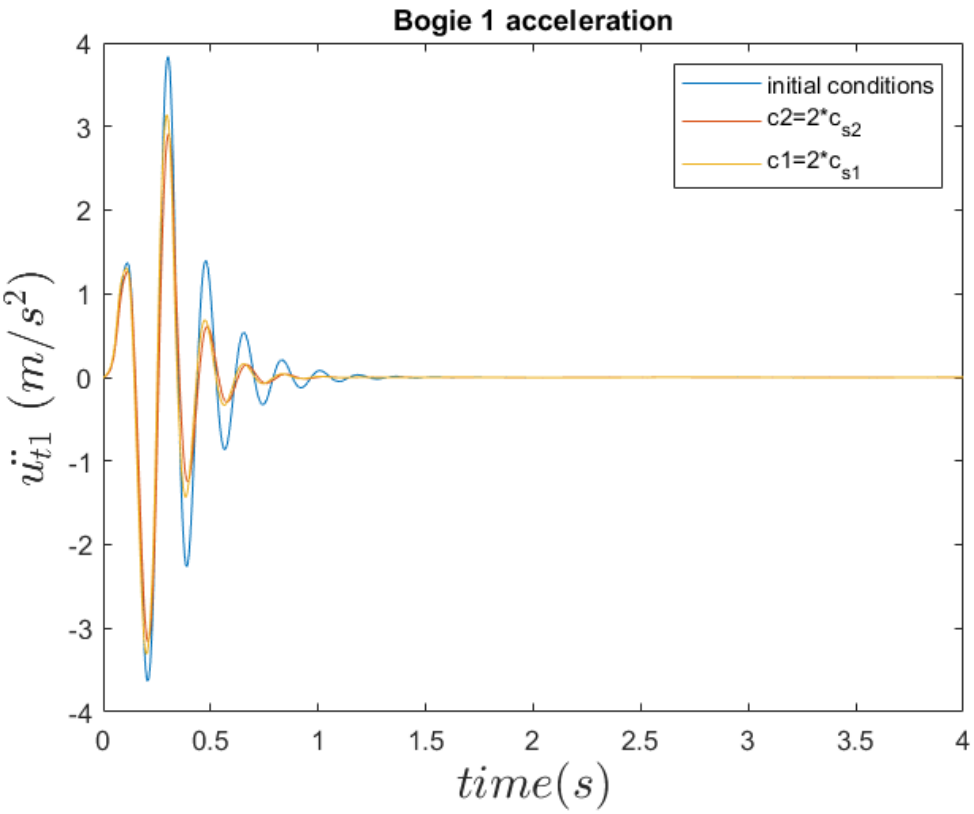

(b)

Figure 4-24 Bogie (a) displacement (b) acceleration -effect of suspension damping

5 Conclusion and future work

5.1 Conclusion

In order to dodge traffic problems in the past years, many cities have expanded their transportation system by adding more and more highway and railway bridges, where citizens can travel by their own vehicles or very frequently by railway trains. For that reason, the investigation of the VBI dynamics is very important to ensure safety and comfort during travelling. In this context, this study examines the influence of various parameters of the vehicle and bridge. This examination is carried out using Lagrange and EMBS method to solve the VBI system and Newmark-β time-integration method to simulate the corresponding response in MATLAB software.

As the simulation results show, the speed of the vehicle has a noteworthy impact in the dynamic responses of the system. In general, when the vehicle travels with high velocities the vibrations present higher amplitude. Similar results occur in case the vehicle's mass increases. Moreover, it should be noted that changes in the suspension system can have crucial effect in the acceleration responses of the vehicle, which directly acts on the riding comfort and safety of the passengers. One more factor that threatens the passenger's comfort is the road irregularities, where even small discontinuities on the bridge's surface can cause significant elevation in the car's body response.

The influence of both vehicle's and bridge parameters indicate the importance of studying the dynamics of VBI system and design both vehicles and bridges considering the safety of the passengers.

5.2 Future work

Nowadays, due to novel materials and construction methods, there is a substantial variation in bridge structures and vehicles. In this thesis, the dynamics of VBI system is simulated for a two-dimensional model for the vehicle. The model of the bridge's subsystem is also simplified to a simply supported Euler-Bernoulli beam. For this reason, a fully (3D) representation for both vehicle and bridge could examine the VBI system mechanisms in a more complete way. Last but not least, more solving methods should be considered in order to validate the accuracy of the simulation's responses.

6 References

[1] Yeong-Bin Yang_ Zhongda Yao_ Y S Wu - “Vehicle-Bridge Interaction Dynamics With Applications to High-Speed Railway.”

[2] Anil K. Chopra -“DYNAMICS OF STRUCTURES.”

[3] C. D. Stoura, E. Paraskevopoulos, E. G. Dimitrakopoulos, and S. Natsiavas, “A Dynamic Partitioning Method to solve the vehicle-bridge interaction problem,” *Comput Struct*, vol. 251, Jul. 2021, doi: 10.1016/j.compstruc.2021.106547.

[4] C. D. Stoura and E. G. Dimitrakopoulos, “MDOF extension of the Modified Bridge System method for vehicle–bridge interaction,” *Nonlinear Dyn*, vol. 102, no. 4, pp. 2103–2123, Dec. 2020, doi: 10.1007/s11071-020-06022-6.

[5] Q. Zeng, C. D. Stoura, and E. G. Dimitrakopoulos, “A localized lagrange multipliers approach for the problem of vehicle-bridge-interaction,” *Eng Struct*, vol. 168, pp. 82–92, Aug. 2018, doi: 10.1016/j.engstruct.2018.04.040.

[6] C. D. Stoura and E. G. Dimitrakopoulos, “MDOF extension of the Modified Bridge System method for vehicle–bridge interaction,” *Nonlinear Dyn*, vol. 102, no. 4, pp. 2103–2123, Dec. 2020, doi: 10.1007/s11071-020-06022-6.

[7] Comsol, “The Structural Mechanics Module User’s Guide,” 2018. [Online]. Available: www.comsol.com/blogs

[8] W. Zhait and Z. Cai$$, “PII: s0045-7949p6po4o14 DYNAMIC INTERACTION BETWEEN A LUMPED MASS VEHICLE AND A DISCRETELY SUPPORTED CONTINUOUS RAIL TRACK,” 1991.

[9] J. D. Yau, M. D. Martínez-Rodrigo, and A. Doménech, “An equivalent additional damping approach to assess vehicle-bridge interaction for train-induced vibration of short-span railway bridges,” *Eng Struct*, vol. 188, pp. 469–479, Jun. 2019, doi: 10.1016/j.engstruct.2019.01.144.

[10] C. Stoura, “Analytical and Numerical Examination of the Vehicle-Bridge Interaction Problem in Railway Bridges.”

[11] J. M. Gere, “Mechanics of Material, 7th Edition.”

[12] “L. Fryba - Dynamics of Railway Bridges-Thomas Telford Publishing (1996)”.

[13] P. Salcher and C. Adam, “Modeling of dynamic train–bridge interaction in high-speed railways,” *Acta Mech*, vol. 226, no. 8, pp. 2473–2495, Aug. 2015, doi: 10.1007/s00707-015-1314-6.

Appendix A

Simulation of Bridge Irregularities

Road irregularities are commonly considered to be one of the main factors affecting the dynamic response of the bridge and the vehicle system. There are random vertical road irregularities (elevation irregularities) resulting from the construction and maintenance of the road that led to deviations from the ideal geometry of the road layout. In this study elevation irregularity is studied, which in mainly caused by wear, initial installation errors, degradation of support materials, improper clearances, bridge support or pier settlement and their combinations. The modes of irregularity can be expressed as stationary processes in space, specifically, as random functions in terms of the longitudinal coordinate x. In road engineering, the irregularity is frequently characterized by the one-sided power spectral density (PSD) function of the road geometry [1],[12]. The PSD function used in the study for the elevation irregularity is given as follows:

$$\boldsymbol{S_{v,a}(\Omega) = \frac{A_v \Omega_c^2}{(\Omega^2 + \Omega_r^2)(\Omega^2 + \Omega_c^2)}} \quad \text{(A.1)}$$

Where $\boldsymbol{\Omega = 1/L_r}$ denotes the spatial frequency (Hz) and L_r is the length of the irregularity (m). Table tade contains the values for the coefficients involved in eqs tade, which are equivalent to Classes 4, 5 and 6 of track classification used by the Federal Railroad Administration (FRA). The track classes refer to track designations that range from 1 to 6, with class 6 indicating the best and class 1 the worst. However, the PSD function cannot be directly used in time-domain analysis because of its frequency-based nature. To overcome the problem, the spectral representation method was implemented to generate the vertical profile and alignment irregularity of the road from the PSD functions as described in eqs () . By applying the spectral representation method, the deviations in the vertical profile, $r_v(x)$, of the track can be written along the longitudinal axis x as:

$$\boldsymbol{r_v(x) = \sqrt{2} \sum_{n=0}^{N-1} A_n \cos(\Omega_n x + a_n)} \quad \text{(A.2)}$$

Where N denotes the total number of discrete spatial frequencies considered, and Ω_n is the nth discrete frequency, which is computed as

$$\boldsymbol{\Omega_n = n\Delta\Omega = n\,\frac{(\Omega_u - \Omega_l)}{N}} \quad \text{(A.3)}$$

Where Ω_u and Ω_l respectively denote the uppermost and lowest frequencies considered, and $n = 1,2, \dots, N-1$.
The coefficients A_n are defined as:

$$\begin{aligned} \boldsymbol{A_0} &= \boldsymbol{0} \\ \boldsymbol{A_1} &= \sqrt{\left(\frac{\boldsymbol{1}}{\boldsymbol{\pi}}\boldsymbol{S_{v,a}(\Delta\Omega)} + \frac{\boldsymbol{4}}{\boldsymbol{6\pi}}\boldsymbol{S_{v,a}(0)}\right)\boldsymbol{\Delta\Omega}} \\ \boldsymbol{A_2} &= \sqrt{\left(\frac{\boldsymbol{1}}{\boldsymbol{\pi}}\boldsymbol{S_{v,a}(2\Delta\Omega)} + \frac{\boldsymbol{1}}{\boldsymbol{6\pi}}\boldsymbol{S_{v,a}(0)}\right)\boldsymbol{\Delta\Omega}} \\ \boldsymbol{A_n} &= \sqrt{\left(\frac{\boldsymbol{1}}{\boldsymbol{\pi}}\boldsymbol{S_{v,a}(n\Delta\Omega)}\right)\boldsymbol{\Delta\Omega}}\,, \boldsymbol{for\ n = 3,4,\dots,N-1} \end{aligned} \tag{A.4}$$

The independent random phase angles a_n $(n = 1,2, \dots, N-1)$ are uniformly distributed in the range $[0,2\pi]$. The results presented below are computed for FRA track Classes 4,5 and 6 (fig ()).
In the simulation, the following are assumed: $\Omega_l = 0.0209\ rad/m$, $\Omega_u = 12.5664\ rad/m$ and $N = 3540$.

Note that if the length for the irregular track needed in analysis exceeds the sampling length which is selected in the study, the same irregularities should be used repeatedly in certain manner until the entire length of the track is fully covered. In order to compute the irregularity profile needed for the analysis the longitudinal coordinate x should be equal with the vehicle's position at each time, i.e., $\boldsymbol{x = v * t}$ where $\boldsymbol{v}$ is the vehicle's speed and $\boldsymbol{t}$ is the current time of interest. If the original profile has been established for different $\boldsymbol{x}$ the values from eq () should be computed through interpolation.

Table A-1 Track PSD model parameters

Quality (FRA class)	Very poor (4)	Poor (5)	Moderate (6)
A_v(m)	2.39×10^{-5}	9.35×10^{-6}	1.50×10^{-6}
Ω_s(rad/m)	1.130	0.821	0.438
Ω_r(rad/m)	2.06×10^{-2}	2.06×10^{-2}	2.06×10^{-2}
Ω_c(rad/m)	0.825	0.825	0.825

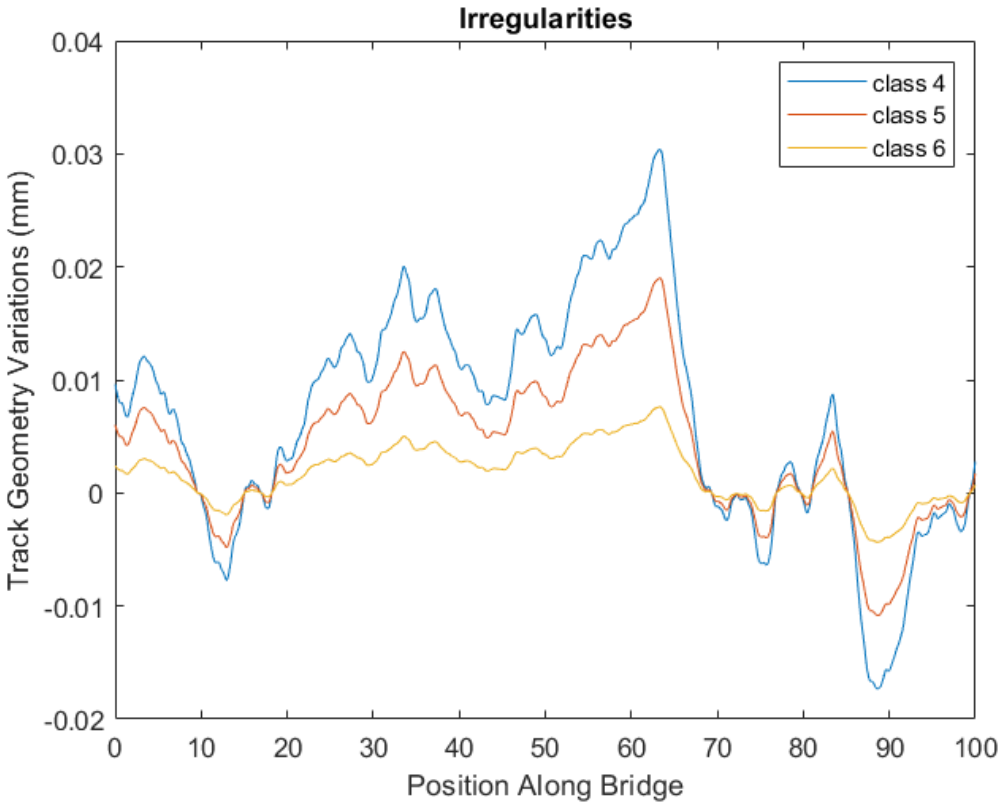

Figure A-1 Bridge Irregularities

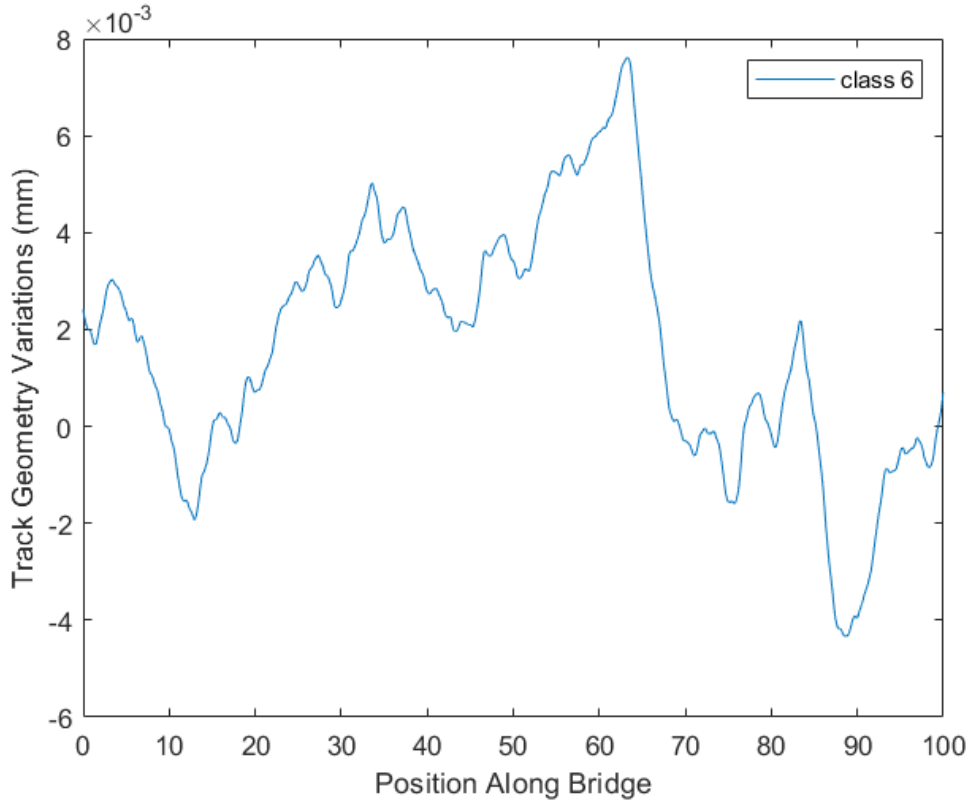

Figure A-2 Track irregularities used in 4.5.1 application

Appendix B

Newmark's-β method

A great number of dynamic problems encountered in engineering appears in the form of second-order differential equations. As so in the VBI problem the systems EOMs are being solved with Newmark's-β method. In a multi degrees of freedom problem, finite difference methods are often called to solve the second-order differential equations, which have been referred to as the direct integration methods. Newmark's-β method represents a special category of finite difference methods that have frequently been used by engineers and researchers in solving the second-order differential equations. The following is a summary of the method proposed by Newmark (1959), as presented in [1],[13].
In a step-by-step nonlinear analysis, we are interested in the behavior of the system within the incremental step from time *t* to *t*+Δ*t*, where Δ*t* denotes a small-time increment. The following are the equations of motion for the system at time *t*+Δ*t*:

$$[\boldsymbol{M}]\{\ddot{\boldsymbol{U}}\}_{\boldsymbol{t+\Delta t}} + [\boldsymbol{C}]\{\dot{\boldsymbol{U}}\}_{\boldsymbol{t+\Delta t}} + [\boldsymbol{K}]\{\boldsymbol{U}\}_{\boldsymbol{t+\Delta t}} = \{\boldsymbol{P}\}_{\boldsymbol{t+\Delta t}} \tag{B.1}$$

Where:
$[M], [C]$ and $[K]$ denote the mass, damping and stiffness matrices
$\{\ddot{U}\}, \{\dot{U}\}$ and $\{U\}$ denote the acceleration, velocity and displacement vectors
$\{P\}$ the applied load vector

The method proposed by Newmark is a single-step method, which requires only information of the system at time *t*. The following are the two basic equations proposed by Newmark for determining the displacements and velocities of the system at time *t*+Δ*t*:

$$\{\boldsymbol{U}\}_{\boldsymbol{t+\Delta t}} = \{\boldsymbol{U}\}_{\boldsymbol{t}} + \{\dot{\boldsymbol{U}}\}_{\boldsymbol{t}}\boldsymbol{\Delta t} + \left[\left(\frac{\mathbf{1}}{\mathbf{2}} - \boldsymbol{\beta}\right)\{\ddot{\boldsymbol{U}}\}_{\boldsymbol{t}} + \boldsymbol{\beta}\{\ddot{\boldsymbol{U}}\}_{\boldsymbol{t+\Delta t}}\right](\boldsymbol{\Delta t})^2 \tag{B.2}$$

$$\{\dot{\boldsymbol{U}}\}_{\boldsymbol{t+\Delta t}} = \{\dot{\boldsymbol{U}}\}_{\boldsymbol{t}} + \left[(\mathbf{1}-\boldsymbol{\gamma})\{\ddot{\boldsymbol{U}}\}_{\boldsymbol{t}} + \boldsymbol{\gamma}\{\ddot{\boldsymbol{U}}\}_{\boldsymbol{t+\Delta t}}\right]\boldsymbol{\Delta t} \tag{B.3}$$

Where a dot denotes differentiation with respect to time *t*. The parameter β denotes the variation of acceleration during the incremental step from t to $t + \Delta t$. Different values of β imply different schemes of interpolation for the acceleration over a time step. The values $\beta = 0$ indicates a scheme equivalent to the central difference method, the value $\beta = 0.25$ is a constant average acceleration method, and the value $\beta = 1/6$ is a linear acceleration method. On the other hand, the parameter γ relates to the property of numerical or artificial damping introduced by discretization in time domain. For the case with $\gamma < 0.5$, there exist some artificial negative damping, while for $\gamma > 0.5$, artificial positive damping will occur. The method has been demonstrated to be unconditionally stable under the conditions when $\gamma \geq 0.5$ and $\beta \geq 0.25(0.5 + \gamma)^2$. Throughout this study, the combination

$\gamma = 0.5$ and $\beta = 0.25$ will be selected.

From eq (), the accelerations and velocities of the system at time *t*+Δ*t* can be solved as:

$$\{\ddot{\boldsymbol{U}}\}_{t+\Delta t} = \boldsymbol{a_0}(\{\boldsymbol{U}\}_{t+\Delta t} - \{\boldsymbol{U}\}_t) - \boldsymbol{a_2}\{\dot{\boldsymbol{U}}\}_t - \boldsymbol{a_3}\{\ddot{\boldsymbol{U}}\}_t \tag{B.4}$$

$$\{\dot{\boldsymbol{U}}\}_{t+\Delta t} = \{\dot{\boldsymbol{U}}\}_t + \boldsymbol{a_6}\{\ddot{\boldsymbol{U}}\}_t + \boldsymbol{a_7}\{\ddot{\boldsymbol{U}}\}_{t+\Delta t} \tag{B.5}$$

Where the coefficients $\boldsymbol{a_0}$~$\boldsymbol{a_7}$ are given as follows:

$$\boldsymbol{a_0} = \frac{1}{\beta \Delta t^2}, \boldsymbol{a_1} = \frac{\gamma}{\beta \Delta t}, \boldsymbol{a_2} = \frac{1}{\beta \Delta t}, \boldsymbol{a_3} = \frac{1}{2\beta} - \boldsymbol{1}, \boldsymbol{a_4} = \frac{\gamma}{\beta} - \boldsymbol{1} \tag{B.6}$$
$$\boldsymbol{a_5} = \frac{\Delta t}{2}\left(\frac{\gamma}{\beta} - \boldsymbol{2}\right), \boldsymbol{a_6} = \boldsymbol{\Delta t}(\boldsymbol{1} - \boldsymbol{\gamma}), \boldsymbol{a_7} = \boldsymbol{\gamma \Delta t}$$

Substituting the preceding expression () into () yields the equivalent stiffness equations

$$[\boldsymbol{K_{eff}}]\{\boldsymbol{U}\}_{t+\Delta t} = \{\boldsymbol{P_{eff}}\}_{t+\Delta t} \tag{B.7}$$

Where the effective stiffness matrix $[\boldsymbol{K_{eff}}]$ and the effective load vector $\{\boldsymbol{P_{eff}}\}_{t+\Delta t}$ are defined as follows:

$$[\boldsymbol{K_{eff}}] = a_0[\boldsymbol{M}] + a_1[\boldsymbol{C}] + [\boldsymbol{K}], \tag{B.8}$$
$$\{\boldsymbol{P_{eff}}\}_{t+\Delta t} = \{\boldsymbol{P}\}_{t+\Delta t} + [\boldsymbol{M}]\left(\boldsymbol{a_0}\{\boldsymbol{U}\}_t + \boldsymbol{a_2}\{\dot{\boldsymbol{U}}\}_t + \boldsymbol{a_3}\{\ddot{\boldsymbol{U}}\}_t\right)$$
$$+ [\boldsymbol{C}]\left(\boldsymbol{a_1}\{\boldsymbol{U}\}_t + \boldsymbol{a_4}\{\dot{\boldsymbol{U}}\}_t + \boldsymbol{a_5}\{\ddot{\boldsymbol{U}}\}_t\right)$$

From (), the system's displacements $\{\boldsymbol{U}\}$ at time $\boldsymbol{t} + \boldsymbol{\Delta t}$ can be solved as:

$$\{\boldsymbol{U}\}_{t+\Delta t} = [\boldsymbol{K_{eff}}]^{-1}\{\boldsymbol{P_{eff}}\}_{t+\Delta t} \tag{B.9}$$

Appendix C

Shape functions

3D beam

In the beam local system, the displacements, $\boldsymbol{u}$,and rotations $\boldsymbol{\theta}$, are interpolated as

$$\begin{Bmatrix} \boldsymbol{u} \\ \boldsymbol{\theta} \end{Bmatrix} = [\boldsymbol{N}] \begin{Bmatrix} \boldsymbol{u_A} \\ \boldsymbol{\theta_A} \\ \boldsymbol{u_B} \\ \boldsymbol{\theta_B} \end{Bmatrix} \tag{C.1}$$

Where the subscript refers to the two nodes of the element.

and $\boldsymbol{N}$ is a matrix of shape functions.

$$[\boldsymbol{N}] = \begin{bmatrix} \boldsymbol{N_1} & \boldsymbol{0} & \boldsymbol{0} & \boldsymbol{0} & \boldsymbol{0} & \boldsymbol{0} & \boldsymbol{N_2} & \boldsymbol{0} & \boldsymbol{0} & \boldsymbol{0} & \boldsymbol{0} & \boldsymbol{0} \\ \boldsymbol{0} & \boldsymbol{N_3} & \boldsymbol{0} & \boldsymbol{0} & \boldsymbol{0} & \boldsymbol{N_5} & \boldsymbol{0} & \boldsymbol{N_4} & \boldsymbol{0} & \boldsymbol{0} & \boldsymbol{0} & \boldsymbol{N_6} \\ \boldsymbol{0} & \boldsymbol{0} & \boldsymbol{N_3} & \boldsymbol{0} & \boldsymbol{-N_5} & \boldsymbol{0} & \boldsymbol{0} & \boldsymbol{0} & \boldsymbol{N_4} & \boldsymbol{0} & \boldsymbol{-N_6} & \boldsymbol{0} \\ \boldsymbol{0} & \boldsymbol{0} & \boldsymbol{0} & \boldsymbol{M_1} & \boldsymbol{0} & \boldsymbol{0} & \boldsymbol{0} & \boldsymbol{0} & \boldsymbol{0} & \boldsymbol{M_2} & \boldsymbol{0} & \boldsymbol{0} \\ \boldsymbol{0} & \boldsymbol{0} & \boldsymbol{M_3} & \boldsymbol{0} & \boldsymbol{M_5} & \boldsymbol{0} & \boldsymbol{0} & \boldsymbol{0} & \boldsymbol{M_4} & \boldsymbol{0} & \boldsymbol{M_6} & \boldsymbol{0} \\ \boldsymbol{0} & \boldsymbol{-M_3} & \boldsymbol{0} & \boldsymbol{0} & \boldsymbol{0} & \boldsymbol{M_5} & \boldsymbol{0} & \boldsymbol{-M_4} & \boldsymbol{0} & \boldsymbol{0} & \boldsymbol{0} & \boldsymbol{M_6} \end{bmatrix}$$

The shape functions for the Euler-Bernoulli case are expressed in the local coordinate $\boldsymbol{\xi}$, as:

$$\begin{aligned} &\boldsymbol{N_1 = 1 - \xi} \quad \boldsymbol{N_2 = \xi} \\ &\boldsymbol{N_3 = 1 - 3\xi^2 + 2\xi^3} \quad \boldsymbol{N_4 = 3\xi^2 - 2\xi^3} \quad \boldsymbol{N_5 = L_{el}\left(\xi - 2\xi^2 + 3\xi^3\right)} \\ &\boldsymbol{N_6 = L_{el}\left(-\xi^2 + \xi^3\right)} \\ &\boldsymbol{M_1 = 1 - \xi} \; \boldsymbol{M_2 = \xi} \\ &\boldsymbol{M_3 = -\frac{6}{L_{el}}\left(\xi - \xi^2\right)} \quad \boldsymbol{M_4 = \frac{6}{L_{el}}\left(\xi - \xi^2\right)} \\ &\boldsymbol{M_5 = 1 - 4\xi + 3\xi^2} \; \boldsymbol{M_6 = -2\xi + 3\xi^2} \end{aligned} \tag{C.2}$$

Where $\boldsymbol{L_{el}}$ is the length of the beam element

And

$$\boldsymbol{\xi = \left(x_N - x_{j-1}\right)/\left(L_{el}\right)} \tag{C.3}$$

Where, $\boldsymbol{x_N}$ is the position of the N-wheel of the vehicle and $\boldsymbol{x_{j-1}}$ is the coordinate of the left node of the beam element that interacts with the N-wheel at the time, which is extracted from the COMSOL software, as mentioned above. Subsequently, ξ ranges from 0 to 1.

Note that the axial extension and the twist around the beam axis are represented by a linear shape function (N_1, N_2, M_1, M_2) while the bending displacement and corresponding rotation is represented by cubic shape functions, $(N_3, N_4, N_5, N_6, M_3, M_4, M_5, M_6)$, the Hermitian shape functions.